Geophys. J. Int. (2007) **170,** 44–80 doi: 10.1111/j.1365-246X.2007.03390.x

Electromagnetic fields in planarly layered anisotropic media

L. O. Løseth[1] and B. Ursin[2]

[1]*Department of Physics, NTNU,* N-7491 *Trondheim, Norway. E-mail: lars.loseth@phys.ntnu.no*
[2]*Department of Petroleum Engineering and Applied Geophysics, NTNU,* N-7491 *Trondheim, Norway*

Accepted 2007 January 16. Received 2007 January 3; in original form 2006 February 20

SUMMARY

This paper presents a method for calculating the electromagnetic field from a dipole source in stratified media with general anisotropy. The formulation can be applied to geophysical applications such as ground-penetrating radar and marine controlled source electromagnetic (CSEM) methods. In stratified media, the propagation of fields can be considered in the frequency–wavenumber domain. The resulting set of ordinary differential equations consists of a field vector, a system matrix, and a source vector. In each piecewise homogeneous region, the system matrix is given by the material properties and the horizontal slownesses. The vertical slownesses are the eigenvalues of the system matrix. A diagonalization of the system matrix transforms the field vector into a mode-field that contains upgoing and downgoing field constituents. For system matrices that account for general anisotropy, it is shown how the electromagnetic field from any of the four basic dipole types can be calculated at any desired position in the stratified medium. It is furthermore shown how the reflection and transmission response from a stack can be calculated by a recursive scheme. Potential numerical instabilities due to using propagators are avoided by using this reflectivity method. Due to an energy-flux normalization of the eigenvector matrices, the reciprocity relations for reflection and transmission of electromagnetic fields in general anisotropic media can be derived. Several other useful relations between the reflection and transmission matrices are obtained as well. The propagator method is dependent on the ability to calculate eigenvalues and eigenvectors of the system matrix for all layers. In simple cases with isotropy or transversal isotropy in the direction of medium variation, the eigenvalue problem can be solved explicitly. These eigenvector matrices have useful properties, e.g. when processing data. The possibility to remove layers above or below the receiver layer follows from the decomposition of a field into upgoing and downgoing polarization modes. The propagator theory was implemented in order to model anisotropy in marine CSEM. A modelling study shows that responses are affected by horizontal, vertical, and dipping anisotropy in different manners. This suggests that when anisotropy is present at a survey site, careful planning and interpretation are required in order to correctly account for the responses.

Key words: anisotropy, electromagnetic modelling.

1 INTRODUCTION

Anisotropy is a phenomenon that occurs on various scales, and it is a concern or an advantage (depending on how it can be exploited), in a variety of geophysical applications such as ground penetrating radar (GPR), which is towards the high frequency end of applications, and marine controlled source electromagnetic (CSEM) methods or SeaBed Logging (SBL), which are applications that use very low frequencies.

In electromagnetic surveying of the subsurface, anisotropy effects will almost certainly be encountered to some extent. Thus it is important to have an understanding of how various forms will affect the measurements. In elastic theory, a lot of work on anisotropy has been performed. Helbig & Thomsen (2005) review its history in elastic wave propagation. One of their main points is that anisotropy in many cases can be exploited in the exploration. Anisotropic effects when measuring electromagnetic fields in geophysical applications have also been studied for quite some time. Much of this work has been for media with stratification and transversal isotropy in the same direction, e.g. Maillet (1947), O'Brien & Morrison (1967), Sinha & Bhattacharyya (1967), Kong (1972), Chlamtac & Abramovici (1981) and Edwards *et al.* (1984). Another type of anisotropy configuration that has been studied, is transversal isotropy in a direction normal to a layered structure, e.g. Li & Pedersen (1991) and Yu & Edwards (1992). Everett & Constable (1999) studied the effects of such anisotropy on CSEM-data, and Yu *et al.* (1997)

considered triaxial (orthorhombic) anisotropy. For the modelling of GPR, Carcione & Schoenberg (2000) and Carcione & Cavallini (2001) treated anisotropy with orthorhombic symmetry in 3-D structures. Arbitrary anisotropy was considered for the DC-resistivity method in layered media by Yin & Weidelt (1999). Their solution approach, in terms of potentials, was extended to the controlled source audio-magnetotelluric (CSAMT) method by Yin & Maurer (2001). Moreover, Yin (2006) considered the marine magnetotellurics (MT) forward problem formulated for stratified media with arbitrary anisotropy.

There are many material configurations in the subsurface that might lead to anisotropy (Negi & Saraf 1989). It might be that there are some preferred directions in the subsurface rocks, or some preferred orientation of grains in the sediments. Fine layering or a pronounced strike direction might lead to an effective anisotropy. Alternations of sandstone and shales may give reservoir anisotropies. Kennedy & Herrick (2004) examined the consequences of anisotropy in reservoir rocks.

Anisotropic material properties can often be described in terms of different parameters along three orthogonal coordinate axes in a principal coordinate system for each property. Anisotropic media are furthermore often classified as triclinic, meaning that the various material properties have no principal axes in common, monoclinic meaning they have one principal axis in common, or orthorhombic, which means that the principal axes coincide for all the medium properties (Carcione & Schoenberg 2000). When two parameters in the principal coordinate frame for an orthorhombic medium are equal, the medium can be referred to as transversally isotropic. In this case, we will refer to the axis with the distinct parameter as the axis of anisotropy. In optics, one often works with anisotropy related to crystal classes. It is in this case common to consider uniaxial and biaxial media meaning either one or two anisotropy axes, respectively (Born & Wolf 1999; Huard 1997; Stamnes & Sithambaranathan 2001).

In the following, we study stratified media with arbitrary anisotropy by using a matrix propagator method. There are several reasons for studying plane-layered media. The calculation of electromagnetic fields in such media is often useful in order to simplify a problem for interpretational purposes. In case of anisotropy, the added complication to the interpretation makes it worthwhile to study anisotropy effects in 1-D models. In addition, plane-layer modelling-codes are fast and useful in, e.g. more complicated modelling-schemes and inversion. Plane-layer modelling is also important as a verification tool for numerical algorithms that handle 2-D or 3-D structures.

The matrix propagator methods are well known techniques for treating wave propagation in stratified media: *cf.* Berremann (1972) in optics, Suchy & Altman (1975) in plasma physics, Kong (1972) for the geophysical electromagnetic problem in stratified media with transversal isotropy in the direction of medium changes, Griffiths & Steinke (2000) for wave propagation in locally periodic media, Kennett (1983) for seismic wave propagation, Ursin (1983) reviewing elastic and electromagnetic wave propagation, and White & Zhou (2006) for electroseismic prospecting in layered media.

However, to our knowledge, there has not been many applications of propagator techniques to electromagnetic problems in stratified media with general anisotropy and loss. In the following, we derive equations that describe electromagnetic field propagation from any of the basic dipole sources in general anisotropic media. An implementation and application of the theory will be presented after the theory sections. During the derivation of the formalism, several useful relations for reflection and transmission in anisotropic media are derived.

The constitutive relations between the field variables are considered in terms of dyadic material parameters (second rank tensors). It will be assumed that these dyads can be given in an orthogonal principal frame where they have only diagonal elements. This means that a rotation into another (the main) coordinate frame will preserve the symmetry of the dyads (Onsager 1931). In geophysical applications where one uses low frequencies, the important material parameter will be the dyadic conductivity. In applications such as GPR, the electric permittivity is also important. Even if the magnetic permeability in many applications is assumed to be that of free space, all the material parameters are taken to be dyads for completeness. Non-linear effects are however not considered, and the entries in the material dyads are assumed to be frequency–domain scalars, meaning that they are local parameters in space. It should also be noted that crosscoupling between electric and magnetic fields in the constitutive relations, so-called bianisotropy, is not considered since we expect these effects to be minimal in geophysical applications.

Since the medium varies in one direction, the electromagnetic fields are Fourier transformed into the frequency–wavenumber domain. This leads to a set of ordinary differential equations for the horizontal field components that can be written as in Ursin (1983). This involves a field vector that contains the horizontal electromagnetic field components, a system matrix (4×4) that describes the medium seen by one frequency–wavenumber component, and a source vector that can either be an infinitesimal electric or magnetic dipole. The system matrix will in the general anisotropic case have no non-zero elements, but because of the assumption of symmetric material parameters, it will contain symplectic symmetries (Chapman 1994). The eigenvalues of the system matrix can be obtained by solving a quartic equation, and they correspond to vertical wavenumbers or slownesses (wavenumber divided by frequency). An alternative to solving the quartic equation, is solving the eigenvalue problem with standard routines from linear algebra libraries. To this end it should be noted that the structure of the matrix resembles the structure found in Hamiltonian systems (Bunse-Gerstner *et al.* 1992; Faßbender *et al.* 2001).

By introducing an ad hoc field, we show that the eigenvector matrix, which is used for the similarity transform of the system matrix, should be chosen to be flux-normalized. In lossless media this is straightforward, but in lossy media, a general 'energy invariant' which corresponds to the Poynting vector in the vertical direction for lossless media is introduced. A discussion of adjoint and conjugate fields for these purposes can be found in Altman & Suchy (1998).

In a homogeneous region, the transformed physical field, using the flux-normalized eigenvectors, will be referred to as the upgoing and downgoing mode-field. From considering propagation of the mode-field in a homogeneous region, across a source, across an interface or a stack of layers, expressions for the electromagnetic field anywhere in the layered system are obtained. In homogeneous regions the differential equation is decoupled, and from the boundary conditions a description of reflection and transmission in terms of the eigenvector matrices (2×2) at each side can be obtained. The reflection and transmission in a stack of layers can be described by a recursive scheme similar to that found in Kennett (1983), Chapman (2004), Ursin & Stovas (2002) and Stovas & Ursin (2003). By using the recursive expressions, one avoids the problem with exponentially large terms.

In order to handle a stack of layers that can contain general anisotropy as well as isotropy, various special cases of anisotropy configurations are considered. In addition to arbitrary anisotropy which normally leads to four different magnitudes of the system matrix' eigenvalues, up/down-symmetric media, meaning that the eigenvalues for the upgoing and downgoing mode-fields are equal in magnitude are treated. A medium with transversal isotropy in the horizontal direction (TIH) is an example of an up/down-symmetric configuration. With transversal isotropy in the vertical direction (TIV), the eigenvalues and eigenvectors reduce to simple expressions. The polarization modes of the field vector do not couple at the interfaces in this case. Even if this might happen for some wavenumbers in more complicated anisotropic structures, it is only for TIV-media and isotropic media that the eigenvalues of the system matrix correspond to pure polarization modes which are decoupled at interfaces between homogeneous regions for the entire wavenumber spectrum. The decoupling means that the 2×2-matrix problem reduces to a scalar problem.

In most of the realistic problems in geophysics, the source medium will be TIV or isotropic. Assuming that the receiver (the position where the field is calculated) layer has the same characteristics, but not necessarily is the same layer as that of the source, we derive explicit expressions for the electromagnetic fields. In these formulas, other layers than the source and receiver layers may have general anisotropy. It should be noted that the derived field components correspond to Green' functions when normalized properly. The expressions have been implemented in FORTRAN 90, and a modelling study of some scenarios from CSEM/SBL has been performed.

In the last appendix, an application of the separation into upgoing and downgoing field constituents is demonstrated. Depending on the choice of eigenvector matrix, it is possible to remove the effect of a stack of layers above the source in the measured electromagnetic field. In order to do this 'free-surface' removal, the horizontal field components should be known throughout a 2-D plane.

2 MAXWELL'S EQUATIONS

Maxwell' equations in the frequency domain are (*cf.* Stratton 1941; Jackson 1998; Kong 2000)

$$\nabla \cdot \mathbf{D} = \rho, \tag{1a}$$

$$\nabla \cdot \mathbf{B} = 0, \tag{1b}$$

$$\nabla \times \mathbf{E} - i\omega \mathbf{B} = \mathbf{0}, \tag{1c}$$

$$\nabla \times \mathbf{H} + i\omega \mathbf{D} = \mathbf{J}, \tag{1d}$$

where $\mathbf{E}$ is the complex electric field intensity and $\mathbf{H}$ is the complex magnetic field intensity. The fields vary with position $\mathbf{x} = [x, y, z]$ and frequency ω. In the equations there are two more field quantities which are normally referred to as the electric displacement $\mathbf{D}$ and the magnetic induction $\mathbf{B}$. The density of free charges is described by ρ, and $\mathbf{J}$ is the current density. The charge-conservation is described by the relation $-i\omega\rho = \nabla \cdot \mathbf{J}$. In conductive media, it is convenient to split the current density $\mathbf{J}$ into a source term $\mathbf{J}_0$ and a conduction current density $\mathbf{J}_c$. For macroscopic media it might furthermore be advantageous to introduce a magnetic source term $\mathbf{J}_{0M}$ into Faraday' law (eq. 1c) which in this case is modified to $\nabla \times \mathbf{E} - i\omega \mathbf{B} = -\mathbf{J}_{0M}$. Charge-conservation then leads to the modification $\nabla \cdot \mathbf{B} = \rho_M$ where ρ_M is the magnetic source charge density. Although magnetic sources have not yet been found to exist, their introduction into the equations is justified by the equivalence principle (Kong 2000). Since magnetic sources have been introduced, we will in the following refer to the source term $\mathbf{J}_0$ as the electric source.

In macroscopic media the constitutive relations between the field quantities might be very complicated (Nabighian 1987; Jackson 1998; Kong 2000). In the following, non-linear effects found in ferroelectric and ferromagnetic materials are not taken into account. Unless otherwise noted, only (piecewise) homogeneous regions are considered, and possible non-local effects in space of the material parameters are ignored. The constitutive relations may then be written as

$$\mathbf{D} = \boldsymbol{\varepsilon}(\omega)\mathbf{E}, \tag{2a}$$

$$\mathbf{B} = \boldsymbol{\mu}(\omega)\mathbf{H}, \tag{2b}$$

and in conductive media the relation between the conduction current density $\mathbf{J}_c$ and the electric field (Ohm' law) is

$$\mathbf{J}_c = \boldsymbol{\sigma}(\omega)\mathbf{E}, \tag{2c}$$

where $\boldsymbol{\sigma}$ is the electric conductivity. The material parameters $\boldsymbol{\varepsilon}$, $\boldsymbol{\mu}$, and $\boldsymbol{\sigma}$ are dyads. The principal axes of the medium property dyads can be illustrated using Fig. 1, where the main coordinate system *xyz* is sketched along with a rotated system $x'y'z'$. This rotated system may represent the principal axes of one of the material dyads, e.g. conductivity. The dyads, which are diagonal in the principal coordinate frame, will be symmetric after a rotation into a new coordinate frame when the principal axes are orthogonal (Onsager 1931).

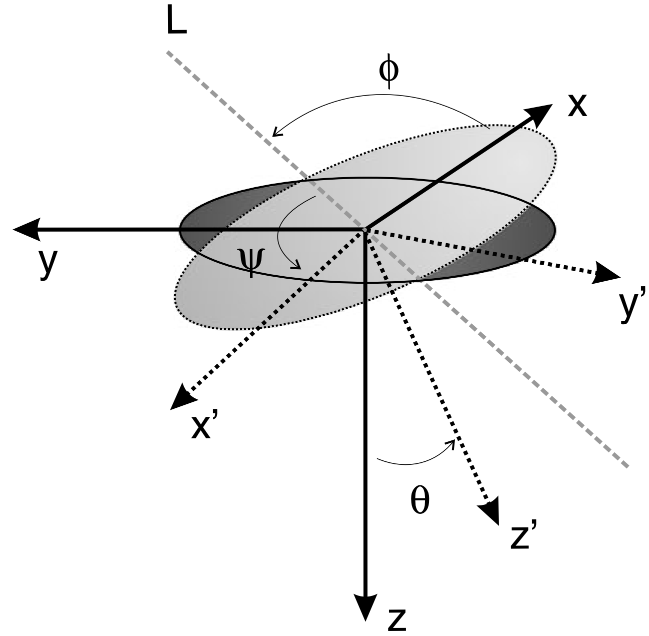

Figure 1. The main coordinate frame *xyz* and a principal system $x'y'z'$. Rotation from the main frame to the principal system (and vice versa) can be performed in terms of the Euler angles ϕ, θ, and ψ. L represents the line of nodes.

In the following it will be assumed that the material dyads have been rotated from their principal system into the main coordinate system. A procedure for doing so is presented in Appendix A. To simplify notation, the permittivity and conductivity can be written as a complex electric permittivity

$$\tilde{\boldsymbol{\varepsilon}} = \boldsymbol{\varepsilon} + i\boldsymbol{\sigma}/\omega, \tag{3}$$

in the main coordinate frame. Note that by doing this, the meaning of the electric flux density changes. The charge density in Gauss' law now describes source charges instead of free charges.

As sources of the electromagnetic field in the stratified medium, electric and magnetic dipoles with general orientation are considered. An infinitesimal electric dipole antenna can be represented by a periodic line current of length $\mathbf{l} = l_x\hat{\mathbf{x}} + l_y\hat{\mathbf{y}} + l_z\hat{\mathbf{z}}$ with current amplitude $I(\omega)$. The frequency domain source current density can then be written as:

$$\mathbf{J}_0 = I(\omega)\left[l_x\hat{\mathbf{x}} + l_y\hat{\mathbf{y}} + l_z\hat{\mathbf{z}}\right]\delta(\mathbf{r}), \tag{4}$$

where $\mathbf{r}$ is the distance from the source, i.e. the radial vector is described in terms of Cartesian coordinates as $\mathbf{r} = \mathbf{x} - \mathbf{x}_s$, where the source position is given as $\mathbf{x}_s = [x_s, y_s, z_s]$. If the electric dipole moment is represented by $\mathbf{P}$ (polarization), the dipole current moment becomes $-i\omega\mathbf{P}$. The magnetic dipole moment is given by $\mathbf{m} = \boldsymbol{\mu}I(\omega)\,\mathbf{a}$, where $\mathbf{a}$ is the area of a current carrying loop with direction normal to the loop. Analogous to the source current density for the electric dipole in eq. (4), an infinitesimal magnetic dipole source can be introduced as

$$\mathbf{J}_{0M} = -i\omega\boldsymbol{\mu}I(\omega)\mathbf{a}\delta(\mathbf{r}) = \begin{pmatrix} -i\omega I(\omega)\left[\mu_{xx}a_x + \mu_{xy}a_y + \mu_{xz}a_z\right]\delta(\mathbf{r}) \\ -i\omega I(\omega)\left[\mu_{yx}a_x + \mu_{yy}a_y + \mu_{yz}a_z\right]\delta(\mathbf{r}) \\ -i\omega I(\omega)\left[\mu_{zx}a_x + \mu_{zy}a_y + \mu_{zz}a_z\right]\delta(\mathbf{r}) \end{pmatrix}, \tag{5}$$

where possible anisotropic effects have been taken into account.

In planarly stratified media the electromagnetic properties vary in one direction only. Consider a layered medium as depicted in Fig. 2, and assume that the medium properties vary in the z-direction. The Fourier transform pair

$$\phi(k_x, k_y, z, \omega) = \int_{-\infty}^{\infty} dx\, dy\, dt\, \phi(x, y, z, t)\exp\left[-i(k_x x + k_y y - \omega t)\right], \tag{6a}$$

$$\phi(x, y, z, t) = \frac{1}{(2\pi)^3}\int_{-\infty}^{\infty} dk_x\, dk_y\, d\omega\, \phi(k_x, k_y, z, \omega)\exp\left[i(k_x x + k_y y - \omega t)\right], \tag{6b}$$

where k_x and k_y are the wavenumbers in the x- and y-directions, respectively, describe a transformation between the space-time and frequency–wavenumber domains. Eq. (6a) transforms Maxwell's equations in the time domain into the frequency–wavenumber domain and implies the following operations: $\partial_t \to -i\omega$, $\partial_x \to ik_x$, and $\partial_y \to ik_y$. The time and frequency part of eq. (6a) has already been applied in order to obtain eq. (1) from the time-domain Maxwell's equations. In the time domain, the variables in Maxwell's equations are real, whereas in both the frequency and frequency–wavenumber domains the variables might be complex. From Faraday's law (eq. 1c) with source term and Ampère's

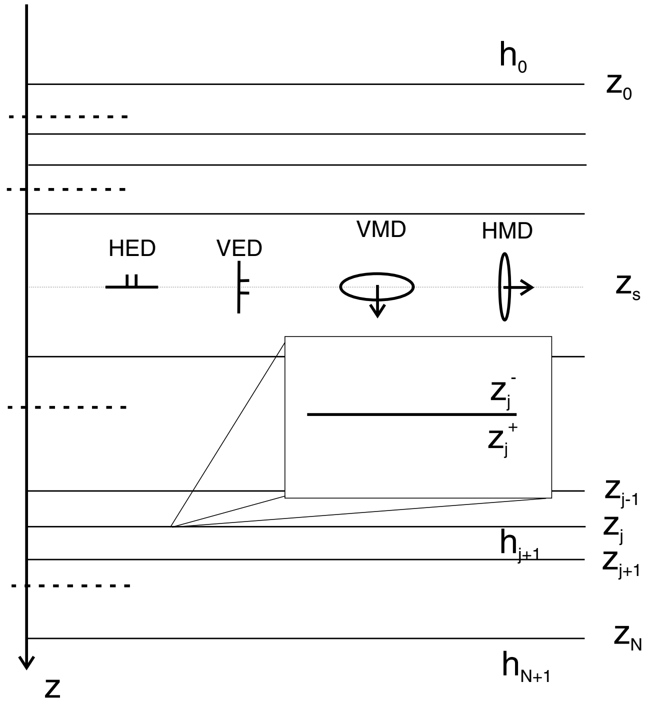

Figure 2. A sketch of the multilayer system. Four types of sources are considered: the horizontal electric dipole (HED), vertical electric dipole (VED), vertical magnetic dipole (VMD), and horizontal magnetic dipole (HMD).

law (eq. 1d), a set of ordinary differential equations are obtained after using the wavenumber part of the transformation in eq. (6a):

$$\frac{dE_x}{dz} = \quad i\omega B_y + ik_x E_z - J_y^M, \tag{7a}$$

$$\frac{dE_y}{dz} = -i\omega B_x + ik_y E_z + J_x^M, \tag{7b}$$

$$-\frac{dH_y}{dz} = -i\omega D_x - ik_y H_z + J_x, \tag{7c}$$

$$\frac{dH_x}{dz} = -i\omega D_y + ik_x H_z + J_y. \tag{7d}$$

The components in the z-direction are related to the horizontal components as

$$D_z = \frac{1}{i\omega}(-ik_x H_y + ik_y H_x + J_z), \tag{8a}$$

$$B_z = \frac{1}{i\omega}\left(ik_x E_y - ik_y E_x + J_z^M\right). \tag{8b}$$

The variables J_n and J_n^M $(n = x, y, z)$ denote the Cartesian components of the frequency–wavenumber domain appearance of the electric and magnetic source, respectively. Likewise the field components E_n, D_n, H_n, and B_n are frequency–wavenumber domain quantities. In order to simplify notation it is convenient to introduce the slowness variables $p_x = k_x/\omega$ and $p_y = k_y/\omega$. With the constitutive relations $D_n = \tilde{\varepsilon}_{nm} E_m$ and $B_n = \mu_{nm} H_m (m = x, y, z)$, the system of equations can be written as

$$\left(\boldsymbol{I}\frac{d}{dz} + i\omega\boldsymbol{A}\right)\boldsymbol{b} = \boldsymbol{\mathcal{L}}\boldsymbol{b} = \boldsymbol{s}, \tag{9}$$

with field vector

$$\boldsymbol{b} = \begin{pmatrix} \boldsymbol{b}_E \\ \boldsymbol{b}_H \end{pmatrix}, \quad \boldsymbol{b}_E = \begin{pmatrix} E_x \\ E_y \end{pmatrix}, \quad \boldsymbol{b}_H = \begin{pmatrix} -H_y \\ H_x \end{pmatrix}, \tag{10}$$

identity matrix $\boldsymbol{I}$, system matrix $\boldsymbol{A}$, and source vector $\boldsymbol{s}$. In addition, the operator $\boldsymbol{\mathcal{L}}$ has been introduced. The system matrix is

$$\boldsymbol{A} = \begin{pmatrix} \boldsymbol{A}_0 & \boldsymbol{A}_1 \\ \boldsymbol{A}_2 & \boldsymbol{A}_3 \end{pmatrix} = \begin{pmatrix} a_{11} & a_{12} & a_{13} & a_{14} \\ a_{21} & a_{22} & a_{23} & a_{24} \\ a_{31} & a_{32} & a_{33} & a_{34} \\ a_{41} & a_{42} & a_{43} & a_{44} \end{pmatrix}, \tag{11}$$

where

$$a_{11} = \frac{\tilde{\varepsilon}_{zx}}{\tilde{\varepsilon}_{zz}} p_x + \frac{\mu_{yz}}{\mu_{zz}} p_y, \qquad a_{12} = \frac{\tilde{\varepsilon}_{zy}}{\tilde{\varepsilon}_{zz}} p_x - \frac{\mu_{yz}}{\mu_{zz}} p_x, \tag{12a}$$

$$a_{13} = \mu_{yy} - \frac{\mu_{yz}\mu_{zy}}{\mu_{zz}} - \frac{p_x^2}{\tilde{\varepsilon}_{zz}}, \qquad a_{14} = -\mu_{yx} + \frac{\mu_{yz}\mu_{zx}}{\mu_{zz}} - \frac{p_x p_y}{\tilde{\varepsilon}_{zz}}, \tag{12b}$$

$$a_{21} = \frac{\tilde{\varepsilon}_{zx}}{\tilde{\varepsilon}_{zz}} p_y - \frac{\mu_{xz}}{\mu_{zz}} p_y, \qquad a_{22} = \frac{\tilde{\varepsilon}_{zy}}{\tilde{\varepsilon}_{zz}} p_y + \frac{\mu_{xz}}{\mu_{zz}} p_x, \tag{12c}$$

$$a_{23} = -\mu_{xy} + \frac{\mu_{xz}\mu_{zy}}{\mu_{zz}} - \frac{p_x p_y}{\tilde{\varepsilon}_{zz}}, \qquad a_{24} = \mu_{xx} - \frac{\mu_{xz}\mu_{zx}}{\mu_{zz}} - \frac{p_y^2}{\tilde{\varepsilon}_{zz}}, \tag{12d}$$

$$a_{31} = \tilde{\varepsilon}_{xx} - \frac{\tilde{\varepsilon}_{xz}\tilde{\varepsilon}_{zx}}{\tilde{\varepsilon}_{zz}} - \frac{p_y^2}{\mu_{zz}}, \qquad a_{32} = \tilde{\varepsilon}_{xy} - \frac{\tilde{\varepsilon}_{xz}\tilde{\varepsilon}_{zy}}{\tilde{\varepsilon}_{zz}} + \frac{p_x p_y}{\mu_{zz}}, \tag{12e}$$

$$a_{33} = \frac{\tilde{\varepsilon}_{xz}}{\tilde{\varepsilon}_{zz}} p_x + \frac{\mu_{zy}}{\mu_{zz}} p_y, \qquad a_{34} = \frac{\tilde{\varepsilon}_{xz}}{\tilde{\varepsilon}_{zz}} p_y - \frac{\mu_{zx}}{\mu_{zz}} p_y, \tag{12f}$$

$$a_{41} = \tilde{\varepsilon}_{yx} - \frac{\tilde{\varepsilon}_{yz}\tilde{\varepsilon}_{zx}}{\tilde{\varepsilon}_{zz}} + \frac{p_x p_y}{\mu_{zz}}, \qquad a_{42} = \tilde{\varepsilon}_{yy} - \frac{\tilde{\varepsilon}_{yz}\tilde{\varepsilon}_{zy}}{\tilde{\varepsilon}_{zz}} - \frac{p_x^2}{\mu_{zz}}, \tag{12g}$$

$$a_{43} = \frac{\tilde{\varepsilon}_{yz}}{\tilde{\varepsilon}_{zz}} p_x - \frac{\mu_{zy}}{\mu_{zz}} p_x, \qquad a_{44} = \frac{\tilde{\varepsilon}_{yz}}{\tilde{\varepsilon}_{zz}} p_y + \frac{\mu_{zx}}{\mu_{zz}} p_x. \tag{12h}$$

In the following it will be assumed that all the material dyads have a set of orthogonal principal axes. Thus the material parameters are symmetric, and because of this reciprocity, 6 of the 16 entries in $\boldsymbol{A}$ are equal:

$$\begin{aligned} a_{23} &= a_{14}, \quad a_{33} = a_{11}, \quad a_{34} = a_{21}, \\ a_{41} &= a_{32}, \quad a_{43} = a_{12}, \quad a_{44} = a_{22}. \end{aligned} \tag{13}$$

This implies that the system matrix is on the form

$$\boldsymbol{A} = \begin{pmatrix} \boldsymbol{A}_0 & \boldsymbol{A}_1 \\ \boldsymbol{A}_2 & \boldsymbol{A}_0^T \end{pmatrix}, \tag{14}$$

with $\boldsymbol{A}_1^T = \boldsymbol{A}_1$ and $\boldsymbol{A}_2^T = \boldsymbol{A}_2$.

The vertical components of the electromagnetic field are given in terms of the horizontal components as

$$E_z = \frac{1}{\tilde{\varepsilon}_{zz}} \left(p_y H_x - p_x H_y - \tilde{\varepsilon}_{zx} E_x - \tilde{\varepsilon}_{zy} E_y + \frac{1}{i\omega} J_z \right), \tag{15a}$$

$$H_z = \frac{1}{\mu_{zz}} \left(- p_y E_x + p_x E_y - \mu_{zx} H_x - \mu_{zy} H_y + \frac{1}{i\omega} J_z^M \right). \tag{15b}$$

The source vector consists of an electric source vector $\boldsymbol{s}_E$ and a magnetic source vector $\boldsymbol{s}_M (\boldsymbol{s} = \boldsymbol{s}_E + \boldsymbol{s}_M)$:

$$\boldsymbol{s}_E = \begin{pmatrix} p_x J_z / \tilde{\varepsilon}_{zz} \\ p_y J_z / \tilde{\varepsilon}_{zz} \\ J_x - \frac{\tilde{\varepsilon}_{xz}}{\tilde{\varepsilon}_{zz}} J_z \\ J_y - \frac{\tilde{\varepsilon}_{yz}}{\tilde{\varepsilon}_{zz}} J_z \end{pmatrix} \quad \text{and} \quad \boldsymbol{s}_M = \begin{pmatrix} -J_y^M + \frac{\mu_{yz}}{\mu_{zz}} J_z^M \\ J_x^M - \frac{\mu_{xz}}{\mu_{zz}} J_z^M \\ -p_y J_z^M / \mu_{zz} \\ p_x J_z^M / \mu_{zz} \end{pmatrix}. \tag{16}$$

The x- and y-components of the electric and magnetic sources will be referred to as the horizontal electric dipole (HED) and horizontal magnetic dipole (HMD). In a plane-layer model the coordinate system may be rotated so that the horizontal component of the electric or magnetic dipoles points in the x-direction, but it is sometimes advantageous to let the HED and HMD have components in both the x- and y-direction. The vertical components of the electric and magnetic dipoles are referred to as the VED and VMD, respectively. In the frequency–wavenumber domain the HED-components are

$$J_x = I(\omega) l_x \delta(z - z_s), \tag{17a}$$

$$J_y = I(\omega) l_y \delta(z - z_s), \tag{17b}$$

where $x_s = y_s = 0$, and the VED-component is

$$J_z = I(\omega) l_z \delta(z - z_s). \tag{17c}$$

The HMD-components become

$$J_x^M = -i\omega I(\omega)(\mu_{xx} a_x + \mu_{xy} a_y + \mu_{xz} a_z)\delta(z - z_s), \tag{17d}$$

$$J_y^M = -i\omega I(\omega)(\mu_{yx} a_x + \mu_{yy} a_y + \mu_{yz} a_z)\delta(z - z_s), \tag{17e}$$

and the VMD-component is

$$J_z^M = -i\omega I(\omega)(\mu_{zx} a_x + \mu_{zy} a_y + \mu_{zz} a_z)\delta(z - z_s). \tag{17f}$$

The infinitesimal or Hertzian dipoles are good approximations for any physical dipole source with finite length or size when the wavelength of the radiated signal, or distances at which the fields are considered, are larger than the dimensions of the dipole (length of the electric dipole and diameter of the magnetic dipole).

3 SYMMETRY RELATIONS AND ENERGY FLUX

From eq. (14) it can be seen that $\boldsymbol{A}$ has a symplectic symmetry (Goldstein 1980; Chapman 1994) which can be exploited in order to find invariants and reciprocity relations. Consider eq. (9) in source free regions ($\boldsymbol{\mathcal{L}b} = \mathbf{0}$). Introduce an operator $\tilde{\boldsymbol{\mathcal{L}}}$ in order to construct a new set of equations for a field vector $\tilde{\boldsymbol{b}}$:

$$\tilde{\boldsymbol{\mathcal{L}}}\tilde{\boldsymbol{b}} = \left(\boldsymbol{I}\frac{d}{dz} - i\omega\boldsymbol{A}\right)\tilde{\boldsymbol{b}} = \mathbf{0}. \tag{18}$$

By using the property $\boldsymbol{KA} = (\boldsymbol{KA})^T$ with

$$\boldsymbol{K} = \boldsymbol{K}^{-1} = \boldsymbol{K}^T = \begin{pmatrix} \mathbf{0} & \boldsymbol{I} \\ \boldsymbol{I} & \mathbf{0} \end{pmatrix}, \tag{19}$$

one obtains the invariant

$$\frac{d}{dz}(\tilde{\boldsymbol{b}}^T\boldsymbol{Kb}) = 0. \tag{20}$$

The time averaged Poynting vector in the z-direction is $\langle S_z \rangle = \frac{1}{2}\mathrm{Re}(\mathbf{E} \times \mathbf{H}^*)_z$ which can be written as:

$$\langle S_z \rangle = \frac{1}{4}\left(E_x H_y^* - E_y H_x^* + E_x^* H_y - E_y^* H_x\right) = -\frac{1}{4}\boldsymbol{b}^\dagger\boldsymbol{Kb}. \tag{21}$$

The superscript † denotes complex conjugate transpose. In *lossless* media $\boldsymbol{A}$ is real, and from eq. (9) and (18) it can be seen that $\tilde{\boldsymbol{b}} = \boldsymbol{b}^*$ *in this case*. The consequence is that $\tilde{\boldsymbol{b}}^T\boldsymbol{Kb} = -4\langle S_z \rangle$ meaning that the time averaged energy flux in the z-direction is constant for lossless media.

Next, introduce an operator $\bar{\boldsymbol{\mathcal{L}}}$ which is obtained from $\boldsymbol{\mathcal{L}}$ by reversing the directions of the horizontal slowness components $p_x, p_y \to -p_x, -p_y$. The set of equations for the field vector $\bar{\boldsymbol{b}}$ is then:

$$\bar{\boldsymbol{\mathcal{L}}}\bar{\boldsymbol{b}} = \left(\boldsymbol{I}\frac{d}{dz} + i\omega\boldsymbol{A}'\right)\bar{\boldsymbol{b}} = \mathbf{0}, \tag{22}$$

where $\boldsymbol{A}'$ is obtained from $\boldsymbol{A}$ by changing the signs of $\boldsymbol{A}_0$ and $\boldsymbol{A}_0^T$:

$$\boldsymbol{A}' = \begin{pmatrix} -\boldsymbol{A}_0 & \boldsymbol{A}_1 \\ \boldsymbol{A}_2 & -\boldsymbol{A}_0^T \end{pmatrix}. \tag{23}$$

By using that $(\boldsymbol{K}'\,\boldsymbol{A}')^T = \boldsymbol{K}'\,\boldsymbol{A}$ where

$$\boldsymbol{K}' = -\boldsymbol{K}'^{-1} = -\boldsymbol{K}'^T = \begin{pmatrix} \mathbf{0} & \boldsymbol{I} \\ -\boldsymbol{I} & \mathbf{0} \end{pmatrix}, \tag{24}$$

one obtains the invariant

$$\frac{d}{dz}\left(\bar{\boldsymbol{b}}^T\boldsymbol{K}'\boldsymbol{b}\right) = 0. \tag{25}$$

4 DECOMPOSITION INTO UPGOING AND DOWNGOING FIELDS

The system matrix $\boldsymbol{A}$ is diagonalizable when there is a set of four linearly independent eigenvectors of $\boldsymbol{A}$ (Horn & Johnson 1985). Then the similarity transformation

$$\boldsymbol{AN} = \boldsymbol{N\Lambda}, \tag{26}$$

where the eigenvector-matrix $\boldsymbol{N}$ is formed by the set of eigenvectors as columns, implies that the diagonal matrix $\boldsymbol{\Lambda}$ contains the four eigenvalues of $\boldsymbol{A}$ along its diagonal. By using eq. (26), the differential eq. (9) can be written as

$$\frac{d\boldsymbol{w}}{dz} = -i\omega\boldsymbol{\Lambda w} - \boldsymbol{N}^{-1}\frac{d\boldsymbol{N}}{dz}\boldsymbol{w} + \boldsymbol{N}^{-1}\boldsymbol{s}, \tag{27}$$

where the physical field vector $\boldsymbol{b}$ has been transformed into a mode-field vector $\boldsymbol{w}$:

$$\boldsymbol{b} = \boldsymbol{Nw} \quad \text{and} \quad \boldsymbol{w} = \boldsymbol{N}^{-1}\boldsymbol{b} = \begin{pmatrix} \boldsymbol{u} \\ \boldsymbol{d} \end{pmatrix}. \tag{28}$$

Since $\boldsymbol{\Lambda}$ is diagonal, the solution of eq. (27) in a source free and homogeneous region

$$\boldsymbol{w}(z) = \exp\left[-i\omega\boldsymbol{\Lambda}(z - z_0)\right]\boldsymbol{w}_0(z_0), \tag{29}$$

reveals that the mode-field vector $\boldsymbol{w}$ consists of upgoing ($\boldsymbol{u}$) and downgoing ($\boldsymbol{d}$) field constituents. Thus the eigenvalues of $\boldsymbol{A}$ are the vertical slownesses and it is convenient to write $\boldsymbol{\Lambda}$ as

$$\boldsymbol{\Lambda} = \begin{pmatrix} \acute{\mathbf{p}}_{\mathbf{z}} & \mathbf{0} \\ \mathbf{0} & -\grave{\mathbf{p}}_{\mathbf{z}} \end{pmatrix} = \mathrm{diag}\{p_{z\mathrm{I}}, p_{z\mathrm{II}}, p_{z\mathrm{III}}, p_{z\mathrm{IV}}\}, \tag{30}$$

where $\acute{\mathbf{p}}_{\mathbf{z}} = \mathrm{diag}\{p_{z\mathrm{I}}, p_{z\mathrm{II}}\}$ and $\grave{\mathbf{p}}_{\mathbf{z}} = \mathrm{diag}\{-p_{z\mathrm{III}}, -p_{z\mathrm{IV}}\}$. The two eigenvalues in $\acute{\mathbf{p}}_{\mathbf{z}}$ are related to the upgoing field, and the two eigenvalues in $\grave{\mathbf{p}}_{\mathbf{z}}$ are related to the downgoing field.

Since it will simplify many derivations and relations at later stages, the eigenvector-matrix $\boldsymbol{N}$ and its inverse should be normalized with respect to vertical energy flux. In order to achieve this, consider source free and homogeneous media and use the invariant in eq. (20). A decomposition of the ad hoc field vector $\tilde{\boldsymbol{b}}$ into $\tilde{\boldsymbol{b}} = \tilde{\boldsymbol{N}}\tilde{\boldsymbol{w}}$ then leads to

$$\frac{d\tilde{\boldsymbol{w}}}{dz} = i\omega\tilde{\boldsymbol{\Lambda}}\tilde{\boldsymbol{w}}, \tag{31}$$

by using the similarity transform

$$\boldsymbol{A}\tilde{\boldsymbol{N}} = \tilde{\boldsymbol{N}}\tilde{\boldsymbol{\Lambda}}. \tag{32}$$

Now $\tilde{\boldsymbol{\Lambda}}$ must contain the same eigenvalues as $\boldsymbol{\Lambda}$. From

$$\tilde{\boldsymbol{\Lambda}} = \begin{pmatrix} -\grave{\mathbf{p}}_{\mathbf{z}} & \mathbf{0} \\ \mathbf{0} & \acute{\mathbf{p}}_{\mathbf{z}} \end{pmatrix}, \tag{33}$$

the invariant

$$\frac{d}{dz}\left(\tilde{\boldsymbol{w}}^T \boldsymbol{K}\boldsymbol{w}\right) = 0 \tag{34}$$

is obtained by using that $\boldsymbol{K}\tilde{\boldsymbol{\Lambda}} = \boldsymbol{K}\boldsymbol{\Lambda}$. In order for $\boldsymbol{N}$ to be energy normalized, the following relation must hold:

$$\tilde{\boldsymbol{w}}^T \boldsymbol{K}\boldsymbol{w} = \tilde{\boldsymbol{b}}^T \boldsymbol{K}\boldsymbol{b}. \tag{35}$$

By using that $\boldsymbol{b} = \boldsymbol{N}\boldsymbol{w}$ and $\tilde{\boldsymbol{b}} = \tilde{\boldsymbol{N}}\tilde{\boldsymbol{w}}$ this means that

$$\tilde{\boldsymbol{N}}^T \boldsymbol{K}\boldsymbol{N} = \boldsymbol{K}. \tag{36}$$

A relation between $\tilde{\boldsymbol{N}}$ and $\boldsymbol{N}$ can now be obtained by multiplying eq. (26) by $\boldsymbol{K}'$ from the right and using that $\boldsymbol{\Lambda}\boldsymbol{K}' = \boldsymbol{K}'\tilde{\boldsymbol{\Lambda}}$. This leads to $\boldsymbol{A}\boldsymbol{N}\boldsymbol{K}' = \boldsymbol{N}\boldsymbol{K}'\tilde{\boldsymbol{\Lambda}}$ which is consistent with eq. (32) if $\tilde{\boldsymbol{N}} = \boldsymbol{N}\boldsymbol{K}'$. The latter result combined with eq. (36) yields

$$\boldsymbol{N}^{-1} = \boldsymbol{J}\boldsymbol{N}^T\boldsymbol{K}, \tag{37}$$

where

$$\boldsymbol{J} = \boldsymbol{J}^{-1} = \boldsymbol{J}^T = \begin{pmatrix} \boldsymbol{I} & \mathbf{0} \\ \mathbf{0} & -\boldsymbol{I} \end{pmatrix}. \tag{38}$$

The choice of sign in the derivation of $\tilde{\boldsymbol{N}} = \boldsymbol{N}\boldsymbol{K}'$ is justified by considering the lossless case. The energy contained in the mode-field in the vertical direction for lossless media is:

$$\langle S_z \rangle = \frac{1}{4}\left(\boldsymbol{d}^\dagger\boldsymbol{d} - \boldsymbol{u}^\dagger\boldsymbol{u}\right) = -\frac{1}{4}\boldsymbol{w}^\dagger\boldsymbol{J}\boldsymbol{w}. \tag{39}$$

Eq. (39) must be equal to the energy expression in eq. (21). This yields eq. (37) in the lossless case by using that the energy-normalized eigenvector matrix in the lossless medium is real.

The eigenvector-matrix $\boldsymbol{N}$ can be written in terms of submatrices as

$$\boldsymbol{N} = \frac{1}{\sqrt{2}}\begin{pmatrix} \acute{\boldsymbol{N}}_E & \grave{\boldsymbol{N}}_E \\ \acute{\boldsymbol{N}}_H & -\grave{\boldsymbol{N}}_H \end{pmatrix}. \tag{40a}$$

Eq. (37) then implies that the inverse eigenvector matrix is given in terms of the submatrices transposed:

$$\boldsymbol{N}^{-1} = \frac{1}{\sqrt{2}}\begin{pmatrix} \acute{\boldsymbol{N}}_H^T & \acute{\boldsymbol{N}}_E^T \\ \grave{\boldsymbol{N}}_H^T & -\grave{\boldsymbol{N}}_E^T \end{pmatrix}, \tag{40b}$$

which means that the electromagnetic energy in the field vector $\boldsymbol{b}$ is preserved within the mode-field vector $\boldsymbol{w}$ after the transformation $\boldsymbol{w} = \boldsymbol{N}^{-1}\boldsymbol{b}$.

5 PROPAGATION OF UPGOING AND DOWNGOING FIELDS

The mode-field vector $\boldsymbol{w}$ can be used to describe propagation of electromagnetic fields in homogeneous regions, across interfaces, and in a system of layers. Now, represent propagation of $\boldsymbol{w}$ downwards in the positive z-direction in terms of the propagator $\grave{\boldsymbol{Q}}$, and propagation upwards in the negative z-direction by $\acute{\boldsymbol{Q}}$. Since the z-axis is pointing downwards, this means that if $z > z_0$:

$$\boldsymbol{w}(z) = \grave{\boldsymbol{Q}}(z, z_0)\boldsymbol{w}(z_0), \tag{41a}$$

$$\boldsymbol{w}(z_0) = \acute{\boldsymbol{Q}}(z_0, z)\boldsymbol{w}(z). \tag{41b}$$

The relation between a propagator and its inverse is thus

$$\acute{\boldsymbol{Q}}(z_0, z) = \grave{\boldsymbol{Q}}^{-1}(z, z_0). \tag{42}$$

5.1 Source-free homogeneous regions

In a source-free homogeneous region, eq. (27) simplifies to $d\boldsymbol{w}/dz = -i\omega\boldsymbol{\Lambda}\boldsymbol{w}$ with solution $\boldsymbol{w}(z) = \exp[-i\omega\boldsymbol{\Lambda}\,(z - z_0)]\ \boldsymbol{w}_0(z_0)$. Thus propagation downwards within a homogeneous region from z_0 to z is described in terms of the propagator matrix $\grave{\boldsymbol{Q}}$ in eq. (41a) where

$$\grave{\boldsymbol{Q}}(z, z_0) = \begin{pmatrix} \mathrm{e}^{-i\omega\acute{\mathbf{p}}_{\mathbf{z}}(z-z_0)} & \mathbf{0} \\ \mathbf{0} & \mathrm{e}^{i\omega\grave{\mathbf{p}}_{\mathbf{z}}(z-z_0)} \end{pmatrix}. \tag{43}$$

The propagation upwards is related to the propagation downwards as described in eq. (42).

5.2 Propagation across a source

A *point source* causes a discontinuity in the mode-field vector $\boldsymbol{w}$. The transformation of the source in eq. (27) is denoted as

$$\boldsymbol{\Sigma} = \boldsymbol{N}^{-1}\boldsymbol{s}. \tag{44}$$

Propagation across a source can be described by

$$\boldsymbol{w}(z_s^+) = \boldsymbol{\Sigma}(z_s) + \boldsymbol{w}(z_s^-), \tag{45}$$

where z_s denotes the source position and z_s^- and z_s^+ are the positions just above and just below the source, respectively. The mode-domain source can furthermore be written as $\boldsymbol{\Sigma} = (\acute{\boldsymbol{\Sigma}}^T\ \ \grave{\boldsymbol{\Sigma}}^T)^T$, where $\acute{\Sigma}$ describes the upgoing radiation and $\grave{\Sigma}$ describes the downgoing radiation.

5.3 Propagation in continuously varying media

In eq. (27) the term that contains the derivative of the eigenvector matrix describes possible medium variations. In homogeneous regions this term is zero, and the medium-variations are discretized into piecewise homogeneous regions which are connected by applying the appropriate boundary conditions. In several occasions it can be useful to consider medium variations by using the entire differential eq. (27). Write the product of $\boldsymbol{N}^{-1}$ and the derivative of $\boldsymbol{N}$ as:

$$\boldsymbol{N}^{-1}\frac{d\boldsymbol{N}}{dz} = -\begin{pmatrix} \acute{\boldsymbol{F}} & \hat{\boldsymbol{G}} \\ \check{\boldsymbol{G}} & \grave{\boldsymbol{F}} \end{pmatrix}, \tag{46}$$

where

$$\acute{\boldsymbol{F}} = -\frac{1}{2}\left(\acute{\boldsymbol{N}}_H^T\frac{d\acute{\boldsymbol{N}}_E}{dz} + \acute{\boldsymbol{N}}_E^T\frac{d\acute{\boldsymbol{N}}_H}{dz}\right), \tag{47a}$$

$$\grave{\boldsymbol{F}} = -\frac{1}{2}\left(\grave{\boldsymbol{N}}_H^T\frac{d\grave{\boldsymbol{N}}_E}{dz} + \grave{\boldsymbol{N}}_E^T\frac{d\grave{\boldsymbol{N}}_H}{dz}\right), \tag{47b}$$

$$\hat{\boldsymbol{G}} = -\frac{1}{2}\left(\acute{\boldsymbol{N}}_H^T\frac{d\grave{\boldsymbol{N}}_E}{dz} - \acute{\boldsymbol{N}}_E^T\frac{d\grave{\boldsymbol{N}}_H}{dz}\right), \tag{47c}$$

$$\check{\boldsymbol{G}} = -\frac{1}{2}\left(\grave{\boldsymbol{N}}_H^T\frac{d\acute{\boldsymbol{N}}_E}{dz} - \grave{\boldsymbol{N}}_E^T\frac{d\acute{\boldsymbol{N}}_H}{dz}\right). \tag{47d}$$

Then eq. (27) in terms of the upgoing and downgoing fields can be written as

$$\frac{d\boldsymbol{u}}{dz} = -i\omega\acute{\mathbf{p}}_{\mathbf{z}}\boldsymbol{u} + \acute{\boldsymbol{F}}\boldsymbol{u} + \hat{\boldsymbol{G}}\boldsymbol{d} + \acute{\Sigma}, \tag{48a}$$

$$\frac{d\boldsymbol{d}}{dz} = \ \ i\omega\grave{\mathbf{p}}_{\mathbf{z}}\boldsymbol{d} + \grave{\boldsymbol{F}}\boldsymbol{d} + \check{\boldsymbol{G}}\boldsymbol{u} + \grave{\Sigma}. \tag{48b}$$

Considerations of the symmetries in $\boldsymbol{N}$ and $\boldsymbol{N}^{-1}$ lead to $\hat{\boldsymbol{G}} = \check{\boldsymbol{G}}^T$, $\acute{\boldsymbol{F}} = -\acute{\boldsymbol{F}}^T$, and $\grave{\boldsymbol{F}} = -\grave{\boldsymbol{F}}^T$. Thus,

$$\acute{\boldsymbol{F}} = \begin{pmatrix} 0 & \acute{f}_{12} \\ -\acute{f}_{12} & 0 \end{pmatrix} \quad \text{and} \quad \grave{\boldsymbol{F}} = \begin{pmatrix} 0 & \grave{f}_{12} \\ -\grave{f}_{12} & 0 \end{pmatrix}. \tag{49}$$

These relations are useful e.g. when considering slow and continuous medium variations in for instance the WKB-approximation, and in the calculation of approximate expressions for the reflection and transmission matrices at interfaces with weak contrasts as will be shown in the next section.

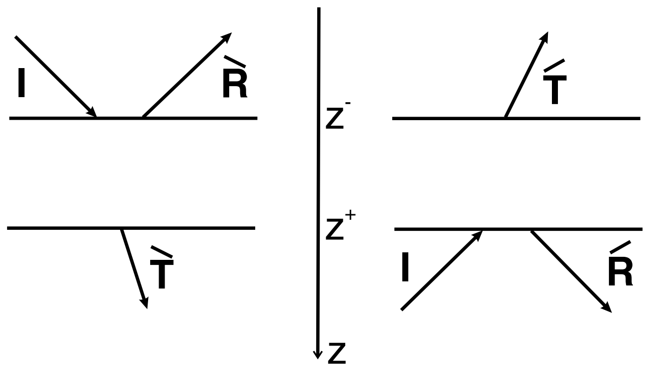

Figure 3. Reflection and transmission for an upgoing and downgoing incident plane-wave through a stack of layers.

6 REFLECTION AND TRANSMISSION RESPONSES

Fig. 3 describes reflection and transmission of a unit incident field in a region between the coordinates z^- and z^+. This region might contain an arbitrary number of layers or just a single interface. The reflection and transmission at an interface when propagating downwards in the positive z-direction can be written in terms of a propagator matrix $\grave{\boldsymbol{Q}}(z^+, z^-)$:

$$\begin{pmatrix} \boldsymbol{0} \\ \grave{\boldsymbol{T}} \end{pmatrix} = \begin{pmatrix} \grave{\boldsymbol{Q}}_{11} & \grave{\boldsymbol{Q}}_{12} \\ \grave{\boldsymbol{Q}}_{21} & \grave{\boldsymbol{Q}}_{22} \end{pmatrix} \begin{pmatrix} \grave{\boldsymbol{R}} \\ \boldsymbol{I} \end{pmatrix} \quad \text{and} \quad \begin{pmatrix} \boldsymbol{I} \\ \acute{\boldsymbol{R}} \end{pmatrix} = \begin{pmatrix} \grave{\boldsymbol{Q}}_{11} & \grave{\boldsymbol{Q}}_{12} \\ \grave{\boldsymbol{Q}}_{21} & \grave{\boldsymbol{Q}}_{22} \end{pmatrix} \begin{pmatrix} \acute{\boldsymbol{T}} \\ \boldsymbol{0} \end{pmatrix}, \tag{50}$$

where $\grave{\boldsymbol{R}}$ and $\grave{\boldsymbol{T}}$ denote reflection and transmission of a downgoing field, and $\acute{\boldsymbol{R}}$ and $\acute{\boldsymbol{T}}$ denote reflection and transmission of an upgoing field. The reflection and transmission coefficients can be written in terms of the elements of $\grave{\boldsymbol{Q}}$:

$$\acute{\boldsymbol{T}} = \grave{\boldsymbol{Q}}_{11}^{-1}, \tag{51a}$$

$$\acute{\boldsymbol{R}} = \grave{\boldsymbol{Q}}_{21} \grave{\boldsymbol{Q}}_{11}^{-1}, \tag{51b}$$

$$\grave{\boldsymbol{R}} = -\grave{\boldsymbol{Q}}_{11}^{-1} \grave{\boldsymbol{Q}}_{12}, \tag{51c}$$

$$\grave{\boldsymbol{T}} = \grave{\boldsymbol{Q}}_{22} - \grave{\boldsymbol{Q}}_{21} \grave{\boldsymbol{Q}}_{11}^{-1} \grave{\boldsymbol{Q}}_{12}. \tag{51d}$$

When propagating upwards in the negative z-direction, the relation between the incoming reflected and transmitted fields in terms of the propagator $\acute{\boldsymbol{Q}}(z^-, z^+)$ is:

$$\begin{pmatrix} \grave{\boldsymbol{R}} \\ \boldsymbol{I} \end{pmatrix} = \begin{pmatrix} \acute{\boldsymbol{Q}}_{11} & \acute{\boldsymbol{Q}}_{12} \\ \acute{\boldsymbol{Q}}_{21} & \acute{\boldsymbol{Q}}_{22} \end{pmatrix} \begin{pmatrix} \boldsymbol{0} \\ \grave{\boldsymbol{T}} \end{pmatrix} \quad \text{and} \quad \begin{pmatrix} \acute{\boldsymbol{T}} \\ \boldsymbol{0} \end{pmatrix} = \begin{pmatrix} \acute{\boldsymbol{Q}}_{11} & \acute{\boldsymbol{Q}}_{12} \\ \acute{\boldsymbol{Q}}_{21} & \acute{\boldsymbol{Q}}_{22} \end{pmatrix} \begin{pmatrix} \boldsymbol{I} \\ \acute{\boldsymbol{R}} \end{pmatrix}, \tag{52}$$

and in terms of $\acute{\boldsymbol{Q}}$, the reflection and transmission coefficients are:

$$\grave{\boldsymbol{T}} = \acute{\boldsymbol{Q}}_{22}^{-1}, \tag{53a}$$

$$\grave{\boldsymbol{R}} = \acute{\boldsymbol{Q}}_{12} \acute{\boldsymbol{Q}}_{22}^{-1}, \tag{53b}$$

$$\acute{\boldsymbol{R}} = -\acute{\boldsymbol{Q}}_{22}^{-1} \acute{\boldsymbol{Q}}_{21}, \tag{53c}$$

$$\acute{\boldsymbol{T}} = \acute{\boldsymbol{Q}}_{11} - \acute{\boldsymbol{Q}}_{12} \acute{\boldsymbol{Q}}_{22}^{-1} \acute{\boldsymbol{Q}}_{21}. \tag{53d}$$

The propagators written in terms of the reflection and transmission coefficients become

$$\grave{\boldsymbol{Q}}(z^+, z^-) = \begin{pmatrix} \acute{\boldsymbol{T}}^{-1} & -\acute{\boldsymbol{T}}^{-1} \grave{\boldsymbol{R}} \\ \acute{\boldsymbol{R}} \acute{\boldsymbol{T}}^{-1} & \grave{\boldsymbol{T}} - \acute{\boldsymbol{R}} \acute{\boldsymbol{T}}^{-1} \grave{\boldsymbol{R}} \end{pmatrix}, \tag{54a}$$

$$\acute{\boldsymbol{Q}}(z^-, z^+) = \begin{pmatrix} \acute{\boldsymbol{T}} - \grave{\boldsymbol{R}} \grave{\boldsymbol{T}}^{-1} \acute{\boldsymbol{R}} & \grave{\boldsymbol{R}} \grave{\boldsymbol{T}}^{-1} \\ -\grave{\boldsymbol{T}}^{-1} \acute{\boldsymbol{R}} & \grave{\boldsymbol{T}}^{-1} \end{pmatrix}, \tag{54b}$$

where $\grave{\boldsymbol{Q}}(z^+, z^-) = \acute{\boldsymbol{Q}}^{-1}(z^-, z^+)$.

6.1 Reciprocity relations

Consider the field-vector $\bar{\boldsymbol{b}}$ in eq. (22). In this system the direction of the slowness vectors are reversed. Thus, the similarity transform of the system matrix $\boldsymbol{A}'$ becomes

$$\boldsymbol{A}'\bar{\boldsymbol{N}} = -\bar{\boldsymbol{N}}\boldsymbol{\Lambda}. \tag{55}$$

By using the diagonal matrix $\boldsymbol{J}$ from eq. (38), the relationship $\boldsymbol{A}'\,\boldsymbol{J} + \boldsymbol{J}\boldsymbol{A} = \boldsymbol{0}$ is obtained. Using this property and comparing the expressions in eqs (55) and eq. (26), gives that $\bar{\boldsymbol{N}} = \boldsymbol{J}\boldsymbol{N}$. Inserted into eq. (37) this means that

$$\bar{\boldsymbol{N}}^T \boldsymbol{K}' \boldsymbol{N} = \boldsymbol{J}. \tag{56}$$

Eq. (25) with the mode-field transformations ($\bar{\boldsymbol{w}} = \bar{\boldsymbol{N}}\bar{\boldsymbol{b}}$ and $\boldsymbol{w} = \boldsymbol{N}\boldsymbol{b}$) and eq. (56) now lead to

$$\bar{\boldsymbol{w}}^T \boldsymbol{J}\boldsymbol{w} = \text{constant}. \tag{57}$$

Consider the preservation of the quantity in eq. (57) between e.g. the interfaces z^- and z^+ (propagation upwards *cf.* eq. 52). For simplicity a matrix where the left column represents the mode-field vector with incidence from above (left side of Fig. 3) and the right column represents the mode-field with incidence from below (right side of Fig. 3) can be formed. Then eq. (57) leads to

$$\begin{pmatrix} \boldsymbol{I} & \grave{\boldsymbol{R}}'^T \\ \boldsymbol{0} & \acute{\boldsymbol{T}}'^T \end{pmatrix} \boldsymbol{J} \begin{pmatrix} \grave{\boldsymbol{R}} & \acute{\boldsymbol{T}} \\ \boldsymbol{I} & \boldsymbol{0} \end{pmatrix} = \begin{pmatrix} \grave{\boldsymbol{T}}'^T & \boldsymbol{0} \\ \acute{\boldsymbol{R}}'^T & \boldsymbol{I} \end{pmatrix} \boldsymbol{J} \begin{pmatrix} \boldsymbol{0} & \boldsymbol{I} \\ \grave{\boldsymbol{T}} & \acute{\boldsymbol{R}} \end{pmatrix}, \tag{58}$$

where the reflection and transmission in the slowness-reversed system are denoted $\boldsymbol{R}'$ and $\boldsymbol{T}'$, respectively. The upgoing and downgoing incident, reflected, and transmitted fields have furthermore been swapped for the slowness reversed mode-field since there is a reversal of the propagation direction in this system. This also implies that the reflection and transmission coefficients have opposite signs for the horizontal slowness parameters in the slowness reversed and 'normal' systems. Thus the following reciprocity relations for the transmission and reflection coefficients become evident:

$$\grave{\boldsymbol{R}}(p_x, p_y) = \grave{\boldsymbol{R}}^T(-p_x, -p_y), \tag{59a}$$

$$\acute{\boldsymbol{R}}(p_x, p_y) = \acute{\boldsymbol{R}}^T(-p_x, -p_y), \tag{59b}$$

$$\grave{\boldsymbol{T}}(p_x, p_y) = \acute{\boldsymbol{T}}^T(-p_x, -p_y). \tag{59c}$$

These expressions are equivalent to the expressions found in Chapman (1994) for elastic anisotropic media.

6.2 Reflection and transmission at a single interface

Explicit expressions for the reflection and transmission coefficients at a single interface can be derived by using the boundary conditions. The horizontal electromagnetic field components represented by $\boldsymbol{b} = \boldsymbol{N}\boldsymbol{w}$ are continuous across an interface which leads to $\boldsymbol{N}(z_j^-)\,\boldsymbol{w}(z_j^-) = \boldsymbol{N}(z_j^+)\,\boldsymbol{w}(z_j^+)$, where z_j^- and z_j^+ are the z-coordinates on each side of the interface at z_j as illustrated in Fig. 2. Thus, the propagators across the interface become

$$\acute{\boldsymbol{Q}}(z_j^-, z_j^+) = \boldsymbol{N}^{-1}(z_j^-)\boldsymbol{N}(z_j^+) \quad \text{and} \quad \grave{\boldsymbol{Q}}(z_j^+, z_j^-) = \boldsymbol{N}^{-1}(z_j^+)\boldsymbol{N}(z_j^-). \tag{60}$$

In order to derive the 2×2 reflection and transmission matrices at an interface, it is convenient to introduce the matrices

$$\acute{\boldsymbol{C}} = \left[\acute{\boldsymbol{N}}_H^-\right]^T \acute{\boldsymbol{N}}_E^+, \qquad \acute{\boldsymbol{D}} = \left[\acute{\boldsymbol{N}}_E^-\right]^T \acute{\boldsymbol{N}}_H^+, \tag{61a}$$

$$\hat{\boldsymbol{C}} = \left[\acute{\boldsymbol{N}}_H^-\right]^T \grave{\boldsymbol{N}}_E^+, \qquad \hat{\boldsymbol{D}} = \left[\acute{\boldsymbol{N}}_E^-\right]^T \grave{\boldsymbol{N}}_H^+, \tag{61b}$$

$$\check{\boldsymbol{C}} = \left[\grave{\boldsymbol{N}}_H^-\right]^T \acute{\boldsymbol{N}}_E^+, \qquad \check{\boldsymbol{D}} = \left[\grave{\boldsymbol{N}}_E^-\right]^T \acute{\boldsymbol{N}}_H^+, \tag{61c}$$

$$\grave{\boldsymbol{C}} = \left[\grave{\boldsymbol{N}}_H^-\right]^T \grave{\boldsymbol{N}}_E^+, \qquad \grave{\boldsymbol{D}} = \left[\grave{\boldsymbol{N}}_E^-\right]^T \grave{\boldsymbol{N}}_H^+, \tag{61d}$$

where the superscripts '$-$' and '$+$' denote eigenvector matrices in the upper and lower homogeneous regions, respectively. The propagators in both directions across the interface can now be written (using equations 60 and 40) as:

$$\acute{\boldsymbol{Q}} = \frac{1}{2}\begin{pmatrix} \acute{\boldsymbol{C}} + \acute{\boldsymbol{D}} & \hat{\boldsymbol{C}} - \hat{\boldsymbol{D}} \\ \check{\boldsymbol{C}} - \check{\boldsymbol{D}} & \grave{\boldsymbol{C}} + \grave{\boldsymbol{D}} \end{pmatrix} \quad \text{and} \quad \grave{\boldsymbol{Q}} = \frac{1}{2}\begin{pmatrix} \acute{\boldsymbol{D}}^T + \acute{\boldsymbol{C}}^T & \check{\boldsymbol{D}}^T - \check{\boldsymbol{C}}^T \\ \hat{\boldsymbol{D}}^T - \hat{\boldsymbol{C}}^T & \grave{\boldsymbol{D}}^T + \grave{\boldsymbol{C}}^T \end{pmatrix}. \tag{62}$$

The propagator elements are related to the reflection and transmission coefficients as described in eqs (51) and (53), and from this the reflection and transmission matrices can be derived in terms of the $\boldsymbol{C}$ and $\boldsymbol{D}$ matrices:

$$\acute{\boldsymbol{t}} = 2\left(\acute{\boldsymbol{C}} + \acute{\boldsymbol{D}}\right)^{-T}, \tag{63a}$$

$$\acute{\boldsymbol{r}} = -\left(\hat{\boldsymbol{C}} - \hat{\boldsymbol{D}}\right)^T \left(\acute{\boldsymbol{C}} + \acute{\boldsymbol{D}}\right)^{-T} = -\left(\grave{\boldsymbol{C}} + \grave{\boldsymbol{D}}\right)^{-1}\left(\check{\boldsymbol{C}} - \check{\boldsymbol{D}}\right), \tag{63b}$$

$$\grave{\boldsymbol{r}} = \left(\hat{\boldsymbol{C}} - \hat{\boldsymbol{D}}\right)\left(\grave{\boldsymbol{C}} + \grave{\boldsymbol{D}}\right)^{-1} = \left(\acute{\boldsymbol{C}} + \acute{\boldsymbol{D}}\right)^{-T}\left(\check{\boldsymbol{C}} - \check{\boldsymbol{D}}\right)^{T}, \tag{63c}$$

$$\grave{\boldsymbol{t}} = 2\left(\grave{\boldsymbol{C}} + \grave{\boldsymbol{D}}\right)^{-1}. \tag{63d}$$

Note the use of small boldface letters to denote reflection $\boldsymbol{r}$ and transmission $\boldsymbol{t}$ from a *single* interface.

6.3 Single interface weak contrast approximation

In case of weak contrasts at an interface, eq. (48) can be used to derive approximate expressions for the reflection and transmission matrices in terms of $\boldsymbol{F}$ and $\boldsymbol{G}$ as in Ursin & Stovas (2002) and Stovas & Ursin (2003). In a source-free region a Taylor expansion of $\boldsymbol{u}$ leads to

$$\boldsymbol{u}(z - \Delta z) \approx \boldsymbol{u}(z) - \frac{d\boldsymbol{u}}{dz}\Delta z = (\boldsymbol{I} + i\omega\acute{\mathbf{p}}_{\mathbf{z}}\Delta z - \acute{\boldsymbol{F}}\Delta z)\boldsymbol{u}(z) - \hat{\boldsymbol{G}}\boldsymbol{d}(z). \tag{64}$$

When $\Delta z \to 0$ this becomes

$$\boldsymbol{u}^{\text{out}} = (\boldsymbol{I} - \acute{\boldsymbol{\mathcal{F}}})\boldsymbol{u}^{\text{in}} - \hat{\boldsymbol{\mathcal{G}}}\boldsymbol{d}^{\text{in}}, \tag{65}$$

where $\boldsymbol{u}^{\text{out}}$ is the resulting upgoing field after transmission of $\boldsymbol{u}^{\text{in}}$ and reflection of $\boldsymbol{d}^{\text{in}}$. The propagation is in the negative z-direction and $\boldsymbol{u}^{\text{out}}$ and $\boldsymbol{d}^{\text{in}}$ are on the upper side of the interface (z_j^-) whereas $\boldsymbol{u}^{\text{in}}$ is on the lower side (z_j^+). The matrices $\boldsymbol{\mathcal{F}}$ and $\boldsymbol{\mathcal{G}}$ refer to $\boldsymbol{F}$ and $\boldsymbol{G}$ with the derivatives replaced by the discontinuity in the parameters, and the parameters replaced by their average values. A Taylor expansion for $\boldsymbol{d}$ leads to

$$\boldsymbol{d}(z + \Delta z) \approx \boldsymbol{d}(z) + \frac{d\boldsymbol{d}}{dz}\Delta z = (\boldsymbol{I} + i\omega\grave{\mathbf{p}}_{\mathbf{z}}\Delta z + \grave{\boldsymbol{F}}\Delta z)\boldsymbol{d}(z) + \check{\boldsymbol{G}}\boldsymbol{u}(z), \tag{66}$$

which when $\Delta z \to 0$ leads to

$$\boldsymbol{d}^{\text{out}} = (\boldsymbol{I} + \grave{\boldsymbol{\mathcal{F}}})\boldsymbol{d}^{\text{in}} + \check{\boldsymbol{\mathcal{G}}}\boldsymbol{u}^{\text{in}}. \tag{67}$$

Thus from eq. (65) it can be seen that

$$\acute{\boldsymbol{t}} \approx \boldsymbol{I} - \acute{\boldsymbol{\mathcal{F}}} \quad \text{and} \quad \grave{\boldsymbol{r}} \approx -\hat{\boldsymbol{\mathcal{G}}}, \tag{68a}$$

whereas eq. (67) gives

$$\grave{\boldsymbol{t}} \approx \boldsymbol{I} + \grave{\boldsymbol{\mathcal{F}}} \quad \text{and} \quad \acute{\boldsymbol{r}} \approx \check{\boldsymbol{\mathcal{G}}}. \tag{68b}$$

6.4 Recursive reflection and transmission responses

The eigenvalues in $\boldsymbol{\Lambda}$ will in general be complex and have a spectrum that contains evanescent waves and attenuation for both upgoing and downgoing waves. A calculation of reflection and transmission responses from a stack of layers can be done by matrix multiplication of all the propagator elements involved. However, in numerical simulations, this procedure may lead to numerical instabilities. It might thus be better to obtain the overall reflection and transmission matrices from a recursive calculation: Consider a propagator through a stack of layers from z_{N+1} to z_j^+ and furthermore propagation through the interface z_j and the homogeneous region up to z_{j-1}^+ (*cf.* Fig. 2):

$$\acute{\boldsymbol{Q}}\left(z_{j-1}^+, z_{N+1}\right) = \acute{\boldsymbol{Q}}\left(z_{j-1}^+, z_j^-\right)\acute{\boldsymbol{Q}}\left(z_j^-, z_j^+\right)\acute{\boldsymbol{Q}}\left(z_j^+, z_{N+1}\right). \tag{69}$$

In the 4×4 propagator $\acute{\boldsymbol{Q}}(z_j^+, z_{N+1})$, the 2×2 reflection and transmission matrices in the right column of eq. (54b) are denoted as $\acute{\boldsymbol{R}}_{j+1}$ and $\acute{\boldsymbol{T}}_{j+1}$. In the propagator $\acute{\boldsymbol{Q}}(z_{j-1}^+, z_{N+1})$, the corresponding reflection and transmission matrices are denoted $\acute{\boldsymbol{R}}_j$ and $\acute{\boldsymbol{T}}_j$. The propagation across the single interface z_j is described by eq. (54b) as well, and in this case the reflection and transmission matrices are written in lowercase letters ($\boldsymbol{r}$ and $\boldsymbol{t}$) with subscript j. For propagation upwards in the homogeneous region, the inverse of the matrix-expression in eq. (43) is used. The following recursion formulas for the downward reflection and transmission matrices are then obtained:

$$\grave{\boldsymbol{R}}_j = \mathrm{e}^{i\omega\acute{\mathbf{p}}_{\mathbf{z}}h_j}\left[\grave{\boldsymbol{r}}_j + \acute{\boldsymbol{t}}_j\grave{\boldsymbol{R}}_{j+1}(\boldsymbol{I} - \acute{\boldsymbol{r}}_j\grave{\boldsymbol{R}}_{j+1})^{-1}\grave{\boldsymbol{t}}_j\right]\mathrm{e}^{i\omega\grave{\mathbf{p}}_{\mathbf{z}}h_j}, \tag{70a}$$

$$\grave{\boldsymbol{T}}_j = \grave{\boldsymbol{T}}_{j+1}(\boldsymbol{I} - \acute{\boldsymbol{r}}_j\grave{\boldsymbol{R}}_{j+1})^{-1}\grave{\boldsymbol{t}}_j\mathrm{e}^{i\omega\grave{\mathbf{p}}_{\mathbf{z}}h_j}, \tag{70b}$$

where $h_j = z_j - z_{j-1}$, and where $\acute{\mathbf{p}}_{\mathbf{z}}$ and $\grave{\mathbf{p}}_{\mathbf{z}}$ are the eigenvalue submatrices in layer j. The initial values are $\grave{\boldsymbol{R}}_{N+1} = \boldsymbol{0}$ and $\grave{\boldsymbol{T}}_{N+1} = \mathrm{e}^{i\omega\grave{\mathbf{p}}_{\mathbf{z}}h_{N+1}}$.

The same procedure can be used for the downgoing propagators to find recursive relations for $\acute{\boldsymbol{R}}_j$ and $\acute{\boldsymbol{T}}_j$:

$$\acute{\boldsymbol{R}}_j = \mathrm{e}^{i\omega\grave{\mathbf{p}}_{\mathbf{z}}h_{j+1}}\left[\acute{\boldsymbol{r}}_j + \grave{\boldsymbol{t}}_j\acute{\boldsymbol{R}}_{j-1}\left(\boldsymbol{I} - \grave{\boldsymbol{r}}_j\acute{\boldsymbol{R}}_{j-1}\right)^{-1}\acute{\boldsymbol{t}}_j\right]\mathrm{e}^{i\omega\acute{\mathbf{p}}_{\mathbf{z}}h_{j+1}}, \tag{71a}$$

$$\acute{\boldsymbol{T}}_j = \acute{\boldsymbol{T}}_{j-1}\left(\boldsymbol{I} - \grave{\boldsymbol{r}}_j\acute{\boldsymbol{R}}_{j-1}\right)^{-1}\acute{\boldsymbol{t}}_j\mathrm{e}^{i\omega\acute{\mathbf{p}}_{\mathbf{z}}h_{j+1}}. \tag{71b}$$

Here, $\acute{\boldsymbol{R}}_{j-1}$ and $\acute{\boldsymbol{T}}_{j-1}$ describe reflection and transmission at z_j^- whereas $\acute{\boldsymbol{R}}_j$ and $\acute{\boldsymbol{T}}_j$ describe reflection and transmission at z_{j+1}^-. The initial values are $\acute{\boldsymbol{R}}_0 = \boldsymbol{0}$ and $\acute{\boldsymbol{T}}_0 = \mathrm{e}^{i\omega\acute{\mathbf{p}}_{\mathbf{z}}h_0}$, and the eigenvalue submatrices are those of layer $j+1$. The initial conditions are not necessarily related to the 'top' and 'bottom' of the stack as the interpretation of Fig. 2 might suggest; the recursion formulas can be applied to substacks anywhere in the medium, but not across a source (*cf.* Fig. 4). Note that the structure of the formulas is the same for both the upward and downward reflection and transmission matrices.

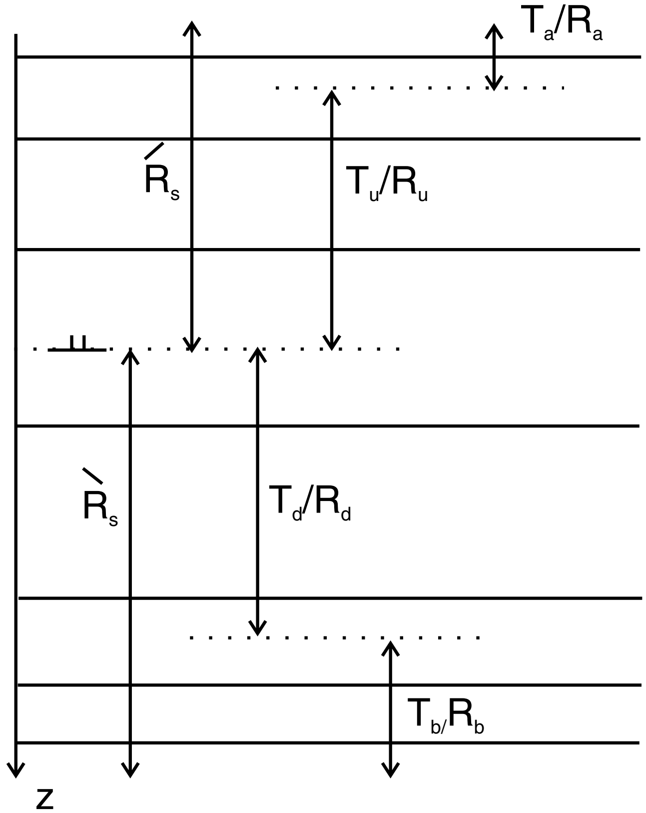

Figure 4. A sketch of the multilayered medium with reflection and transmission responses that must be calculated in order to obtain the field anywhere above or below the source in any layer.

7 System of layers containing a source

A system of homogeneous layers containing a source is shown in Fig. 2. The interfaces are denoted as $0, \ldots j, \ldots N$ along the positive z-direction from the topmost interface to the bottommost interface. Now, consider propagation downwards from the source through the stack below:

$$\boldsymbol{w}(z_N) = \grave{\boldsymbol{Q}}\big(z_N, z_s^+\big)\boldsymbol{w}\big(z_s^+\big) = \grave{\boldsymbol{Q}}\big(z_N, z_s^-\big)\big[\boldsymbol{w}\big(z_s^-\big) + \Sigma(z_s)\big]. \tag{72}$$

In the lower half-space, that is, in the region below the interface z_N, there are only downgoing fields. Furthermore, the downgoing field above the source is the reflected upgoing field: $\boldsymbol{d}(z_s^-) = \acute{\boldsymbol{R}}_s \boldsymbol{u}(z_s^-)$, where $\acute{\boldsymbol{R}}_s$ is the reflection response from a stack above z_s. Thus eq. (72) can be written as

$$\begin{pmatrix} \boldsymbol{0} \\ \boldsymbol{d}(z_N) \end{pmatrix} = \grave{\boldsymbol{Q}}_{11} \begin{pmatrix} \boldsymbol{I} & -\grave{\boldsymbol{R}}_s \\ \grave{\boldsymbol{Q}}_{11}^{-1}\grave{\boldsymbol{Q}}_{21} & \grave{\boldsymbol{Q}}_{11}^{-1}\grave{\boldsymbol{Q}}_{22} \end{pmatrix} \left\{ \begin{pmatrix} \boldsymbol{u}(z_s^-) \\ \acute{\boldsymbol{R}}_s \boldsymbol{u}(z_s^-) \end{pmatrix} + \begin{pmatrix} \acute{\Sigma}(z_s) \\ \grave{\Sigma}(z_s) \end{pmatrix} \right\}, \tag{73}$$

where the relation $\grave{\boldsymbol{R}}_s = -\grave{\boldsymbol{Q}}_{11}^{-1}\grave{\boldsymbol{Q}}_{12}$ from eq. (51c) has been used. The matrix $\grave{\boldsymbol{R}}_s$ represents the reflection response from the stack below z_s. The mode-field vector just above the source now becomes:

$$\boldsymbol{w}(z_s^-) = \begin{pmatrix} \boldsymbol{I} \\ \acute{\boldsymbol{R}}_s \end{pmatrix} \big(\boldsymbol{I} - \grave{\boldsymbol{R}}_s \acute{\boldsymbol{R}}_s\big)^{-1} (-\acute{\Sigma} + \grave{\boldsymbol{R}}_s \grave{\Sigma}). \tag{74}$$

In order to obtain an expression for the mode-field vector anywhere above the source, downward propagation of $\boldsymbol{w}(z)$ to $\boldsymbol{w}(z_s^-)$ where $z < z_s$, is considered by using eq. (54a). The relation between the upgoing mode-fields now gives

$$\boldsymbol{u}(z < z_s) = \big(\boldsymbol{I} - \grave{\boldsymbol{R}}_u \acute{\boldsymbol{R}}_a\big)^{-1} \acute{\boldsymbol{T}}_u \boldsymbol{u}(z_s^-), \tag{75}$$

when the relation $\boldsymbol{d}(z) = \acute{\boldsymbol{R}}_a \boldsymbol{u}(z)$ is used. The notation follows from Fig. 4: The reflection and transmission between $z < z_s$ and z_s are denoted $\acute{\boldsymbol{T}}_u$ and $\grave{\boldsymbol{R}}_u$ whereas the reflection from the above layers is denoted $\acute{\boldsymbol{R}}_a$. The total mode-field vector is thus

$$\boldsymbol{w}(z < z_s) = \begin{pmatrix} \boldsymbol{I} \\ \acute{\boldsymbol{R}}_a \end{pmatrix} (\boldsymbol{I} - \grave{\boldsymbol{R}}_u \acute{\boldsymbol{R}}_a)^{-1} \acute{\boldsymbol{T}}_u (\boldsymbol{I} - \grave{\boldsymbol{R}}_s \acute{\boldsymbol{R}}_s)^{-1} (-\acute{\Sigma} + \grave{\boldsymbol{R}}_s \grave{\Sigma}). \tag{76}$$

Written in this way the mode-field expression contains multiple reflections in the source layer and in the receiver layer. In addition there is a transmission matrix between these two layers.

An expression for the mode-field vector below the source can be found by considering propagation from the source through the upper stack:

$$\boldsymbol{w}(z_0) = \acute{\boldsymbol{Q}}\left(z_0, z_s^-\right)\boldsymbol{w}\left(z_s^-\right) = \acute{\boldsymbol{Q}}\left(z_0, z_s^+\right)\left[\boldsymbol{w}\left(z_s^+\right) - \boldsymbol{\Sigma}(z_s)\right]. \tag{77}$$

The radiation condition for the upper half-space implies that there are only upgoing waves in this region, and the upgoing field below the source equals the reflection response from the downgoing field $\boldsymbol{u}(z_s^+) = \grave{\boldsymbol{R}}_s\boldsymbol{d}(z_s^+)$. This leads to a corresponding relation to eq. (73):

$$\begin{pmatrix} \boldsymbol{u}(z_0) \\ \boldsymbol{0} \end{pmatrix} = \acute{\boldsymbol{Q}}_{22}\begin{pmatrix} \acute{\boldsymbol{Q}}_{22}^{-1}\acute{\boldsymbol{Q}}_{11} & \acute{\boldsymbol{Q}}_{22}^{-1}\acute{\boldsymbol{Q}}_{12} \\ -\acute{\boldsymbol{R}}_s & \boldsymbol{I} \end{pmatrix}\left\{\begin{pmatrix} \grave{\boldsymbol{R}}_s\boldsymbol{d}\left(z_s^+\right) \\ \boldsymbol{d}\left(z_s^+\right) \end{pmatrix} - \begin{pmatrix} \acute{\boldsymbol{\Sigma}}(z_s) \\ \grave{\boldsymbol{\Sigma}}(z_s) \end{pmatrix}\right\}, \tag{78}$$

where $\acute{\boldsymbol{R}}_s = -\acute{\boldsymbol{Q}}_{22}^{-1}\acute{\boldsymbol{Q}}_{21}$ from eq. (53c), and $\acute{\boldsymbol{R}}_s$ is the reflection response from the stack above z_s. The mode-field vector just below the source now becomes

$$\boldsymbol{w}(z_s^+) = \begin{pmatrix} \grave{\boldsymbol{R}}_s \\ \boldsymbol{I} \end{pmatrix}(\boldsymbol{I} - \acute{\boldsymbol{R}}_s\grave{\boldsymbol{R}}_s)^{-1}(\grave{\boldsymbol{\Sigma}} - \acute{\boldsymbol{R}}_s\acute{\boldsymbol{\Sigma}}), \tag{79}$$

and the mode-field vector anywhere below the source $z > z_s$ is found by propagating $\boldsymbol{w}(z)$ up to $\boldsymbol{w}(z_s^+)$ with the propagator in eq. (54b). By using that $\boldsymbol{u}(z) = \grave{\boldsymbol{R}}_b\boldsymbol{d}(z)$, a relation between the downgoing fields can be derived:

$$\boldsymbol{d}(z > z_s) = (\boldsymbol{I} - \acute{\boldsymbol{R}}_d\grave{\boldsymbol{R}}_b)^{-1}\grave{\boldsymbol{T}}_d\boldsymbol{d}\left(z_s^+\right). \tag{80}$$

The reflection and transmission between $z > z_s$ and z_s are denoted $\grave{\boldsymbol{T}}_d$ and $\acute{\boldsymbol{R}}_d$ whereas the reflection from the bottom layers is denoted $\grave{\boldsymbol{R}}_b$ as shown in Fig. 4. The total mode-field vector then becomes

$$\boldsymbol{w}(z > z_s) = \begin{pmatrix} \grave{\boldsymbol{R}}_b \\ \boldsymbol{I} \end{pmatrix}\left(\boldsymbol{I} - \acute{\boldsymbol{R}}_d\grave{\boldsymbol{R}}_b\right)^{-1}\grave{\boldsymbol{T}}_d\left(\boldsymbol{I} - \acute{\boldsymbol{R}}_s\grave{\boldsymbol{R}}_s\right)^{-1}(\grave{\boldsymbol{\Sigma}} - \acute{\boldsymbol{R}}_s\acute{\boldsymbol{\Sigma}}). \tag{81}$$

Note that eq. (76) can be obtained from eq. (81) and vice versa by switching the roles of upgoing and downgoing mode-fields, reflection, transmission, and radiation. In addition, the signs of the mode-fields must be switched.

Within the source layer eqs (76) and (81) reduce to

$$\boldsymbol{w}_s(z < z_s) = \begin{pmatrix} \mathrm{e}^{-i\omega\acute{\mathbf{p}}_{\mathbf{z}}(z-z_s)} \\ \acute{\boldsymbol{R}}_a\mathrm{e}^{-i\omega\acute{\mathbf{p}}_{\mathbf{z}}(z-z_s)} \end{pmatrix}(\boldsymbol{I} - \grave{\boldsymbol{R}}_s\acute{\boldsymbol{R}}_s)^{-1}(-\acute{\boldsymbol{\Sigma}} + \grave{\boldsymbol{R}}_s\grave{\boldsymbol{\Sigma}}), \tag{82a}$$

$$\boldsymbol{w}_s(z > z_s) = \begin{pmatrix} \grave{\boldsymbol{R}}_b\mathrm{e}^{i\omega\grave{\mathbf{p}}_{\mathbf{z}}(z-z_s)} \\ \mathrm{e}^{i\omega\grave{\mathbf{p}}_{\mathbf{z}}(z-z_s)} \end{pmatrix}(\boldsymbol{I} - \acute{\boldsymbol{R}}_s\grave{\boldsymbol{R}}_s)^{-1}(\grave{\boldsymbol{\Sigma}} - \acute{\boldsymbol{R}}_s\acute{\boldsymbol{\Sigma}}), \tag{82b}$$

where $\acute{\boldsymbol{R}}_a$ in this case differs from $\acute{\boldsymbol{R}}_s$ by a phase factor that corresponds to propagation down and up between the receiver and the source, and likewise $\grave{\boldsymbol{R}}_b$ equals $\grave{\boldsymbol{R}}_s$ when the receiver is at the same z-level as the source. The eigenvalue submatrices in eq. (82) are those of the source-medium.

8 EIGENVALUES AND EIGENVECTORS

In the previous section, expressions for the mode-field from an infinitesimal dipole have been derived. The physical field follows from the transformation $\boldsymbol{b} = \boldsymbol{N}\boldsymbol{w}$ (eq. 28). In order to calculate the mode-field, the reflection and transmission from a stack of layers are needed. This is provided by the relations in eqs (71) and (70). The reflection and transmission from a single interface is described by eq. (63). Finally, the expression for the source vector in the mode-domain as given by eq. (44) is required.

In all of the derivations, the relations are obtained from the eigenvalues and eigenvectors of the system matrix $\boldsymbol{A}$. Thus, the calculation of the electromagnetic field is dependent on solving the eigenvalue problem for the system matrix in each homogeneous region. The eigenvalues and eigenvectors of $\boldsymbol{A}$ are dependent on the material parameters in the specified region and the horizontal slownesses p_x and p_y.

8.1 Eigenvalues

The eigenvalues of $\boldsymbol{A}$ are determined by solving $\det(\boldsymbol{A} - p_z\boldsymbol{I}) = 0$. This leads to the quartic equation

$$p_z^4 + b_3\, p_z^3 + b_2\, p_z^2 + b_1\, p_z + b_0 = 0, \tag{83}$$

where

$$b_3 = -2(a_{11} + a_{22}), \tag{84a}$$

$$b_2 = (a_{11} + a_{22})^2 + 2a_{11}a_{22} - 2a_{12}a_{21} - 2a_{14}a_{32} - a_{13}a_{31} - a_{24}a_{42}, \tag{84b}$$

$$b_1 = 2a_{11}[a_{12}a_{21} + a_{14}a_{32} + a_{24}a_{42} - a_{22}(a_{11} + a_{22})] + 2a_{12}(a_{21}a_{22} - a_{24}a_{32} - a_{14}a_{31}),$$
$$+ 2a_{13}(a_{31}a_{22} - a_{21}a_{32}) + 2a_{14}(a_{22}a_{32} - a_{21}a_{42}), \tag{84c}$$

$$b_0 = a_{11}\left[a_{11}\left(a_{22}^2 - a_{24}a_{42}\right) + 2a_{12}(a_{24}a_{32} - a_{21}a_{22}) + 2a_{14}(a_{21}a_{42} - a_{22}a_{32})\right],$$
$$+ a_{12}\left[a_{12}\left(a_{21}^2 - a_{24}a_{31}\right) + 2a_{14}(a_{22}a_{31} - a_{21}a_{32})\right],$$
$$+ a_{13}\left[a_{21}(a_{22}a_{32} - a_{21}a_{42}) + a_{22}(a_{21}a_{32} - a_{22}a_{31}) + a_{24}\left(a_{31}a_{42} - a_{32}^2\right)\right],$$
$$+ a_{14}\left[a_{14}\left(a_{32}^2 - a_{31}a_{42}\right)\right]. \tag{84d}$$

The solution of eq. (83) can be found using the approach in Abramowitz & Stegun (1962), page 17. This implies to determine one solution, e.g. u_1 of the cubic equation

$$u^3 - b_2u^2 + (b_3b_1 - 4b_0)u - \left[b_1^2 + b_0\left(b_3^2 - 4b_2\right)\right] = 0, \tag{85}$$

and then determining the four roots from the two quadratic equations:

$$p_z^2 + \left(\frac{b_3}{2} \mp \sqrt{\frac{b_3^2}{4} + u_1 - b_2}\right) p_z + \left(\frac{u_1}{2} \mp \sqrt{\frac{u_1^2}{4} - b_0}\right) = 0. \tag{86}$$

The derived set of roots p_{zj} (where $j = \{I, II, III, IV\}$) must satisfy the following relations

$$\sum p_{zj} = -b_3, \quad \sum p_{zj}p_{zk}p_{zl} = -b_1, \quad \sum p_{zj}p_{zk} = b_2, \quad \text{and} \quad p_{zI}p_{zII}p_{zIII}p_{zIV} = b_0. \tag{87}$$

The eigenvalues represent slownesses in the vertical direction, and in general, these are all complex parameters. In order for the iterative reflectivity method to work properly, cf. eqs (70) and (71), it is important that the eigenvalues that have positive (negative) imaginary parts are sorted into the upgoing (downgoing) submatrix in eq. (30). Since the horizontal slownesses are real, this requirement (i.e. the radiation condition) corresponds to the requirement that the direction of the energy flow should determine which eigenvalue that relates to upgoing and downgoing constituents (*cf.* Chapman 1994; Carcione & Schoenberg 2000). In case of real eigenvalues, the determination of an eigenvalue being upgoing or downgoing relies on the energy-flow condition. In Appendix C, a method for calculating the energy velocity in a homogeneous region in terms of the slowness and material parameters is presented.

Within each eigenvalue submatrix for upgoing and downgoing constituents, the sorting of the eigenvalues does not matter as shown in Appendix D. If it is desirable to derive the correct physical reflection and transmission matrices at an interface, the eigenvalues must however have the same sorting on each side of the interface. This can be obtained by accounting for signs throughout the solution of the quartic equation. Another method for sorting the eigenvalues is provided through the calculation of the energy velocity in Appendix C.

8.2 Eigenvectors

The eigenvector-matrix $\boldsymbol{N}$ can be written in terms of the eigenvectors, matrix elements, and submatrices as

$$\sqrt{2}\boldsymbol{N} = (\boldsymbol{n}_I \quad \boldsymbol{n}_{II} \quad \boldsymbol{n}_{III} \quad \boldsymbol{n}_{IV}) = \begin{pmatrix} n_{11} & n_{12} & n_{13} & n_{14} \\ n_{21} & n_{22} & n_{23} & n_{24} \\ n_{31} & n_{32} & -n_{33} & -n_{34} \\ n_{41} & n_{42} & -n_{43} & -n_{44} \end{pmatrix} = \begin{pmatrix} \acute{\boldsymbol{N}}_E & \grave{\boldsymbol{N}}_E \\ \acute{\boldsymbol{N}}_H & -\grave{\boldsymbol{N}}_H \end{pmatrix}. \tag{88}$$

Thus, $j = \{I, II, III, IV\}$ in the eigenvectors (and corresponding eigenvalues), appear as $j = \{1, 2, 3, 4\}$ for the second number in the subscript of the eigenvector-matrix elements. The eigenvectors that correspond to the eigenvalues are found from solving

$$\boldsymbol{A}\boldsymbol{n}_j = p_{zj}\boldsymbol{n}_j, \tag{89}$$

and for each eigenvalue p_{zj}, the following relations between the entries in an eigenvector can be obtained:

$$n_{2j} = \frac{\beta_{2j}}{\beta_{1j}}n_{1j}, \quad n_{3j} = \pm\frac{\beta_{3j}}{\beta_{1j}}n_{1j}, \quad \text{and} \quad n_{4j} = \pm\frac{\beta_{4j}}{\beta_{1j}}n_{1j}, \tag{90}$$

where the plus sign is applied when $j = \{1, 2\}$ and minus sign when $j = \{3, 4\}$, and where

$$\beta_{1j} = (a_{11} - p_{zj})(a_{22} - p_{zj})a_{14} - (a_{11} - p_{zj})a_{12}a_{24}$$
$$-(a_{22} - p_{zj})a_{13}a_{21} - a_{14}^2a_{32} + a_{12}a_{14}a_{21} + a_{13}a_{24}a_{32}, \tag{91a}$$

$$\beta_{2j} = a_{24}(a_{11} - p_{zj})^2 - 2a_{14}a_{21}(a_{11} - p_{zj}) + a_{13}\left(a_{21}^2 - a_{24}a_{31}\right) + a_{14}^2a_{31}, \tag{91b}$$

$$\beta_{3j} = a_{21}(a_{11} - p_{zj})(a_{22} - p_{zj}) - a_{24}a_{32}(a_{11} - p_{zj})$$
$$-a_{14}a_{31}(a_{22} - p_{zj}) - a_{12}\left(a_{21}^2 - a_{24}a_{31}\right) + a_{14}a_{21}a_{32}, \tag{91c}$$

$$\beta_{4j} = -(a_{11} - p_{zj})^2(a_{22} - p_{zj}) + (a_{12}a_{21} + a_{14}a_{32})(a_{11} - p_{zj})$$
$$+ a_{13}a_{31}(a_{22} - p_{zj}) - a_{12}a_{14}a_{31} - a_{13}a_{21}a_{32}. \tag{91d}$$

The n_{1j}-entries are obtained from the flux-normalization criterion. The relation $\boldsymbol{N}\boldsymbol{N}^{-1} = \boldsymbol{I}$ in terms of the eigenvector submatrices from eq. (40) implies that

$$\acute{\boldsymbol{N}}_E \acute{\boldsymbol{N}}_H^T \; + \; \grave{\boldsymbol{N}}_E \grave{\boldsymbol{N}}_H^T = 2\boldsymbol{I}, \quad \acute{\boldsymbol{N}}_H \acute{\boldsymbol{N}}_H^T = \grave{\boldsymbol{N}}_H \grave{\boldsymbol{N}}_H^T,$$
$$\acute{\boldsymbol{N}}_H \acute{\boldsymbol{N}}_E^T \; + \; \grave{\boldsymbol{N}}_H \grave{\boldsymbol{N}}_E^T = 2\boldsymbol{I}, \quad \acute{\boldsymbol{N}}_E \acute{\boldsymbol{N}}_E^T = \grave{\boldsymbol{N}}_E \grave{\boldsymbol{N}}_E^T. \tag{92}$$

which provides the set of equations:

$$n_{11}^2 + n_{12}^2 - n_{13}^2 - n_{14}^2 = 0, \tag{93a}$$

$$n_{11}n_{21} + n_{12}n_{22} - n_{13}n_{23} - n_{14}n_{24} = 0, \tag{93b}$$

$$n_{11}n_{31} + n_{12}n_{32} + n_{13}n_{33} + n_{14}n_{34} = 2, \tag{93c}$$

$$n_{11}n_{41} + n_{12}n_{42} + n_{13}n_{43} + n_{14}n_{44} = 0, \tag{93d}$$

where n_{11}, n_{12}, n_{13}, and n_{14} are the unknowns. The solution is given by

$$n_{11}^2 = 2(\alpha_{12}\alpha_{23} - \alpha_{13}\alpha_{22})D_\alpha^{-1}, \qquad n_{12}^2 = 2(\alpha_{13}\alpha_{21} - \alpha_{11}\alpha_{23})D_\alpha^{-1},$$

$$n_{13}^2 = 2(\alpha_{11}\alpha_{22} - \alpha_{12}\alpha_{21})D_\alpha^{-1}, \qquad n_{14}^2 = n_{11}^2 + n_{12}^2 - n_{13}^2,$$

where

$$\alpha_{11} = \beta'_{24} - \beta'_{21}, \qquad \alpha_{12} = \beta'_{24} - \beta'_{22}, \qquad \alpha_{13} = \beta'_{23} - \beta'_{24}, \tag{94a}$$

$$\alpha_{21} = \beta'_{41} - \beta'_{44}, \qquad \alpha_{22} = \beta'_{42} - \beta'_{44}, \qquad \alpha_{23} = \beta'_{44} - \beta'_{43}, \tag{94b}$$

$$\alpha_{31} = \beta'_{31} - \beta'_{34}, \qquad \alpha_{32} = \beta'_{32} - \beta'_{34}, \qquad \alpha_{33} = \beta'_{34} - \beta'_{33}, \tag{94c}$$

the quotient $\beta'_{ij} = \beta_{ij}/\beta_{1j}$ has been introduced, and

$$D_\alpha = \alpha_{11}(\alpha_{22}\alpha_{33} - \alpha_{23}\alpha_{32}) + \alpha_{12}(\alpha_{23}\alpha_{31} - \alpha_{21}\alpha_{33}) + \alpha_{13}(\alpha_{21}\alpha_{32} - \alpha_{22}\alpha_{31}). \tag{94d}$$

The sign of the square root in the solutions for n_{11} and n_{12} can be chosen at will, but the sign of n_{13} and n_{14} must correspond to the selected sign for n_{11} and n_{12}, respectively.

9 UP/DOWN-SYMMETRIC MEDIA

When one of the principal axes in the anistropic medium coincides with the vertical axis of the main coordinate system, the relation between the principal system and the main coordinate is given in terms of one rotation in the horizontal plane (*cf.* Appendix A). This corresponds to a monoclinic medium with the horizontal plane as a mirror plane of symmetry, and the system matrix reduces to:

$$\boldsymbol{A} = \begin{pmatrix} \boldsymbol{0} & \boldsymbol{A}_1 \\ \boldsymbol{A}_2 & \boldsymbol{0} \end{pmatrix}. \tag{95}$$

In this case the entries in the submatrices are denoted

$$\boldsymbol{A}_1 = \begin{pmatrix} a'_{13} & a'_{14} \\ a'_{14} & a'_{24} \end{pmatrix} \quad \text{and} \quad \boldsymbol{A}_2 = \begin{pmatrix} a'_{31} & a'_{32} \\ a'_{32} & a'_{42} \end{pmatrix}, \tag{96}$$

where the same indices as in the general case are used. However, the expressions in the entries simplify compared to the general case and become:

$$a'_{13} = \mu_{yy} - \frac{p_x^2}{\tilde{\varepsilon}_v}, \qquad a'_{14} = -\mu_{xy} - \frac{p_x p_y}{\tilde{\varepsilon}_v}, \tag{97a}$$

$$a'_{24} = \mu_{xx} - \frac{p_y^2}{\tilde{\varepsilon}_v}, \qquad a'_{31} = \tilde{\varepsilon}_{xx} - \frac{p_y^2}{\mu_v}, \tag{97b}$$

$$a'_{32} = \tilde{\varepsilon}_{xy} + \frac{p_x p_y}{\mu_v}, \qquad a'_{42} = \tilde{\varepsilon}_{yy} - \frac{p_x^2}{\mu_v}. \tag{97c}$$

Now, because of the symmetry in the original 4 × 4-matrices, the eigenvalues and eigenvectors can be obtained from 2 × 2-matrices. The product of the submatrices will become useful:

$$\boldsymbol{A}_1\boldsymbol{A}_2 = \begin{pmatrix} \alpha'_{11} & \alpha'_{12} \\ \alpha'_{21} & \alpha'_{22} \end{pmatrix}, \tag{98}$$

where

$$\alpha'_{11} = a'_{13}a'_{31} + a'_{14}a'_{32}, \qquad \alpha'_{12} = a'_{13}a'_{32} + a'_{14}a'_{42},$$
$$\alpha'_{21} = a'_{14}a'_{31} + a'_{24}a'_{32}, \qquad \alpha'_{22} = a'_{14}a'_{32} + a'_{24}a'_{42}. \tag{99}$$

The eigenvalues can be derived from the expression for the eigenvalues in eq. (83) where the terms b_3 and b_1 are zero for the up/down-symmetric (u/d-symmetric) case. This means that the quartic equation reduces to a quadratic equation for the squared eigenvalues, which can be written in terms of the submatrix product as:

$$p_z = \pm \left\{ \frac{1}{2} \left[\mathrm{tr}(\boldsymbol{A}_1 \boldsymbol{A}_2) \pm \sqrt{\mathrm{tr}^2(\boldsymbol{A}_1 \boldsymbol{A}_2) - 4\det(\boldsymbol{A}_1 \boldsymbol{A}_2)} \right] \right\}^{1/2}. \tag{100}$$

The two eigenvalues that correspond to the positive sign in front of the square root are $p_{z\mathrm{I}}$ and $p_{z\mathrm{II}}$. These two quantities are furthermore obtained by using the positive and negative sign inside the square root, respectively. Then $p_{z\mathrm{III}} = -p_{z\mathrm{I}}$ and $p_{z\mathrm{IV}} = -p_{z\mathrm{II}}$, which means that the eigenvalue submatrices in eq. (30) are equal due to the u/d-symmetry: $\acute{\mathbf{p}}_\mathbf{z} = \grave{\mathbf{p}}_\mathbf{z} = \mathbf{p}_\mathbf{z}$.

Because of the symmetry in the upgoing and downgoing field constituents, the submatrices in eq. (88) become pairwise equal:

$$\boldsymbol{N} = \frac{1}{\sqrt{2}} \begin{pmatrix} \boldsymbol{N}_E & \boldsymbol{N}_E \\ \boldsymbol{N}_H & -\boldsymbol{N}_H \end{pmatrix}, \tag{101}$$

where the block inverse and relation from the general expression for the eigenvector matrix (eq. 40) give:

$$\boldsymbol{N}^{-1} = \frac{1}{\sqrt{2}} \begin{pmatrix} \boldsymbol{N}_E^{-1} & \boldsymbol{N}_H^{-1} \\ \boldsymbol{N}_E^{-1} & -\boldsymbol{N}_H^{-1} \end{pmatrix} = \frac{1}{\sqrt{2}} \begin{pmatrix} \boldsymbol{N}_H^T & \boldsymbol{N}_E^T \\ \boldsymbol{N}_H^T & -\boldsymbol{N}_E^T \end{pmatrix}. \tag{102}$$

The following symmetry-relations thus appear:

$$\boldsymbol{N}_E^{-1} = \boldsymbol{N}_H^T, \quad \boldsymbol{N}_H^{-1} = \boldsymbol{N}_E^T. \tag{103}$$

The similarity transform $\boldsymbol{AN} = \boldsymbol{N\Lambda}$, where $\boldsymbol{\Lambda} = \mathrm{diag}\,\{\mathbf{p}_z, -\mathbf{p}_z\}$ then gives the equations:

$$\boldsymbol{A}_1 = \boldsymbol{N}_E \mathbf{p}_\mathbf{z} \boldsymbol{N}_E^T \quad \text{and} \quad \boldsymbol{A}_2 = \boldsymbol{N}_H \mathbf{p}_\mathbf{z} \boldsymbol{N}_H^T. \tag{104}$$

Complex symmetric matrices as $\boldsymbol{A}_1$ and $\boldsymbol{A}_2$ can always be diagonalized as in eq. (104) (Horn & Johnson 1985). It has previously been shown that this choice of eigenvectors corresponds to a flux normalization.

By writing $\boldsymbol{N}_E = (\boldsymbol{n}_\mathrm{I}\ \boldsymbol{n}_\mathrm{II})$, the multiplication of $\boldsymbol{A}_2$ by $\boldsymbol{A}_1$ from the left in eq. (104) leads to:

$$\boldsymbol{A}_1 \boldsymbol{A}_2 \boldsymbol{n}_j = p_{zj}^2 \boldsymbol{n}_j, \tag{105}$$

where $j = \{\mathrm{I}, \mathrm{II}\}$. Using the relations in eq. (103), the eigenvector-submatrices $\boldsymbol{N}_E$ and $\boldsymbol{N}_H$ can be written as:

$$\boldsymbol{N}_E = \begin{pmatrix} n_{11} & n_{12} \\ n_{21} & n_{22} \end{pmatrix}, \quad \boldsymbol{N}_H = \frac{1}{n_{11}n_{22} - n_{12}n_{21}} \begin{pmatrix} n_{22} & -n_{21} \\ -n_{12} & n_{11} \end{pmatrix}. \tag{106}$$

The elements in the eigenvector matrices can now be calculated in terms of the eigenvalues $p_{z\mathrm{I}}$ and $p_{z\mathrm{II}}$ from eq. (100) as follows: Find a relation between the entries in the eigenvectors from eq. (105), and use eq. (104) to obtain a scaling between the eigenvectors that satisfies the flux-normalization condition. It is useful to derive two sets of solutions: The following expressions can be used as long as the anisotropy is not uniaxial and in the y-direction:

$$n_{21} = \left[\frac{a'_{14}\alpha'_{21} + a'_{24}\left(\alpha'_{22} - p_{z\mathrm{II}}^2\right)}{p_{z\mathrm{I}}\left(p_{z\mathrm{I}}^2 - p_{z\mathrm{II}}^2\right)} \right]^{1/2}, \qquad n_{22} = \left[\frac{a'_{14}\alpha'_{21} + a'_{24}\left(\alpha'_{22} - p_{z\mathrm{I}}^2\right)}{p_{z\mathrm{II}}\left(p_{z\mathrm{II}}^2 - p_{z\mathrm{I}}^2\right)} \right]^{1/2}, \tag{107a}$$

$$n_{11} = \frac{p_{z\mathrm{I}}^2 - \alpha'_{22}}{\alpha'_{21}} n_{21}, \qquad n_{12} = \frac{p_{z\mathrm{II}}^2 - \alpha'_{22}}{\alpha'_{21}} n_{22}. \tag{107b}$$

Equivalently the following set of eigenvectors can be used, except when the anisotropy is uniaxial and the direction coincides with the x-direction:

$$n_{11} = \left[\frac{a'_{14}\alpha'_{12} + a'_{13}\left(\alpha'_{11} - p_{z\mathrm{II}}^2\right)}{p_{z\mathrm{I}}\left(p_{z\mathrm{I}}^2 - p_{z\mathrm{II}}^2\right)} \right]^{1/2}, \qquad n_{12} = \left[\frac{a'_{14}\alpha'_{12} + a'_{13}\left(\alpha'_{11} - p_{z\mathrm{I}}^2\right)}{p_{z\mathrm{II}}\left(p_{z\mathrm{II}}^2 - p_{z\mathrm{I}}^2\right)} \right]^{1/2}, \tag{108a}$$

$$n_{21} = \frac{p_{z\mathrm{I}}^2 - \alpha'_{11}}{\alpha'_{12}} n_{11}, \qquad n_{22} = \frac{p_{z\mathrm{II}}^2 - \alpha'_{11}}{\alpha'_{12}} n_{12}. \tag{108b}$$

9.1 Common principal and coordinate axes

The case where the principal axes of anisotropy coincide with the coordinate axes will be denoted as non-rotated orthorhombic. Since the Fourier expansion of dipole radiation in stratified media gives a spectrum of slownesses in terms of p_x and p_y, this orthorhombic case does not in general lead to any simplifications compared to an u/d-symmetric case where the principal axes are rotated with respect to the horizontal coordinate axes. However, the expressions for the eigenvalues simplify for uniaxial non-rotated orthorhombic media. Thus, it might be enlightening to calculate the eigenvalues for biaxial orthorhombic media explicitly. To this end, note that it is possible to always choose the coordinate system to coincide with the principal axes of anisotropy for u/d-symmetric media by decomposing the antenna into x- and y-components that coincide with the principal axes.

For non-rotated orthorhombic media, the material parameter dyads are $\tilde{\boldsymbol{\varepsilon}} = \mathrm{diag}\{\tilde{\varepsilon}_1, \tilde{\varepsilon}_2, \tilde{\varepsilon}_3\}$ and $\boldsymbol{\mu} = \mathrm{diag}\ \{\mu_1, \mu_2, \mu_3\}$. The eigenvalues of $\boldsymbol{A}$ become:

$$p_{z\mathrm{I}} = \left[\frac{1+f(p_x)}{2}\left(\mu_2\tilde{\varepsilon}_1 - \frac{\mu_1}{\mu_3}p_x^2 - \frac{\mu_2}{\mu_3}p_y^2\right) + \frac{1-f(p_x)}{2}\left(\mu_1\tilde{\varepsilon}_2 - \frac{\tilde{\varepsilon}_1}{\tilde{\varepsilon}_3}p_x^2 - \frac{\tilde{\varepsilon}_2}{\tilde{\varepsilon}_3}p_y^2\right)\right]^{1/2}, \tag{109a}$$

$$p_{z\mathrm{II}} = \left[\frac{1+f(p_x)}{2}\left(\mu_1\tilde{\varepsilon}_2 - \frac{\tilde{\varepsilon}_1}{\tilde{\varepsilon}_3}p_x^2 - \frac{\tilde{\varepsilon}_2}{\tilde{\varepsilon}_3}p_y^2\right) + \frac{1-f(p_x)}{2}\left(\mu_2\tilde{\varepsilon}_1 - \frac{\mu_1}{\mu_3}p_x^2 - \frac{\mu_2}{\mu_3}p_y^2\right)\right]^{1/2}, \tag{109b}$$

where

$$f(p_x) = \sqrt{1 + \frac{4\,(\mu_1\tilde{\varepsilon}_2 - \mu_2\tilde{\varepsilon}_1)\,q_1 p_x^2}{\left(\mu_1\tilde{\varepsilon}_2 - \mu_2\tilde{\varepsilon}_1 + q_1 p_x^2 + q_2 p_y^2\right)^2}}, \tag{109c}$$

and $q_1 = \tilde{\varepsilon}_1/\tilde{\varepsilon}_3 - \mu_1/\mu_3$, and $q_2 = \tilde{\varepsilon}_2/\tilde{\varepsilon}_3 - \mu_2/\mu_3$. The eigenvalues can also be written as

$$p_{z\mathrm{I}} = \left[\frac{1+f(p_y)}{2}\left(\mu_1\tilde{\varepsilon}_2 - \frac{\mu_1}{\mu_3}p_x^2 - \frac{\mu_2}{\mu_3}p_y^2\right) + \frac{1-f(p_y)}{2}\left(\mu_2\tilde{\varepsilon}_1 - \frac{\tilde{\varepsilon}_1}{\tilde{\varepsilon}_3}p_x^2 - \frac{\tilde{\varepsilon}_2}{\tilde{\varepsilon}_3}p_y^2\right)\right]^{1/2}, \tag{110a}$$

$$p_{z\mathrm{II}} = \left[\frac{1+f(p_y)}{2}\left(\mu_2\tilde{\varepsilon}_1 - \frac{\tilde{\varepsilon}_1}{\tilde{\varepsilon}_3}p_x^2 - \frac{\tilde{\varepsilon}_2}{\tilde{\varepsilon}_3}p_y^2\right) + \frac{1-f(p_y)}{2}\left(\mu_1\tilde{\varepsilon}_2 - \frac{\mu_1}{\mu_3}p_x^2 - \frac{\mu_2}{\mu_3}p_y^2\right)\right]^{1/2}, \tag{110b}$$

where

$$f(p_y) = \sqrt{1 - \frac{4\,(\mu_1\tilde{\varepsilon}_2 - \mu_2\tilde{\varepsilon}_1)\,q_2 p_y^2}{\left(\mu_1\tilde{\varepsilon}_2 - \mu_2\tilde{\varepsilon}_1 + q_1 p_x^2 + q_2 p_y^2\right)^2}}. \tag{110c}$$

Note that the quantity $f(p_x)$ is equal to one when p_x is zero, and similarly that $f(p_y)$ is equal to one when p_y is zero.

When the anisotropy is uniaxial and in the *x*-direction, the expressions for the eigenvalues simplify since $q_2 = 0$ which means that $f(p_y) = 1$. Thus,

$$p_{z\mathrm{I}} = \sqrt{\mu_1\tilde{\varepsilon}_2 - \frac{\mu_1}{\mu_3}p_x^2 - p_y^2} \quad \text{and} \quad p_{z\mathrm{II}} = \sqrt{\mu_2\tilde{\varepsilon}_1 - \frac{\tilde{\varepsilon}_1}{\tilde{\varepsilon}_3}p_x^2 - p_y^2}. \tag{111}$$

Similarly, when the anisotropy direction is along the y-axis only, $q_1 = 0$ and $f(p_x) = 1$. Then

$$p_{z\mathrm{I}} = \sqrt{\mu_2\tilde{\varepsilon}_1 - p_x^2 - \frac{\mu_2}{\mu_3}p_y^2} \quad \text{and} \quad p_{z\mathrm{II}} = \sqrt{\mu_1\tilde{\varepsilon}_2 - p_x^2 - \frac{\tilde{\varepsilon}_2}{\tilde{\varepsilon}_3}p_y^2}. \tag{112}$$

9.2 Reflection and transmission coefficients

In u/d-symmetric stratified layers the relations in eq. (59) reduce to

$$\acute{\boldsymbol{R}} = \acute{\boldsymbol{R}}^T, \quad \grave{\boldsymbol{R}} = \grave{\boldsymbol{R}}^T, \quad \text{and} \quad \acute{\boldsymbol{T}} = \grave{\boldsymbol{T}}^T. \tag{113}$$

At an interface between two u/d-symmetric media, the relations in eq. (63) reduce to:

$$\acute{\boldsymbol{t}} = 2\,(\boldsymbol{C} + \boldsymbol{D})^{-T}, \tag{114a}$$

$$\acute{\boldsymbol{r}} = -\,(\boldsymbol{C} - \boldsymbol{D})^T\,(\boldsymbol{C} + \boldsymbol{D})^{-T} = -\,(\boldsymbol{C} + \boldsymbol{D})^{-1}\,(\boldsymbol{C} - \boldsymbol{D}), \tag{114b}$$

$$\grave{\boldsymbol{r}} = (\boldsymbol{C} - \boldsymbol{D})\,(\boldsymbol{C} + \boldsymbol{D})^{-1} = (\boldsymbol{C} + \boldsymbol{D})^{-T}\,(\boldsymbol{C} - \boldsymbol{D})^T, \tag{114c}$$

$$\grave{\boldsymbol{t}} = 2\,(\boldsymbol{C} + \boldsymbol{D})^{-1}, \tag{114d}$$

since the relations in eq. (61) now are

$$\boldsymbol{C} = \left[\boldsymbol{N}_H^-\right]^T \boldsymbol{N}_E^+ \quad \text{and} \quad \boldsymbol{D} = \left[\boldsymbol{N}_E^-\right]^T \boldsymbol{N}_H^+, \tag{115}$$

because of the symmetries in the eigenvector submatrices in eq. (103). The superscripts '$-$' and '$+$' denote the upper and lower homogeneous regions, respectively, and the matrices $\boldsymbol{C}$ and $\boldsymbol{D}$ have the property $\boldsymbol{C}\boldsymbol{D}^T = \boldsymbol{I}$. This way of writing reflection and transmission matrices for u/d-symmetric media was introduced by Ursin & Stovas (2002). From eq. (114) it can be verified that the upgoing and downgoing reflection matrices are related as

$$\acute{\boldsymbol{r}} = -\grave{\boldsymbol{t}}\grave{\boldsymbol{r}}\grave{\boldsymbol{t}}^{-1} \quad \text{and} \quad \grave{\boldsymbol{r}} = -\acute{\boldsymbol{t}}\acute{\boldsymbol{r}}\acute{\boldsymbol{t}}^{-1}, \tag{116}$$

and that the reflection matrices are related to the transmission matrices as

$$\acute{\boldsymbol{r}}^2 = \boldsymbol{I} - \grave{\boldsymbol{t}}\acute{\boldsymbol{t}} \quad \text{and} \quad \grave{\boldsymbol{r}}^2 = \boldsymbol{I} - \acute{\boldsymbol{t}}\grave{\boldsymbol{t}}. \tag{117}$$

The relations in continuously varying media also simplify with u/d-symmetry since $\acute{\boldsymbol{F}} = \grave{\boldsymbol{F}} = \boldsymbol{F}$ and $\check{\boldsymbol{G}} = \hat{\boldsymbol{G}} = \boldsymbol{G}$. For *weak contrasts*, the approximations in eq. (68) then imply that $\acute{\boldsymbol{r}} \approx -\grave{\boldsymbol{r}}$.

10 TRANSVERSAL ISOTROPY IN THE VERTICAL DIRECTION

Transversal isotropy in the vertical direction (TIV) means that the electromagnetic properties of a medium are rotationally symmetric about the z-axis. In this case the constitutive relations simplify to $\tilde{\boldsymbol{\varepsilon}} = \mathrm{diag}\{\tilde{\varepsilon}_h, \tilde{\varepsilon}_h, \tilde{\varepsilon}_v\}$ and $\boldsymbol{\mu} = \mathrm{diag}\,\{\mu_h, \mu_h, \mu_v\}$, and the system matrix has the same form as eq. (95) with

$$\boldsymbol{A}_1 = \frac{1}{\tilde{\varepsilon}_v}\begin{pmatrix} \mu_h\tilde{\varepsilon}_v - p_x^2 & -p_x p_y \\ -p_x p_y & \mu_h\tilde{\varepsilon}_v - p_y^2 \end{pmatrix}, \quad \boldsymbol{A}_2 = \frac{1}{\mu_v}\begin{pmatrix} \mu_v\tilde{\varepsilon}_h - p_y^2 & p_x p_y \\ p_x p_y & \mu_v\tilde{\varepsilon}_h - p_x^2 \end{pmatrix}. \tag{118}$$

The eigenvalues of $\boldsymbol{A}$ now become

$$p_{z\mathrm{I}} = -p_{z\mathrm{III}} = \sqrt{\mu_h\tilde{\varepsilon}_h - \frac{\mu_h}{\mu_v}\left(p_x^2 + p_y^2\right)}, \tag{119a}$$

$$p_{z\mathrm{II}} = -p_{z\mathrm{IV}} = \sqrt{\mu_h\tilde{\varepsilon}_h - \frac{\tilde{\varepsilon}_h}{\tilde{\varepsilon}_v}\left(p_x^2 + p_y^2\right)}. \tag{119b}$$

The eigenvector matrix and its inverse from eqs (101) and (102) have the submatrices:

$$\boldsymbol{N}_E = \frac{1}{p_\rho}\begin{pmatrix} p_y\sqrt{\frac{\mu_h}{p_{z\mathrm{I}}}} & p_x\sqrt{\frac{p_{z\mathrm{II}}}{\tilde{\varepsilon}_h}} \\ -p_x\sqrt{\frac{\mu_h}{p_{z\mathrm{I}}}} & p_y\sqrt{\frac{p_{z\mathrm{II}}}{\tilde{\varepsilon}_h}} \end{pmatrix} \quad \text{and} \quad \boldsymbol{N}_H = \frac{1}{p_\rho}\begin{pmatrix} p_y\sqrt{\frac{p_{z\mathrm{I}}}{\mu_h}} & p_x\sqrt{\frac{\tilde{\varepsilon}_h}{p_{z\mathrm{II}}}} \\ -p_x\sqrt{\frac{p_{z\mathrm{I}}}{\mu_h}} & p_y\sqrt{\frac{\tilde{\varepsilon}_h}{p_{z\mathrm{II}}}} \end{pmatrix}, \tag{120}$$

where $p_\rho = \sqrt{p_x^2 + p_y^2}$.

10.1 Reflection and transmission matrices

In the TIV-case, explicit expressions for the reflection and transmission matrices can be derived by inserting eq. (120) into (115) and using eq. (114):

$$\grave{\boldsymbol{t}} = \begin{pmatrix} \frac{2\sqrt{\mu_h^- \mu_h^+ p_{z\mathrm{I}}^- p_{z\mathrm{I}}^+}}{\mu_h^+ p_{z\mathrm{I}}^- + \mu_h^- p_{z\mathrm{I}}^+} & 0 \\ 0 & \frac{2\sqrt{\tilde{\varepsilon}_h^- \tilde{\varepsilon}_h^+ p_{z\mathrm{II}}^- p_{z\mathrm{II}}^+}}{\tilde{\varepsilon}_h^- p_{z\mathrm{II}}^+ + \tilde{\varepsilon}_h^+ p_{z\mathrm{II}}^-} \end{pmatrix} \quad \grave{\boldsymbol{r}} = \begin{pmatrix} \frac{\mu_h^+ p_{z\mathrm{I}}^- - \mu_h^- p_{z\mathrm{I}}^+}{\mu_h^+ p_{z\mathrm{I}}^- + \mu_h^- p_{z\mathrm{I}}^+} & 0 \\ 0 & \frac{\tilde{\varepsilon}_h^- p_{z\mathrm{II}}^+ - \tilde{\varepsilon}_h^+ p_{z\mathrm{II}}^-}{\tilde{\varepsilon}_h^- p_{z\mathrm{II}}^+ + \tilde{\varepsilon}_h^+ p_{z\mathrm{II}}^-} \end{pmatrix}. \tag{121}$$

Since these matrices are diagonal, the relations in eq. (113) and eq. (116) lead to

$$\acute{\boldsymbol{t}} = \grave{\boldsymbol{t}} \quad \text{and} \quad \acute{\boldsymbol{r}} = -\grave{\boldsymbol{r}}. \tag{122}$$

In eq. (121) the reflection coefficients are recognized as the Fresnel coefficients for transversal electric (TE) and transversal magnetic (TM) polarization (*cf.* Stratton 1941; Jackson 1998). Thus, in the TIV-case, the eigenvalue $p_{z\mathrm{I}}$ corresponds to a TE-mode, and the eigenvalue $p_{z\mathrm{II}}$ corresponds to a TM-mode. The transmission coefficients are symmetric across the interface. In order to obtain the Fresnel transmission coefficients, another normalization of the eigenvectors can be chosen as shown in Appendix E.

10.2 Recursive reflection and transmission responses

When the transmission and reflection matrices describing propagation through one interface are diagonal, the expressions in eqs (70) and (71) simplify. The result is scalar recursive reflection and transmission (RT) responses valid for both modes. By using the relations in eq. (117) and (122), one gets:

$$R_m = \frac{r_m + R_{m+1}}{1 + r_m R_{m+1}} \mathrm{e}^{2i\omega p_z h_m}, \tag{123a}$$

$$T_m = \frac{t_m T_{m+1}}{1 + r_m R_{m+1}} \mathrm{e}^{i\omega p_z h_m}, \tag{123b}$$

where $p_z = p_{z\mathrm{I}}$ for the TE-mode and $p_z = p_{z\mathrm{II}}$ for the TM-mode. It is implicit that the eigenvalues take their respective values in the m'th layer. The initial conditions at the start of the stack are $R_{M+1} = 0$ and $T_{M+1} = \mathrm{e}^{i\omega p_z h_{M+1}}$. The expressions can be used both for upgoing and downgoing reflection and transmission coefficients. In both cases h_m describes the thickness from the m'th interface, where r_m and t_m are evaluated, to the z-level of R_m and t_m.

11 ISOTROPIC MEDIA

In isotropic media the system matrix has the same form as in eq. (95), but now

$$\boldsymbol{A}_1 = \frac{1}{\tilde{\varepsilon}}\begin{pmatrix} \mu\tilde{\varepsilon} - p_x^2 & -p_x p_y \\ -p_x p_y & \mu\tilde{\varepsilon} - p_y^2 \end{pmatrix}, \quad \boldsymbol{A}_2 = \frac{1}{\mu}\begin{pmatrix} \mu\tilde{\varepsilon} - p_y^2 & p_x p_y \\ p_x p_y & \mu\tilde{\varepsilon} - p_x^2 \end{pmatrix}, \tag{124}$$

and the eigenvalues are

$$p_z = p_{z\mathrm{I}} = p_{z\mathrm{II}} = -p_{z\mathrm{III}} = -p_{z\mathrm{IV}} = \sqrt{\mu\tilde{\varepsilon} - p_x^2 - p_y^2}. \tag{125}$$

Because of the degeneracy of the eigenvalues there are several possibilities for choosing a linear independent set of 4 eigenvectors that satisfy the flux normalization condition. It will however be convenient to choose the same form of the eigenvector matrix as in the TIV-case. Thus, the same eigenvector matrices as in eq. (120) can be used with $\mu_h = \mu_v = \mu$, $\tilde{\varepsilon}_h = \tilde{\varepsilon}_v = \tilde{\varepsilon}$ and $p_{z\mathrm{I}} = p_{z\mathrm{II}} = p_z$. All the relations that have been derived and will be derived for TIV-media are hence valid for isotropic media.

12 EXPLICIT EXPRESSIONS FOR THE ELECTROMAGNETIC FIELDS

By using eqs (76) and (81) the electromagnetic field in a stratified medium with general anisotropy in *all* the layers can be obtained. However, in many applications in geophysics the source medium is isotropic or transversally isotropic in the vertical direction. The purpose in this section is to derive explicit expressions for the electromagnetic fields from sources that are either a horizontal electric dipole (HED), vertical electric dipole (VED), horizontal magnetic dipole (HMD) or vertical magnetic dipole (VMD), when the source and receiver are situated in TIV or isotropic media. The infinitesimal dipole source is contained in one of the layers as shown in Fig. 2, and the resulting electromagnetic field can be obtained in any TIV or isotropic layer from the explicit expressions that will be derived. In all layers other than the source and receiver layer(s), the anisotropy may be arbitrary.

The field expressions are given in the frequency–wavenumber domain, and a 2-D Fourier transform is required in order to get to the spatial domain. It is only in the case of having TIV or isotropy in all the layers that the transformation to the spatial domain can be reduced to a single integral by using cylindrical coordinates. The field expressions for such cases are given in Appendix F.

12.1 Up/down-symmetry in the source and receiver layer(s)

If the source and receiver layers have u/d-symmetry, the expressions for the mode-field vectors in eqs (76) and (81), and the corresponding physical field vectors $\boldsymbol{b} = (\boldsymbol{b}_E;\ \boldsymbol{b}_H)$, simplify. The resulting fields from the four types of sources (HED, HMD, VED, and VMD) are considered. The source vectors from eq. (16) is split into $\boldsymbol{s}_E = (\boldsymbol{s}_E^v;\ \boldsymbol{s}_E^h)$ and $\boldsymbol{s}_M = (\boldsymbol{s}_M^h;\ \boldsymbol{s}_M^v)$. The different source types in the mode-field domain then become

$$\begin{aligned} &\text{HED}: \grave{\Sigma} = -\acute{\Sigma} = -\boldsymbol{N}_E^T \boldsymbol{s}_E^h/\sqrt{2} \quad \text{and} \quad \text{VED}: \grave{\Sigma} = \acute{\Sigma} = \boldsymbol{N}_H^T \boldsymbol{s}_E^v/\sqrt{2}, \\ &\text{HMD}: \grave{\Sigma} = \acute{\Sigma} = \boldsymbol{N}_H^T \boldsymbol{s}_M^h/\sqrt{2} \quad \text{and} \quad \text{VMD}: \grave{\Sigma} = -\acute{\Sigma} = -\boldsymbol{N}_E^T \boldsymbol{s}_M^v/\sqrt{2}, \end{aligned} \tag{126}$$

where eq. (44) with the eigenvector matrices from eq. (101) has been used. The electromagnetic field is then given for any of these sources by the expression

$$\boldsymbol{b}_E = \boldsymbol{N}_E\, \boldsymbol{\mathcal{R}}\ \grave{\Sigma}/\sqrt{2} \quad \text{and} \quad \boldsymbol{b}_H = \boldsymbol{N}_H\, \boldsymbol{\mathcal{R}}\ \grave{\Sigma}/\sqrt{2}, \tag{127}$$

where the coefficient matrices $\boldsymbol{\mathcal{R}}$ (RT-amplitudes) are, respectively, $\boldsymbol{\mathcal{R}}^A$ and $\boldsymbol{\mathcal{R}}^D$ for the electric and magnetic field components in case of a HED and VMD. When the source is a HMD or a VED, the coefficient matrices for the electric and magnetic fields are $\boldsymbol{\mathcal{R}}^B$ and $\boldsymbol{\mathcal{R}}^C$, respectively. The RT-amplitudes above the source $z < z_s$ are:

$$\acute{\boldsymbol{\mathcal{R}}}^A = (\boldsymbol{I} + \acute{\boldsymbol{R}}_a)(\boldsymbol{I} - \grave{\boldsymbol{R}}_u \acute{\boldsymbol{R}}_a)^{-1} \acute{\boldsymbol{T}}_u (\boldsymbol{I} - \grave{\boldsymbol{R}}_s \acute{\boldsymbol{R}}_s)^{-1} (\grave{\boldsymbol{R}}_s + \boldsymbol{I}), \tag{128a}$$

$$\acute{\boldsymbol{\mathcal{R}}}^B = (\boldsymbol{I} + \acute{\boldsymbol{R}}_a)(\boldsymbol{I} - \grave{\boldsymbol{R}}_u \acute{\boldsymbol{R}}_a)^{-1} \acute{\boldsymbol{T}}_u (\boldsymbol{I} - \grave{\boldsymbol{R}}_s \acute{\boldsymbol{R}}_s)^{-1} (\grave{\boldsymbol{R}}_s - \boldsymbol{I}), \tag{128b}$$

$$\acute{\boldsymbol{\mathcal{R}}}^C = (\boldsymbol{I} - \acute{\boldsymbol{R}}_a)(\boldsymbol{I} - \grave{\boldsymbol{R}}_u \acute{\boldsymbol{R}}_a)^{-1} \acute{\boldsymbol{T}}_u (\boldsymbol{I} - \grave{\boldsymbol{R}}_s \acute{\boldsymbol{R}}_s)^{-1} (\grave{\boldsymbol{R}}_s - \boldsymbol{I}), \tag{128c}$$

$$\acute{\boldsymbol{\mathcal{R}}}^D = (\boldsymbol{I} - \acute{\boldsymbol{R}}_a)(\boldsymbol{I} - \grave{\boldsymbol{R}}_u \acute{\boldsymbol{R}}_a)^{-1} \acute{\boldsymbol{T}}_u (\boldsymbol{I} - \grave{\boldsymbol{R}}_s \acute{\boldsymbol{R}}_s)^{-1} (\grave{\boldsymbol{R}}_s + \boldsymbol{I}), \tag{128d}$$

and the RT-amplitudes below the source $z > z_s$ are:

$$\grave{\boldsymbol{\mathcal{R}}}^A = (\grave{\boldsymbol{R}}_b + \boldsymbol{I})(\boldsymbol{I} - \acute{\boldsymbol{R}}_d \grave{\boldsymbol{R}}_b)^{-1} \grave{\boldsymbol{T}}_d (\boldsymbol{I} - \acute{\boldsymbol{R}}_s \grave{\boldsymbol{R}}_s)^{-1} (\boldsymbol{I} + \acute{\boldsymbol{R}}_s), \tag{128e}$$

$$\grave{\boldsymbol{\mathcal{R}}}^B = (\grave{\boldsymbol{R}}_b + \boldsymbol{I})(\boldsymbol{I} - \acute{\boldsymbol{R}}_d \grave{\boldsymbol{R}}_b)^{-1} \grave{\boldsymbol{T}}_d (\boldsymbol{I} - \acute{\boldsymbol{R}}_s \grave{\boldsymbol{R}}_s)^{-1} (\boldsymbol{I} - \acute{\boldsymbol{R}}_s), \tag{128f}$$

$$\grave{\boldsymbol{\mathcal{R}}}^C = (\grave{\boldsymbol{R}}_b - \boldsymbol{I})(\boldsymbol{I} - \acute{\boldsymbol{R}}_d \grave{\boldsymbol{R}}_b)^{-1} \grave{\boldsymbol{T}}_d (\boldsymbol{I} - \acute{\boldsymbol{R}}_s \grave{\boldsymbol{R}}_s)^{-1} (\boldsymbol{I} - \acute{\boldsymbol{R}}_s), \tag{128g}$$

$$\grave{\boldsymbol{\mathcal{R}}}^D = (\grave{\boldsymbol{R}}_b - \boldsymbol{I})(\boldsymbol{I} - \acute{\boldsymbol{R}}_d \grave{\boldsymbol{R}}_b)^{-1} \grave{\boldsymbol{T}}_d (\boldsymbol{I} - \acute{\boldsymbol{R}}_s \grave{\boldsymbol{R}}_s)^{-1} (\boldsymbol{I} + \acute{\boldsymbol{R}}_s). \tag{128h}$$

The reflection and transmission matrices can be calculated from the relations in eq. (71) and (70). The single interface reflection and transmission are described by eq. (63).

12.2 RT-responses and polarization modes

In TIV or isotropic media the direction of the wavenumber vector for a plane-wave constituent and the electric and magnetic field components form an orthogonal system (*cf.* Appendix C). This means that in presence of an interface, the electromagnetic field can be decomposed into a TE and TM polarization mode. The interface normal and the wavenumber direction form the *plane of incidence*. The electromagnetic field component where the electric field is normal to the plane of incidence is referred to as the TE-mode, and the field component where the magnetic field is normal to the plane of incidence is referred to as the TM-mode.

For reflection and transmission in TIV-media there is no coupling of the polarization modes as seen from eq. (121), since the reflection and transmission matrices are diagonal. From eq. (119) it can be observed that the vertical slowness that corresponds to the TE-mode is governed by anisotropy in the magnetic permeability, whereas the vertical slowness that corresponds to the TM-mode is governed by anisotropy in the complex electric permittivity. The modes are obviously also decoupled for reflection and transmission at interfaces between TIV *and* isotropic media or between isotropic media. For isotropic media the slownesses are equal, *cf.* eq. (125).

At interfaces between media with more complicated anisotropy than TIV, the off-diagonal elements of the reflection and transmission matrices (*cf.* eqs (63) and (114)) are non-zero and thus the polarization modes are coupled. However, in a general anisotropic homogeneous region there are no pure TE- and TM-polarization modes since the propagation direction is not orthogonal to the field components (*cf.* Appendix C). We will refer to the modes in such regions as quasi-TE (qTE) and quasi-TM (qTM). When the anisotropy simplifies into TIV, the qTE-mode should then correspond to the TE-mode, and likewise the qTM-mode should give a TM-mode.

Consider the matrix expressions in eq. (1280) which can be written as:

$$\boldsymbol{\mathcal{R}} = \begin{pmatrix} \mathcal{R}_{11} & \mathcal{R}_{12} \\ \mathcal{R}_{21} & \mathcal{R}_{22} \end{pmatrix}, \tag{129}$$

where the notation $\boldsymbol{\mathcal{R}}$ refers to all the eight different reflection and transmission responses in eq. (128). Let eq. (129) represent the RT-response in a TIV or isotropic medium from an anisotropic stack due to a source in a TIV or isotropic medium. The sorting of eigenvalues in eq. (119) then means that the subscript 1 in the matrix elements in eq. (129) is related to the TE-mode, whereas the subscript 2 is related to the TM-mode. Thus the emitted TE-polarization and the resulting TE-mode response is represented by $\mathcal{R}_{11}$ whereas $\mathcal{R}_{12}$ is the resulting TM-mode from the TE-radiation. In the same manner, the emitted TM-polarization is represented by $\mathcal{R}_{21}$ and $\mathcal{R}_{22}$ where the latter is the TM-mode in the resulting electromagnetic field and $\mathcal{R}_{21}$ is the TE-mode due to the radiated TM-mode. In short, subscript 11 implies TE → TE, 12 is TE → TM, 21 is TM → TE, and 22 is TM → TM. Note however, that in a stack with general anisotropy the $\mathcal{R}_{11}$-response will contain responses which have been converted from TM to TE and then back from TM to TE within the stack. In the same manner the $\mathcal{R}_{22}$-response is not a pure TM-response.

When all the layers in the stratified model are TIV or isotropic, there is no crosscoupling between the modes. Then the entries $\mathcal{R}_{12}$ and $\mathcal{R}_{21}$ are zero, and the calculation of the RT-response reduces to a scalar problem in terms of the TE- and TM-mode.

12.3 Horizontal electric dipole

For a HED in the x-direction, the source vector from eq. (16) is $\boldsymbol{s} = (0\ 0\ J_x\ 0)^T$ where J_x is given by eq. (17a) and the delta function is accounted for in eq. (45). Using eq. (126) this leads to

$$\grave{\boldsymbol{\Sigma}} = -\acute{\boldsymbol{\Sigma}} = -\frac{1}{\sqrt{2}}\boldsymbol{N}_E^T \begin{pmatrix} J_x \\ 0 \end{pmatrix} = -\frac{Il_x}{\sqrt{2}p_\rho} \begin{pmatrix} p_y \mathcal{E}_s \\ p_x \mathcal{M}_s^{-1} \end{pmatrix}, \tag{130}$$

where the eigenvector submatrix from eq. (120) has been used since the source is assumed to be in a TIV layer, and where the variables

$$\mathcal{E} = \sqrt{\frac{\mu_h}{p_{zI}}} \quad \text{and} \quad \mathcal{M} = \sqrt{\frac{\varepsilon_h}{p_{zII}}}, \tag{131}$$

have been introduced to simplify notation. The subscript s implies material parameters within the source layer. The electromagnetic field is given by eq. (127):

$$\boldsymbol{b}(z) = \frac{1}{\sqrt{2}} \begin{pmatrix} \boldsymbol{N}_E \boldsymbol{\mathcal{R}}^A \\ \boldsymbol{N}_H \boldsymbol{\mathcal{R}}^D \end{pmatrix} \grave{\boldsymbol{\Sigma}}(z_s). \tag{132}$$

The expression is valid for $z < z_s$; then $\boldsymbol{\mathcal{R}} \to \acute{\boldsymbol{\mathcal{R}}}$, and $z > z_s$ which implies that $\boldsymbol{\mathcal{R}} \to \grave{\boldsymbol{\mathcal{R}}}$. Written explicitly, the electric and magnetic fields become:

$$E_x = -\frac{Il_x}{2p_\rho^2}\left[\mathcal{E}\mathcal{E}_s p_y^2 \mathcal{R}_{11}^A + \frac{\mathcal{E}}{\mathcal{M}_s} p_y p_x \mathcal{R}_{12}^A + \frac{\mathcal{E}_s}{\mathcal{M}} p_x p_y \mathcal{R}_{21}^A + \frac{1}{\mathcal{M}\mathcal{M}_s} p_x^2 \mathcal{R}_{22}^A\right], \tag{133a}$$

$$E_y = -\frac{Il_x}{2p_\rho^2}\left[-\mathcal{E}\mathcal{E}_s p_x p_y \mathcal{R}_{11}^A - \frac{\mathcal{E}}{\mathcal{M}_s} p_x^2 \mathcal{R}_{12}^A + \frac{\mathcal{E}_s}{\mathcal{M}} p_y^2 \mathcal{R}_{21}^A + \frac{1}{\mathcal{M}\mathcal{M}_s} p_y p_x \mathcal{R}_{22}^A\right], \tag{133b}$$

$$H_y = +\frac{Il_x}{2p_\rho^2}\left[\frac{\mathcal{E}_s}{\mathcal{E}} p_y^2 \mathcal{R}_{11}^D + \frac{1}{\mathcal{E}\mathcal{M}_s} p_y p_x \mathcal{R}_{12}^D + \mathcal{M}\mathcal{E}_s p_x p_y \mathcal{R}_{21}^D + \frac{\mathcal{M}}{\mathcal{M}_s} p_x^2 \mathcal{R}_{22}^D\right], \tag{133c}$$

$$H_x = -\frac{Il_x}{2p_\rho^2}\left[-\frac{\mathcal{E}_s}{\mathcal{E}}p_x p_y \mathcal{R}_{11}^D - \frac{1}{\mathcal{E}\mathcal{M}_s}p_x^2\mathcal{R}_{12}^D + \mathcal{M}\mathcal{E}_s p_y^2\mathcal{R}_{21}^D + \frac{\mathcal{M}}{\mathcal{M}_s}p_y p_x \mathcal{R}_{22}^D\right]. \tag{133d}$$

The z-components of the electric and magnetic fields are found using eq. (15a) and (b), respectively, and become:

$$E_z = -\frac{Il_x}{2\tilde{\varepsilon}_v}\left[\mathcal{M}\mathcal{E}_s p_y \mathcal{R}_{21}^D + \frac{\mathcal{M}}{\mathcal{M}_s}p_x \mathcal{R}_{22}^D\right], \tag{133e}$$

$$H_z = \frac{Il_x}{2\mu_v}\left[\mathcal{E}\mathcal{E}_s p_y \mathcal{R}_{11}^A + \frac{\mathcal{E}}{\mathcal{M}_s}p_x \mathcal{R}_{12}^A\right]. \tag{133f}$$

The electromagnetic field from a HED in the y-direction is found by letting $p_x J_x \to p_y J_y$ and $p_y J_x \to -p_x J_y$ in the equations above. When performing the substitution in expressions where both p_x and p_y is present, it is the rightmost slowness parameter that must be used (i.e. by the notation used here it is this slowness parameter that can be ascribed to the source transformation).

In cases where all the layers are TIV (or isotropic), the RT-response simplifies. The crosscoupling coefficients are $\mathcal{R}_{12} = 0$ and $\mathcal{R}_{21} = 0$ in this case. The responses for the TE- and the TM-mode ($\mathcal{R}_{11}$ and $\mathcal{R}_{22}$, respectively) are then given by the same scalar expression. For $z > z_s$ the RT-amplitudes are

$$\grave{\mathcal{R}}_A = \grave{T}_d \frac{\grave{R}_b + 1}{1 - \acute{R}_d \grave{R}_b}\frac{1 + \acute{R}_s}{1 - \acute{R}_s \grave{R}_s}, \tag{134a}$$

$$\grave{\mathcal{R}}_D = \grave{T}_d \frac{\grave{R}_b - 1}{1 - \acute{R}_d \grave{R}_b}\frac{1 + \acute{R}_s}{1 - \acute{R}_s \grave{R}_s}, \tag{134b}$$

and for $z < z_s$ the RT-amplitudes are

$$\acute{\mathcal{R}}_A = \acute{T}_u \frac{1 + \acute{R}_a}{1 - \grave{R}_u \acute{R}_a}\frac{1 + \grave{R}_s}{1 - \grave{R}_s \acute{R}_s}, \tag{134c}$$

$$\acute{\mathcal{R}}_D = \acute{T}_u \frac{1 - \acute{R}_a}{1 - \grave{R}_u \acute{R}_a}\frac{1 + \grave{R}_s}{1 - \grave{R}_s \acute{R}_s}. \tag{134d}$$

12.4 Horizontal magnetic dipole

A HMD implies that the source term from eq. (16) becomes $\boldsymbol{s} = (0 \;\; J_x^M \;\; 0 \;\; 0)^T$. In TIV-media the HMD-source in eq. (17d) reduces to $J_x^M = -i\omega\mu_h I a_x \delta(z - z_s)$. The source in the mode-domain can thus be written:

$$\grave{\boldsymbol{\Sigma}} = \acute{\boldsymbol{\Sigma}} = \frac{1}{\sqrt{2}}\boldsymbol{N}_H^T\begin{pmatrix}0\\ J_x^M\end{pmatrix} = \frac{-i\omega\mu_h^s I a_x}{\sqrt{2}p_\rho}\begin{pmatrix}-p_x\mathcal{E}_s^{-1}\\ p_y\mathcal{M}_s\end{pmatrix}, \tag{135}$$

where the superscript s on μ_h refers to the permeability in the source layer. To obtain the electromagnetic field, the expression in eq. (127) is used:

$$\boldsymbol{b}(z) = \frac{1}{\sqrt{2}}\begin{pmatrix}\boldsymbol{N}_E\boldsymbol{\mathcal{R}}^B\\ \boldsymbol{N}_H\boldsymbol{\mathcal{R}}^C\end{pmatrix}\grave{\boldsymbol{\Sigma}}(z_s). \tag{136}$$

Written explicitly the electric and magnetic fields become:

$$E_x = -\frac{i\omega\mu_h^s I a_x}{2p_\rho^2}\left[-\frac{\mathcal{E}}{\mathcal{E}_s}p_y p_x \mathcal{R}_{11}^B + \mathcal{E}\mathcal{M}_s p_y^2\mathcal{R}_{12}^B - \frac{1}{\mathcal{M}\mathcal{E}_s}p_x^2\mathcal{R}_{21}^B + \frac{\mathcal{M}_s}{\mathcal{M}}p_x p_y \mathcal{R}_{22}^B\right], \tag{137a}$$

$$E_y = -\frac{i\omega\mu_h^s I a_x}{2p_\rho^2}\left[\frac{\mathcal{E}}{\mathcal{E}_s}p_x^2\mathcal{R}_{11}^B - \mathcal{E}\mathcal{M}_s p_x p_y \mathcal{R}_{12}^B - \frac{1}{\mathcal{M}\mathcal{E}_s}p_y p_x \mathcal{R}_{21}^B + \frac{\mathcal{M}_s}{\mathcal{M}}p_y^2\mathcal{R}_{22}^B\right], \tag{137b}$$

$$H_y = +\frac{i\omega\mu_h^s I a_x}{2p_\rho^2}\left[-\frac{1}{\mathcal{E}\mathcal{E}_s}p_y p_x \mathcal{R}_{11}^C + \frac{\mathcal{M}_s}{\mathcal{E}}p_y^2\mathcal{R}_{12}^C - \frac{\mathcal{M}}{\mathcal{E}_s}p_x^2\mathcal{R}_{21}^C + \mathcal{M}\mathcal{M}_s p_x p_y \mathcal{R}_{22}^C\right], \tag{137c}$$

$$H_x = -\frac{i\omega\mu_h^s I a_x}{2p_\rho^2}\left[\frac{1}{\mathcal{E}\mathcal{E}_s}p_x^2\mathcal{R}_{11}^C - \frac{\mathcal{M}_s}{\mathcal{E}}p_x p_y \mathcal{R}_{12}^C - \frac{\mathcal{M}}{\mathcal{E}_s}p_y p_x \mathcal{R}_{21}^C + \mathcal{M}\mathcal{M}_s p_y^2\mathcal{R}_{22}^C\right]. \tag{137d}$$

The z-components are found using eq. (15):

$$E_z = -\frac{i\omega\mu_h^s I a_x}{2\tilde{\varepsilon}_v}\left[-\frac{\mathcal{M}}{\mathcal{E}_s}p_x \mathcal{R}_{21}^C + \mathcal{M}\mathcal{M}_s p_y \mathcal{R}_{22}^C\right], \tag{137e}$$

$$H_z = -\frac{i\omega\mu_h^s I a_x}{2\mu_v}\left[\frac{\mathcal{E}}{\mathcal{E}_s}p_x \mathcal{R}_{11}^B - \mathcal{E}\mathcal{M}_s p_y \mathcal{R}_{12}^B\right]. \tag{137f}$$

It can be seen from eqs (133) and (137) that there is a duality between the electromagnetic field from a magnetic and an electric dipole, a subject that is treated in Appendix B. The fields from a source in the y-direction can be found by letting $p_x J_x^M \to p_y J_y^M$ and $p_y J_x^M \to -p_x J_y^M$.

If all the layers are TIV or isotropic, the crosscoupling terms are zero and the TE-mode and TM-mode responses are both given by:

$$\grave{\mathcal{R}}_B = \grave{T}_d \frac{\grave{R}_b + 1}{1 - \acute{R}_d \grave{R}_b} \frac{1 - \acute{R}_s}{1 - \acute{R}_s \grave{R}_s}, \tag{138a}$$

$$\grave{\mathcal{R}}_C = \grave{T}_d \frac{\grave{R}_b - 1}{1 - \acute{R}_d \grave{R}_b} \frac{1 - \acute{R}_s}{1 - \acute{R}_s \grave{R}_s}, \tag{138b}$$

when $z > z_s$. For $z < z_s$ the RT-amplitudes are

$$\acute{\mathcal{R}}_B = \acute{T}_u \frac{1 + \acute{R}_a}{1 - \grave{R}_u \acute{R}_a} \frac{\grave{R}_s - 1}{1 - \grave{R}_s \acute{R}_s}, \tag{138c}$$

$$\acute{\mathcal{R}}_C = \acute{T}_u \frac{1 - \acute{R}_a}{1 - \grave{R}_u \acute{R}_a} \frac{\grave{R}_s - 1}{1 - \grave{R}_s \acute{R}_s}. \tag{138d}$$

12.5 Vertical electric dipole

The source term for a VED is given by eq. (16) as $\boldsymbol{s} = (p_x J_z/\tilde{\varepsilon}_v \;\; p_y J_z/\tilde{\varepsilon}_v \;\; 0 \;\; 0)^T$ where J_z is given by eq. (17c). Thus,

$$\grave{\boldsymbol{\Sigma}} = \acute{\boldsymbol{\Sigma}} = \frac{J_z}{\sqrt{2}\tilde{\varepsilon}_v^s} \boldsymbol{N}_H^T \begin{pmatrix} p_x \\ p_y \end{pmatrix} = \frac{I l_z p_\rho}{\sqrt{2}\tilde{\varepsilon}_v^s} \begin{pmatrix} 0 \\ \mathcal{M}_s \end{pmatrix}, \tag{139}$$

where the superscript s on $\tilde{\varepsilon}_h$ refers to the complex premittivity in the source layer. Since the upgoing radiation of the mode-source vector equals the downgoing radiation, the VED has the same scattering coefficients as the HMD in eq. (136). Since the uppermost element in eq. (139) is zero this means that

$$E_x = \frac{I l_z}{2\tilde{\varepsilon}_v^s} \left[\mathcal{E}\mathcal{M}_s p_y \mathcal{R}_{12}^B + \frac{\mathcal{M}_s}{\mathcal{M}} p_x \mathcal{R}_{22}^B \right], \tag{140a}$$

$$E_y = \frac{I l_z}{2\tilde{\varepsilon}_v^s} \left[-\mathcal{E}\mathcal{M}_s p_x \mathcal{R}_{12}^B + \frac{\mathcal{M}_s}{\mathcal{M}} p_y \mathcal{R}_{22}^B \right], \tag{140b}$$

$$H_y = -\frac{I l_z}{2\tilde{\varepsilon}_v^s} \left[\frac{\mathcal{M}_s}{\mathcal{E}} p_y \mathcal{R}_{12}^C + \mathcal{M}\mathcal{M}_s p_x \mathcal{R}_{22}^C \right], \tag{140c}$$

$$H_x = \frac{I l_z}{2\tilde{\varepsilon}_v^s} \left[-\frac{\mathcal{M}_s}{\mathcal{E}} p_x \mathcal{R}_{12}^C + \mathcal{M}\mathcal{M}_s p_y \mathcal{R}_{22}^C \right]. \tag{140d}$$

The vertical electric and magnetic components become (using eq. 15):

$$E_z = \frac{I l_z p_\rho^2}{2\tilde{\varepsilon}_v^s \tilde{\varepsilon}_v} \mathcal{M}\mathcal{M}_s \mathcal{R}_{22}^C + \frac{1}{i\omega\tilde{\varepsilon}_v^s} I l_z \delta(z_s), \tag{140e}$$

$$H_z = -\frac{I l_z p_\rho^2}{2\tilde{\varepsilon}_v^s \mu_v} \mathcal{E}\mathcal{M}_s \mathcal{R}_{12}^B. \tag{140f}$$

When all the layers are TIV or isotropic the VED has pure TM-polarization components only, and there is no vertical magnetic field ($H_z = 0$).

12.6 Vertical magnetic dipole

The VMD-source is described by eq. (16) as $\boldsymbol{s} = (0 \; 0 - p_y J_z^M/\mu_v \; p_x J_z^M/\mu_v)^T$. By using the expression for J_z^M from eq. (17f), which in TIV-media reduces to $J_z^M = -i\omega\mu_v I a_z \delta(z - z_s)$, one gets

$$\grave{\boldsymbol{\Sigma}} = -\acute{\boldsymbol{\Sigma}} = -\frac{J_z^M}{\sqrt{2}\mu_v^s} \boldsymbol{N}_E^T \begin{pmatrix} -p_y \\ p_x \end{pmatrix} = \frac{-i\omega I a_z p_p}{\sqrt{2}} \begin{pmatrix} \mathcal{E}_s \\ 0 \end{pmatrix}. \tag{141}$$

Since $\grave{\boldsymbol{\Sigma}} = -\acute{\boldsymbol{\Sigma}}$, the VMD has the same scattering coefficients as the field from a HED, *cf.* eq. (132). Then

$$E_x = -\frac{i\omega I a_z}{2} \left[\mathcal{E}\mathcal{E}_s p_y \mathcal{R}_{11}^A + \frac{\mathcal{E}_s}{\mathcal{M}} p_x \mathcal{R}_{21}^A \right], \tag{142a}$$

$$E_y = -\frac{i\omega I a_z}{2}\left[-\mathcal{E}\mathcal{E}_s p_x \mathcal{R}_{11}^A + \frac{\mathcal{E}_s}{\mathcal{M}} p_y \mathcal{R}_{21}^A\right], \tag{142b}$$

$$H_y = \frac{i\omega I a_z}{2}\left[\frac{\mathcal{E}_s}{\mathcal{E}} p_y \mathcal{R}_{11}^D + \mathcal{M}\mathcal{E}_s p_x \mathcal{R}_{21}^D\right], \tag{142c}$$

$$H_x = -\frac{i\omega I a_z}{2}\left[-\frac{\mathcal{E}_s}{\mathcal{E}} p_x \mathcal{R}_{11}^D + \mathcal{M}\mathcal{E}_s p_y \mathcal{R}_{21}^D\right]. \tag{142d}$$

The z-components are found using eq. (15):

$$E_z = -\frac{i\omega I a_z p_\rho^2}{2\tilde{\varepsilon}_v}\mathcal{M}\mathcal{E}_s \mathcal{R}_{21}^D, \tag{142e}$$

$$H_z = \frac{i\omega I a_z p_\rho^2}{2\mu_v}\mathcal{E}\mathcal{E}_s \mathcal{R}_{11}^A - I a_z \delta(z_s). \tag{142f}$$

When all the layers are TIV or isotropic the VMD produces pure TE-polarization components and the vertical electric field is zero ($E_z = 0$).

13 NUMERICAL RESULTS

The theory for electromagnetic field propagation in stratified anisotropic media has been presented in a rather general form. As long as the constitutive relations are as given in eq. (2), the formalism can be applied to electromagnetic problems in geophysics from e.g. GPR to marine CSEM or SBL. The expressions in eqs (76) and (81) can be used to model electromagnetic fields from electric and magnetic dipole sources in stratified media with arbitrary anisotropy. Here, we apply the method to plane-layer marine CSEM modelling. We assume that the source and receiver layers are TIV, and thus, eqs (133), (137), (140), and (142) can be used to calculate the electromagnetic fields. Other layers than the source and receiver layer(s) may then have arbitrary anisotropy.

The expressions in eqs (133), (137), (140), and (142) are given in the frequency–wavenumber domain. In order to calculate the fields in the spatial domain, the 2-D inverse Fourier transform in eq. (6b) must be applied. We consider the frequency-domain field expressions since single frequency components of the source signal is studied. If the stratified medium is TIV in all the layers, the 2-D Fourier transform can be reduced to a 1-D Hankel transform due to the rotational symmetry. Explicit formulas for this are given in Appendix F.

The field expressions were implemented in FORTRAN 90. Since marine CSEM is a low-frequency application in conductive regions, the dielectric part of the permittivity dyad in eq. (3) is totally dominated by the conductivity dyad in all of the homogeneous regions, except in the air half-space. This implies that the wavenumber-domain field components will have large variations in strength, and in order to accurately calculate the fields in the spatial domain, the integration in the wavenumber domain requires large wavenumbers and careful sampling. We implemented the 2-D Fourier transform using adaptive Gauss-Legendre quadrature, and the integration was performed between zero crossings of the sine-function (extrema of the cosine-function). Series summation acceleration was implemented using continued fractions and Euler's method as described in Hänggi *et al.* (1998) and Press *et al.* (1997), respectively. For the types of input functions encountered here, numerical solutions to the Fourier transform that use logarithmic spacing are often very efficient. The digital filter method described by e.g. Anderson (1979), Mohsen & Hashish (1994) and Christensen (1990), was thus implemented. The efficiency and accuracy of the two different methods (numerical quadrature and digital filter) depend on the input function (Anderson 1989).

The various models that have been considered are shown in Fig. 5. For simplicity, the permeability is taken to be constant. Thus, this dyad is diagonal with all entries equal. The sea water is isotropic. In all of the figures the water depth is 300 m, the source height is 30 m, the thickness of the overburden is 1 km, and the reservoir is 100 m thick. Anisotropy in the overburden and reservoir is considered separately and for the two different cases of having a resistive reservoir and a conductive reservoir. The isotropic conductivities are $\sigma = 3.2\ \mathrm{S\,m^{-1}}$ for sea water and $\sigma_1 = 1.0\ \mathrm{S\,m^{-1}}$ for the overburden and bottom half-space ($\sigma_3 = \sigma_1$). The conductivity in the reservoir is $\sigma_2 = 0.01\ \mathrm{S\,m^{-1}}$ for the resistive case and $\sigma_2 = 0.5\ \mathrm{S\,m^{-1}}$ for the conductive case. To simplify interpretation, the anisotropy is taken to be transversally isotropic (uniaxial). We refer to the direction with different conductivity than the two other as the direction of anisotropy. In addition to the isotropic case, scenarios with transversal isotropy in the vertical direction (TIV), transversal isotropy in the horizontal direction (TIH), and dipping transversal isotropy (TID), are modelled. The conductivity in the anisotropy direction is taken to be one-fourth of the isotropic conductivity. This means for example that in the model with a TIV-overburden, the vertical conductivity is $\sigma_{1v} = 0.25\ \mathrm{S\,m^{-1}}$ whereas the horizontal conductivity is $\sigma_{1h} = 1.0\ \mathrm{S\,m^{-1}}$. For the resistive reservoir case, the vertical conductivity in a TIV-model is $\sigma_{2v} = 0.0025\ \mathrm{S\,m^{-1}}$, whereas the horizontal conductivity is $\sigma_{2h} = 0.01\ \mathrm{S\,m^{-1}}$. In the TIH-model, the azimuth angle between the direction of the source and anisotropy is 15° (*cf.* Fig. 1). When the model has dipping TID, the anisotropy direction has a 30° tilt from the vertical axis. This dip is furthermore taken to be in the direction of the source antenna. The source frequency is 0.25 Hz.

For simplicity we consider the inline electric field from a HED (e.g. the field component in the same direction as the source dipole). The plots are shown in Fig. 6 for the resistive reservoir case and Fig. 7 for the conductive reservoir. In both cases, Fig. (a) shows the magnitude versus offset (MVO) when the overburden is anisotropic, and Fig. b shows the phase response versus offset (PVO). Figs (c) and (d) show the MVO- and PVO-plots when the reservoir is anisotropic.

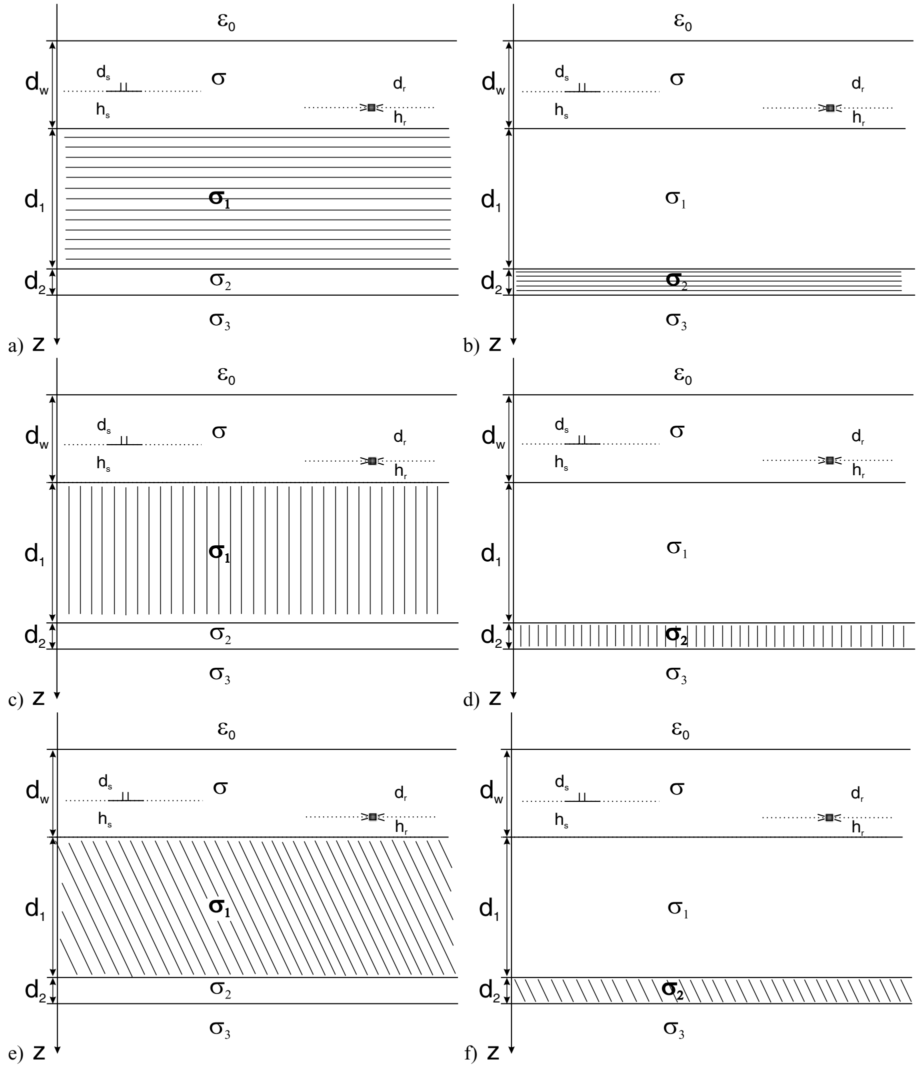

Figure 5. Anisotropy models for some idealized CSEM/SBL-scenarios. The figures to the left (right) illustrate anisotropy in the overburden (reservoir). Three basic uniaxial models are considered. Figures a and b show TIV-media, c and d illustrate TIH-media, and in e and f, media with dipping anisotropy (TID) are sketched.

In the resistive reservoir case, the MVO plot that describes anisotropy effects in the overburden shows an increase in response when anisotropy is present. This is due to the conductivity being less than in the isotropic case. Moreover, the response is largest for a TIH-overburden since it is this direction that has the strongest support of field propagation between the seafloor and the reservoir. To this end, note that there is a crosscoupling of polarization modes in the TIH-case. Using the same line of arguments, the effect of a dipping anisotropy should come out with magnitude in between the TIV- and the TIH-cases as shown in the modelling. The phase behaviour is a bit more involved. The signals propagate faster when anisotropy is present since they experience less conductivity. In consistency with the amplitude responses, at far offsets the TIH-model leads to faster propagation than the TID-model, and the TID-model implies faster propagation than the TIV-model. At intermediate distances, the behaviour is a bit more complicated since, in this case, the response from the guiding in the reservoir and the lateral field propagation along the seabed are nearly equal in magnitude.

A rough interpretation of the consequences of anisotropy effects in the reservoir can be made along the following lines: The response from the thin resistive layer is due to propagation in the horizontal direction of the reservoir and the important conductivity parameter is the vertical conductivity. The TIV-reservoir has less conductivity in the vertical direction than the isotropic model, and thus, the TIV-case should be expected to give an increase in the reservoir response. The same effect, but less, should be expected for the TID-reservoir, whereas TIH in the reservoir should not influence the response to any particular extent. From Figs 6(c) and (d) it can be observed that the behaviour of the modelled data has these characteristics. The dip in the phase curves for the isotropic and TIH case is due to the sea-surface response.

In the conductive reservoir case the thin layer has almost the same resistivity as the surrounding overburden and underburden (half the value). From Fig. 7 it can be observed that anisotropy in the overburden have pronounced effects on the response. The small variation in the isotropic conductivities leads to larger sensitivity to the anisotropy effects. The interplay between the lateral field propagation at the sea-surface and seafloor along with the reflection from the reservoir, leads to the TIV-model having the strongest response for small distances

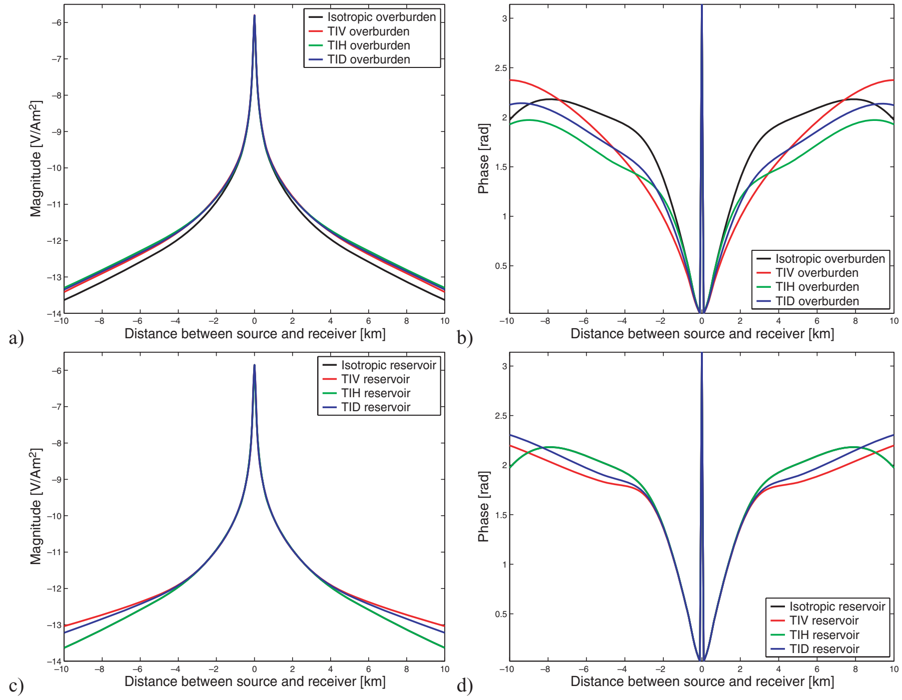

Figure 6. Modelling results for the anisotropic models in Fig. 5. Fig. (a) shows the amplitude response for various kinds of anisotropy effects in the overburden, whereas Fig. (b) shows the phase response. Figs (c) and (d) are the corresponding responses for an anisotropic reservoir. In all the figures the isotropic conductivity-contrast between the overburden and the reservoir is 100.

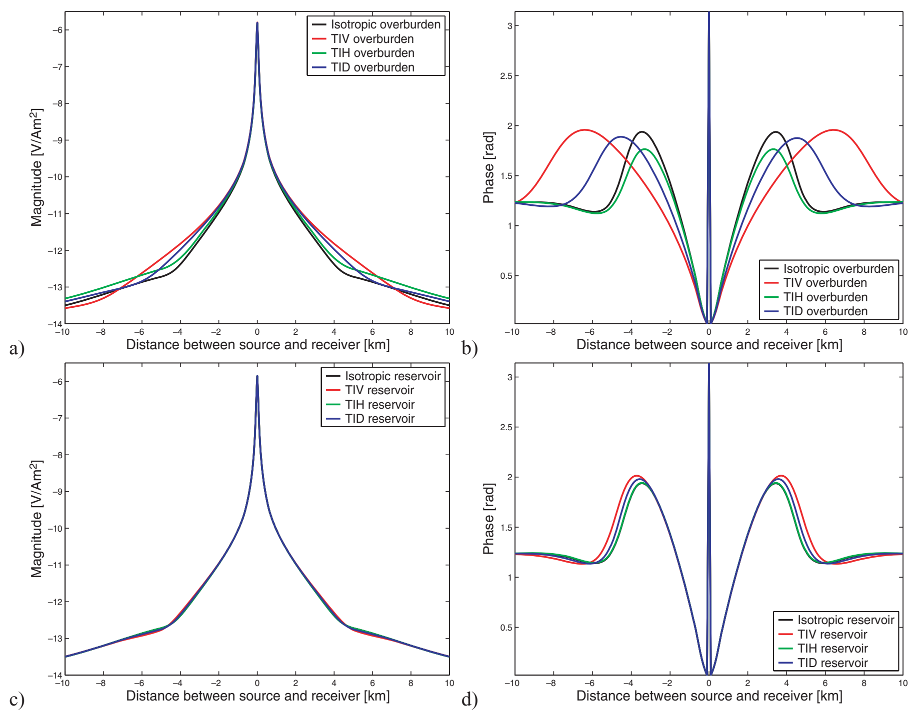

Figure 7. Modelling results for the anisotropic models in Fig. 5. The isotropic conductivity-contrast between the overburden and the reservoir is 2 in these simulations. Figs (a) and (b) show the effect of anisotropy in the overburden, and Figs (c) and (d) show the responses for an anisotropic reservoir with low resistivity.

and the TIH-model having the strongest response for larger distances. As seen from Figs 7(c) and (d), anisotropy in the reservoir has small effects on the response when the reservoir is conductive.

The purpose of the modelling examples is to illustrate some of the effects of anisotropy. Even if responses from isotropic models can be made to resemble more complicated anisotropic models (by carefully selecting the conductivity parameters in the direction normal to the propagation direction of the strongest signal contribution), isotropic models will seldom account for all the anisotropy effects. With one more degree of freedom, a TIV-model can obviously account for anisotropic effects better than an isotropic model, but not fully explain more complicated anisotropy phenomena. Another point to make by the simple modelling examples made here, is that anisotropy effects in the overburden might confuse the interpretation of the response from a reservoir if not carefully rendered.

14 CONCLUSIONS

Electromagnetic field propagation from electric and magnetic dipoles in planarly layered lossy anisotropic media has been considered. The set of first order ordinary differential equations in terms of the horizontal electromagnetic field components in the frequency–wavenumber domain has been evaluated in terms of a system matrix. This matrix is dependent on the medium properties for a specific layer and the horizontal wavenumbers for a plane-wave component in the wavenumber spectrum.

By evaluating the eigenvalues and corresponding eigenvectors of the system matrix, it has been shown that the resulting diagonalization leads to two decoupled differential equations with upgoing and downgoing field constituents in a homogeneous region. The eigenvalues of the system matrix correspond to the vertical slownesses. The reflection and transmission (RT) at an interface can be calculated from the eigenvector matrices on each side, and a recursive scheme for calculating the RT-response across a stack of layers has been derived. Thus we were able to obtain expressions for the field vector in any layer at any position in terms of eigenvalues, eigenvector matrices, RT-response matrices, and the source function.

The assumption that the property dyads are symmetric, and the energy-flux normalization of the eigenvector matrices, made it possible to obtain reciprocity relations for reflection and transmission responses. An example of an application of the reciprocity relations is that the number of calculations in the inverse Fourier transform can be reduced by 50 per cent.

In addition to media with general anisotropy, configurations with simpler anisotropies have been studied. In anisotropic media the diagonalized system matrix is in general not up/down-symmetric. Up/down-symmetry follows if one of the principal axes of the anisotropic medium coincides with the coordinate axis normal to the planar interfaces. Then the diagonal submatrices in the system matrix are zero. In vertically transversely isotropic (TIV) media, the mode-field is decoupled in a TE- and TM-mode throughout the layered system.

For a source and receiver in a TIV-medium, explicit expressions for the electromagnetic fields from the source dipoles HED, HMD, VED, and VMD have been derived. If the entire stratified medium is characterized by TIV or isotropy, the recursive relations for the RT-responses simplify to scalar equations. In this case the 2-D Fourier transform can be reduced to a 1-D Hankel transform.

A numerical implementation of the algorithms and a modelling study have been performed. The modelling example was taken from a marine CSEM-setting. The obtained responses show different behaviour for different anisotropy configurations.

Finally, an application of the propagator method for isotropic media has been demonstrated in Appendix G.

ACKNOWLEDGMENTS

We are grateful to Lasse Amundsen, Rune Mittet, and Ola Hunderi for valuable discussions. L.O.L. would like to thank Statoil' VISTA programme for financial support. B.U. is appreciative to the Norwegian Research Council, Norsk Hydro, Statoil ASA, and ElectroMagnetic GeoServices AS for supporting this research.

REFERENCES

Abramowitz, M. & Stegun, I.A., 1962. *Handbook of Mathematical Functions*, 9th edn, Dover, New York.

Altman, C. & Suchy, K., 1998. The Maxwell and adjoint systems for complex media: physical significance and applications, *International Journal of Applied Electromagnetics and Mechanics,* **9**(1), 135–142.

Amundsen, L., Løseth, L.O., Mittet, R., Ellingsrud, S. & Ursin, B., 2006. Decomposition of electromagnetic fields into upgoing and downgoing components, *Geophysics,* **71**(5), G211–G223.

Anderson, W.L., 1979. Computer program, numerical integration of related Hankel transforms of orders 0 and 1 by adaptive digital filtering, *Geophysics,* **44**(7), 1287–1305.

Anderson, W.L., 1989. A hybrid fast Hankel transform algorithm for electromagnetic modeling, *Geophysics,* **54**(2), 263–266.

Berremann, D.W., 1972. Optics in stratified and anisotropic media: 4 × 4-matrix formulation, *Journal of the Optical Society of America,* **62**(4), 502–510.

Born, M. & Wolf, E., 1999. *Principles of Optics*, 7th edn, University Press, Cambridge, 7th rdn.

Bunse-Gerstner, A., Byers, R. & Mehrmann, V., 1992. A chart of numerical methods for structured eigenvalue problems, *SIAM Journal of Matrix Analysis and Its Applications,* **13**, 419–453.

Carcione, J.M. & Cavallini, F., 2001. A semianalytical solution for the propagation of electromagnetic waves in 3-D lossy orthotropic media, *Geophysics,* **66**(4), 1141–1148.

Carcione, J.M. & Schoenberg, M.A., 2000. 3-D ground-penetrating radar simulation and plane-wave theory in anisotropic media, *Geophysics,* **65**(5), 1527–1541.

Chapman, C., 2004. *Fundamentals of Seismic Wave Propagation*, University Press, Cambridge.

Chapman, C.H., 1994. Reflection/transmission coefficient reciprocities in anisotropic media, *Geophys. J. Int.,* **116**, 498–501.

Chlamtac, M. & Abramovici, F., 1981. The electromagnetic fields of a horizontal dipole over a vertically inhomogeneous and anisotropic earth, *Geophysics,* **46**, 904–915.

Christensen, N.B., 1990. Optimized fast Hankel transform filters, *Geophys. Prospect.,* **38**, 545–568.

Edwards, R.N., Nobes, D.C. & Gómes-Treviño, E., 1984. Offshore electrical exploration of sedimentary basins: the effects of anisotropy in horizontally isotropic, layered media, *Geophysics,* **49**(5), 566–576.

Everett, M.E. & Constable, S., 1999. Electric dipole fields over an anisotropic seafloor: theory and application to the structure of 40 Ma Pacific Ocean lithosphere, *Geophys. J. Int.,* **136**, 41–56.

Faßbender, H., Mackey, D.S. & Mackey, N., 2001. Hamilton and Jacobi come full circle: Jacobi algorithms for structured Hamiltonian eigenproblems, *Linear Algebra and Its Applications,* **332–334**, 37–80.

Goldstein, H., 1980. *Classical Mechanics*, Addison-Wesley, London, 2nd edn.

Gradshteyn, I.S. & Ryzhik, I.M., 1980. *Table of Integrals, Series, and Products*, Academic Press, San Diego, CA.

Griffiths, D.J. & Steinke, C.A., 2000. Waves in locally periodic media, *American Journal of Physics,* **69**(2), 137–154.

Hänggi, P., Roesel, F. & Trautman, D., 1998. Evaluation of infinite series by use of continued fraction expansions: a numerical study, *Journal of Computational Physics,* **37**, 242–258.

Helbig, K. & Thomsen, L., 2005. 75-plus years of anisotropy in exploration and reservoir seismics: a historical review of concepts and methods, *Geophysics,* **70**(6), 9ND–23ND.

Horn, R.A. & Johnson, C.A., 1985. *Matrix Analysis*, Cambridge University Press, Cambridge.

Huard, S., 1997. *Polarization of Light*, John Wiley & Sons, New York.

Jackson, J.D., 1998. *Classical Electrodynamics*, John Wiley & Sons, New York, 3rd edn.

Kennedy, W.D. & Herrick, D.C., 2004. Conductivity anisotropy in shale-free sandstone, *Petrophysics,* **45**(1), 38–58.

Kennett, B.L.N., 1983. *Seismic Wave Propagation in Stratified Media*, Cambridge University Press, Cambridge.

Kong, J.A., 1972. Electromagnetic fields due to dipole antennas over stratified anisotropic media, *Geophysics,* **37**(6), 985–996.

Kong, J.A., 2000. *Electromagnetic Wave Theory*, EMW Publishing, Cambridge, Massachusetts.

Li, X. & Pedersen, L.B., 1991. The electromagnetic response of an azimuthally anisotropic half-space, *Geophysics,* **56**(9), 1462–1473.

Maillet, R., 1947. The fundamental equations of electrical propspecting, *Geophysics,* **12**(4), 529–556.

Mohsen, A.A. & Hashish, E.A., 1994. The fast Hankel transform, *Geophys. Prospect.,* **34**, 131–139.

Nabighian, M.N., 1987. *Electromagnetic Methods in Applied Geophysics, Vol. 1: Theory, Vol. 2: Applications, Series: Investigations in Applied Geophysics; No. 3*, Society of Exploration Geophysicists, Oklahoma.

Negi, J.G. & Saraf, P.D., 1989. *Anisotropy in Geoelectromagnetism*, Elsevier, New York.

O'Brien, D.P. & Morrison, H.F., 1967. Electromagnetic fields in an N-layer anisotropic half-space, *Geophysics,* **32**(4), 668–677.

Onsager, L., 1931. Reciprocal relations in irreversible processes I, *Physical Review,* **37**, 405–425.

Press, W.H., Teukolsky, S.A., Vetterling, W.T. & Flannery, B.P., 1997. *Numerical Recipes in Fortran 77*, 2nd edn, Cambridge University Press, New York, 2nd edn.

Sinha, A.K. & Bhattacharyya, P.K., 1967. Electric dipole over an anisotropic and inhomogeneous earth, *Geophysics,* **32**(4), 652–667.

Stamnes, J.J. & Sithambaranathan, G.S., 2001. Reflection and refraction of an arbitrary electromagnetic wave at a plane interface separating an isotropic and a biaxial medium, *Journal of Optical Society of America A,* **18**(12), 3119–3129.

Stovas, A. & Ursin, B., 2003. Reflection and transmission responses of layered transversely isotropic viscoeleastic media, *Geophys. Prospect.,* **51**, 447–477.

Stratton, J.A., 1941. *Electromagnetic Theory*, McGraw-Hill, New York.

Suchy, K. & Altman, C., 1975. The Maxwell field, its adjoint field and the 'conjugate' field in anisotropic absorbing media, *Journal of Plasma Physics,* **13**, part 2, 299–316.

Ursin, B., 1983. Review of elastic and electromagnetic wave propagation in horizontally layered media, *Geophysics,* **48**, 1063–1081.

Ursin, B. & Stovas, A., 2002. Reflection and transmission responses of a layered isotropic viscoelastic medium, *Geophysics,* **67**(1), 307–323.

White, B.S. & Zhou, M., 2006. Electroseismic prospecting in layered media, *SIAM Journal on Applied Mathematics*, **67**(1), 69–98.

Yin, C., 2006. MMT forward modeling for a layered earth with arbitrary anisotropy, *Geophysics,* **71**(3), G115–G128.

Yin, C. & Maurer, H.M., 2001. Electromagnetic induction in a layered earth with arbitrary anisotropy, *Geophysics,* **66**(5), 1405–1416.

Yin, C. & Weidelt, P., 1999. Geoelectrical fields in a layered earth with arbitrary anisotropy, *Geophysics,* **64**(2), 426–434.

Yu, L. & Edwards, R.N., 1992. The detection of lateral anisotropy of the ocean floor by electromagnetic methods, *Geophys. J. Int.,* **108**, 433–441.

Yu, L., Evans, R.L. & Edwards, R.N., 1997. Transient electromagnetic responses in seafloor with triaxial anisotropy, *Geophys. J. Int.,* **129**, 292–304.

APPENDIX A: ROTATION OF THE ANISOTROPY PRINCIPAL AXES

The electromagnetic property dyads are determined by three different values in their principal axes system. The axes of the principal system are referred to as (1, 2, 3), and in a medium with triclinic anisotropy, each of the property dyads may have their own set of principal axes. In order to rotate the principal coordinate system into the main coordinate frame (x, y, z), it is convenient to use Euler angles (ϕ, θ, ψ). The convention used by Goldstein (1980) is followed. Now, as seen in Fig. 1, ϕ is the angle between the x-axis and the line of nodes, θ is the angle between the z-axis and the 3-axis, and finally, ψ is the angle between the line of nodes and the 1-axis. Note that the 'line of nodes' is the line defined by the intersection of the xy-plane and the 12-plane (horizontal planes of the coordinate frames). The entries of a property dyad in the main coordinate frame are then obtained by transforming the dyad from the principal system as follows:

$$\boldsymbol{\sigma} = \begin{pmatrix} \sigma_{xx} & \sigma_{xy} & \sigma_{xz} \\ \sigma_{yx} & \sigma_{yy} & \sigma_{yz} \\ \sigma_{zx} & \sigma_{zy} & \sigma_{zz} \end{pmatrix} = \begin{pmatrix} e_{11} & e_{12} & e_{13} \\ e_{21} & e_{22} & e_{23} \\ e_{31} & e_{32} & e_{33} \end{pmatrix} \begin{pmatrix} \sigma_1 & 0 & 0 \\ 0 & \sigma_2 & 0 \\ 0 & 0 & \sigma_3 \end{pmatrix} \begin{pmatrix} e_{11} & e_{21} & e_{31} \\ e_{12} & e_{22} & e_{32} \\ e_{13} & e_{23} & e_{33} \end{pmatrix}, \tag{A1}$$

where

$$e_{11} = \cos\phi\cos\psi - \sin\phi\cos\theta\sin\psi, \tag{A2a}$$

$$e_{12} = -\cos\phi\sin\psi - \sin\phi\cos\theta\cos\psi, \tag{A2b}$$

$$e_{13} = \sin\phi\sin\theta, \tag{A2c}$$

$$e_{21} = \sin\phi\cos\psi + \cos\phi\cos\theta\sin\psi, \tag{A2d}$$

$$e_{22} = -\sin\phi\sin\psi + \cos\phi\cos\theta\cos\psi, \tag{A2e}$$

$$e_{23} = -\cos\phi\sin\theta, \tag{A2f}$$

$$e_{31} = \sin\theta\sin\psi, \tag{A2g}$$

$$e_{32} = \sin\theta\cos\psi, \tag{A2h}$$

$$e_{33} = \cos\theta. \tag{A2i}$$

This procedure $\boldsymbol{\sigma} = \boldsymbol{e}\boldsymbol{\sigma}_p\,\boldsymbol{e}^T$, where $\boldsymbol{e}$ is the coordinate rotation matrix with elements $e_{ij} = e_{ji}$, and $\boldsymbol{\sigma}_p$ is the dyad in the principal system, can be performed for all the three property dyads. In general, the principal axes may be different for all these dyads (which obviously requires different rotation angles for each property dyad).

The entries in the conductivity matrix in the main coordinate frame are given by the rotation angles and the principal values as:

$$\sigma_{xx} = \sigma_1 e_{11}^2 + \sigma_2 e_{12}^2 + \sigma_3 e_{13}^2, \tag{A3a}$$

$$\sigma_{xy} = \sigma_1 e_{11}e_{21} + \sigma_2 e_{12}e_{22} + \sigma_3 e_{13}e_{23}, \tag{A3b}$$

$$\sigma_{xz} = \sigma_1 e_{11}e_{31} + \sigma_2 e_{12}e_{32} + \sigma_3 e_{13}e_{33}, \tag{A3c}$$

$$\sigma_{yy} = \sigma_1 e_{21}^2 + \sigma_2 e_{22}^2 + \sigma_3 e_{23}^2, \tag{A3d}$$

$$\sigma_{yz} = \sigma_1 e_{21}e_{31} + \sigma_2 e_{22}e_{32} + \sigma_3 e_{23}e_{33}, \tag{A3e}$$

$$\sigma_{zz} = \sigma_1 e_{31}^2 + \sigma_2 e_{32}^2 + \sigma_3 e_{33}^2, \tag{A3f}$$

In u/d-symmetric media, the relation between the principal and main coordinate systems is described by one rotation only (for each property dyad) in the horizontal plane (i.e. ϕ in equation A2). The conductivity dyad can in this case be written as

$$\begin{pmatrix} \sigma_{xx} & \sigma_{xy} & 0 \\ \sigma_{yx} & \sigma_{yy} & 0 \\ 0 & 0 & \sigma_v \end{pmatrix} = \begin{pmatrix} \cos\phi & \sin\phi & 0 \\ -\sin\phi & \cos\phi & 0 \\ 0 & 0 & 1 \end{pmatrix} \begin{pmatrix} \sigma_1 & 0 & 0 \\ 0 & \sigma_2 & 0 \\ 0 & 0 & \sigma_v \end{pmatrix} \begin{pmatrix} \cos\phi & -\sin\phi & 0 \\ \sin\phi & \cos\phi & 0 \\ 0 & 0 & 1 \end{pmatrix}, \tag{A4}$$

whence

$$\begin{aligned} \sigma_{xx} &= \sigma_1^2\cos^2\phi + \sigma_2^2\sin^2\phi, \quad \sigma_{yy} = \sigma_1^2\sin^2\phi + \sigma_2^2\cos^2\phi, \\ \sigma_{xy} &= \sigma_{yx} = (\sigma_2 - \sigma_1)\sin\phi\cos\phi. \end{aligned} \tag{A5}$$

The relations presented in this section in terms of the conductivity dyad are equally valid for the permittivity and permeability dyads.

APPENDIX B: DUALITY IN THE FIELD EXPRESSIONS

When magnetic sources are introduced into Maxwell' equations, Faraday' and Ampère's laws can be written as

$$\nabla\times\mathbf{E} = -\mathbf{J}_{0M} + i\omega\boldsymbol{\mu}\mathbf{H}, \tag{B1a}$$

$$\nabla\times\mathbf{H} = \mathbf{J}_0 - i\omega\tilde{\boldsymbol{\varepsilon}}\mathbf{E}, \tag{B1b}$$

where $\mathbf{J}_0$ is the electric source and $\mathbf{J}_{0M}$ is the magnetic source. Using the equations of charge-conservation, the divergence equations can be written in terms of the source current density as

$$\nabla\cdot(\tilde{\boldsymbol{\varepsilon}}\mathbf{E}) = -\frac{1}{i\omega}\nabla\cdot\mathbf{J}_0, \tag{B1c}$$

$$\nabla\cdot(\boldsymbol{\mu}\mathbf{H}) = -\frac{1}{i\omega}\nabla\cdot\mathbf{J}_{0M}. \tag{B1d}$$

From these equations one observes a simple relationship between the fields from a magnetic dipole and an electric dipole. Starting with Faraday's law (eq. B1a) and the corresponding divergence eq. (B1c), one can arrive at Ampère's law (eq. B1b) and its corresponding divergence eq. (B1d) by doing the following change of variables:

$$\mathbf{E}\to\mathbf{H}, \tag{B2a}$$

$$\mathbf{H}\to-\mathbf{E}, \tag{B2b}$$

$$\boldsymbol{\mu}\to\tilde{\boldsymbol{\varepsilon}}, \tag{B2c}$$

$$\tilde{\boldsymbol{\varepsilon}}\to\boldsymbol{\mu}, \tag{B2d}$$

$$\mathbf{J}_0\to\mathbf{J}_{0M}. \tag{B2e}$$

The opposite 'transformation', from Ampère's law to Faraday's law and their corresponding divergence equations, also holds. In this case the relation

$$\mathbf{J}_{0M}\to-\mathbf{J}_0 \tag{B2f}$$

is needed. In terms of the dipole sources used in eqs (4) and (5), the source transformations become:

$$I\mathbf{l} \rightarrow -i\omega\boldsymbol{\mu}I\mathbf{a} \quad \text{and} \quad i\omega\boldsymbol{\mu}I\mathbf{a} \rightarrow I\mathbf{l}. \tag{B3}$$

In the main text, RT-responses from a multilayered medium are considered. If a change of variables as described above is performed, a change in polarization modes and signs in the reflection coefficients must be taken into account due to the interchange of the electric and magnetic field variables.

The explicit field expressions for the HMD and VMD (HED and VED) can be derived from the expressions for the HED and VED (HMD and VMD), respectively, by using the change of variables in eqs (B2a) to (B2d) and (B3). In addition, the following change of variables for the RT-response coefficients must be performed:

$$\mathcal{R}^A_{11} \leftrightarrow -\mathcal{R}^C_{22}, \qquad \mathcal{R}^A_{12} \leftrightarrow +\mathcal{R}^C_{21}, \tag{B4a}$$

$$\mathcal{R}^A_{21} \leftrightarrow +\mathcal{R}^C_{12}, \qquad \mathcal{R}^A_{22} \leftrightarrow -\mathcal{R}^C_{11}, \tag{B4b}$$

$$\mathcal{R}^B_{11} \leftrightarrow -\mathcal{R}^D_{22}, \qquad \mathcal{R}^B_{12} \leftrightarrow +\mathcal{R}^D_{21}, \tag{B4c}$$

$$\mathcal{R}^B_{21} \leftrightarrow +\mathcal{R}^D_{12}, \qquad \mathcal{R}^B_{22} \leftrightarrow -\mathcal{R}^D_{11}. \tag{B4d}$$

APPENDIX C: ENERGY VELOCITY OF A PLANE-WAVE COMPONENT

The energy velocity can be defined as (Kong 2000; Carcione & Schoenberg 2000):

$$\mathbf{v}_e = \frac{\mathrm{Re}(\mathbf{S})}{\mathrm{Re}(u_e + u_m)}, \tag{C1}$$

where $\mathbf{S} = \frac{1}{2}\mathbf{E} \times \mathbf{H}^*$ is the complex Poynting vector, $u_e = \frac{1}{4}\mathbf{E} \cdot \mathbf{D}^*$ is the electric energy, and $u_m = \frac{1}{4}\mathbf{H} \cdot \mathbf{B}^*$ is the magnetic energy. Consider a plane electromagnetic wave in a homogeneous source-free medium. Then Maxwell's equations can be written as:

$$\mathbf{p} \cdot \mathbf{D} = 0, \tag{C2a}$$

$$\mathbf{p} \cdot \mathbf{B} = 0, \tag{C2b}$$

$$\mathbf{p} \times \mathbf{E} = \mathbf{B}, \tag{C2c}$$

$$\mathbf{p} \times \mathbf{H} = -\mathbf{D}, \tag{C2d}$$

where **p** is the slowness vector. From these equations it is seen that the slowness is in a direction perpendicular to both the **D**- and **B**-field. It is thus convenient to rotate the coordinate system so that one of the axes coincides with the direction of the slowness. Some caution must however be taken here; since the slowness vector is complex, the 'rotation' must be performed with complex angles. Thus the coordinate system is rather transformed into a new state. We will as in Kong (2000) refer to the system after the transformation as the kDB-system, in which the axes are denoted as 123. (*cf.* Fig. 1 where $x'y'z'$ can be pictured as 123). Note that the axes in the kDB-system are not the same as any principal anisotropy axes. Now, an expression for the energy velocity in terms of the material and slowness parameters can be obtained. From Fig. 1 it is seen that a rotation into the kDB-system described by the angles ϕ and θ can be written as:

$$\boldsymbol{e}_{\mathrm{kDB}} = \begin{pmatrix} e'_{11} & e'_{12} & e'_{13} \\ e'_{21} & e'_{22} & e'_{23} \\ e'_{31} & e'_{32} & e'_{33} \end{pmatrix}, \tag{C3}$$

where

$$e'_{11} = \sin\phi, \qquad e'_{12} = -\cos\phi, \qquad e'_{13} = 0, \tag{C4a}$$

$$e'_{21} = \cos\phi\cos\theta, \qquad e'_{22} = \sin\phi\cos\theta, \qquad e'_{23} = -\sin\theta, \tag{C4b}$$

$$e'_{31} = \cos\phi\sin\theta, \qquad e'_{32} = \sin\phi\sin\theta, \qquad e'_{33} = \cos\theta. \tag{C4c}$$

which would take the values $\phi \in [0, 360^\circ)$, $\theta \in [0, 180^\circ)$ in a lossless case, but here the angles are complex with

$$\cos\phi = \frac{p_x}{\sqrt{p_x^2 + p_y^2}} \quad \text{and} \quad \cos\theta = \frac{p_z}{\sqrt{p_x^2 + p_y^2 + p_z^2}}. \tag{C5}$$

The material parameters in the kDB-system are obtained from the material parameters in the main coordinate frame by the dyadic transformation:

$$\boldsymbol{\chi}' = \boldsymbol{e}_{\mathrm{kDB}}\boldsymbol{\chi}\boldsymbol{e}^T_{\mathrm{kDB}}, \tag{C6}$$

where the resulting matrix is symmetric after the othogonal transformation. Next, a relation between **D** and **B** are needed. It is thus convenient to introduce the impermeability and the complex impermittivity, which are the inverses of the permeability and complex permittivity, respectively (Kong 2000):

$$\mathbf{E} = \tilde{\varepsilon}^{-1}\mathbf{D} = \boldsymbol{\kappa}\mathbf{D} \quad \text{and} \quad \mathbf{H} = \mu^{-1}\mathbf{B} = \boldsymbol{\nu}\mathbf{B}. \tag{C7}$$

From the curl equations in (C2), the following relations between **D** and **B** can be obtained in the kDB-system:

$$D_1 = p(\nu'_{21}B_1 + \nu'_{22}B_2), \tag{C8a}$$

$$D_2 = -p(\nu'_{11}B_1 + \nu'_{12}B_2), \tag{C8b}$$

$$B_1 = -p(\kappa'_{21}D_1 + \kappa'_{22}D_2), \tag{C8c}$$

$$B_2 = p(\kappa'_{11}D_1 + \kappa'_{12}D_2), \tag{C8d}$$

where $p = |\mathbf{p}\,|$ is the slowness in the $\hat{\mathbf{e}}_3$-direction. Note that by definition, this is the direction of the total slowness. Note also that $B_3 = 0$ and $D_3 = 0$. From eq. (C8), the dispersion relation

$$u^2 = -\frac{1}{2}\left[b_u \pm \sqrt{b_u^2 - 4c_u}\right], \tag{C9a}$$

$$b_u = \left(\kappa'_{21}\nu'_{21} + \kappa'_{12}\nu'_{12} - \kappa'_{11}\nu'_{22} - \kappa'_{22}\nu'_{11}\right), \tag{C9b}$$

$$\begin{aligned} c_u = {} & \left(\kappa'_{21}\nu'_{21} - \kappa'_{11}\nu'_{22}\right)\left(\kappa'_{12}\nu'_{12} - \kappa'_{22}\nu'_{11}\right) \\ & - \left(\kappa'_{22}\nu'_{21} - \kappa'_{12}\nu'_{22}\right)\left(\kappa'_{11}\nu'_{12} - \kappa'_{21}\nu'_{11}\right), \end{aligned} \tag{C9c}$$

and a relation between D_1 and D_2 can be obtained:

$$\frac{D_2}{D_1} = \frac{u^2 + \kappa'_{21}\nu'_{21} - \kappa'_{11}\nu'_{22}}{\kappa'_{12}\nu'_{22} - \kappa'_{22}\nu'_{21}} = \frac{\kappa'_{21}\nu'_{11} - \kappa'_{11}\nu'_{12}}{u^2 + \kappa'_{12}\nu'_{12} - \kappa'_{22}\nu'_{11}} = \Psi, \tag{C9d}$$

where the complex velocity $u = 1/p$.

Hence, the electric field in the kDB-system in terms of D_1 can be written as

$$\mathbf{E}_{\text{kDB}} = \boldsymbol{\kappa}'\mathbf{D}_{\text{kDB}} = \begin{pmatrix} \kappa'_{11} + \kappa'_{12}\Psi \\ \kappa'_{21} + \kappa'_{22}\Psi \\ \kappa'_{31} + \kappa'_{32}\Psi \end{pmatrix} D_1, \tag{C10}$$

whereas the magnetic field in the kDB-system is obtained using Faraday's law:

$$\mathbf{H}_{\text{kDB}} = \boldsymbol{\nu}'(\mathbf{p} \times \mathbf{E}_{\text{kDB}}) = p\begin{pmatrix} (\nu'_{12}\kappa'_{11} - \nu'_{11}\kappa'_{21}) + (\nu'_{12}\kappa'_{12} - \nu'_{11}\kappa'_{22})\Psi \\ (\nu'_{22}\kappa'_{11} - \nu'_{21}\kappa'_{21}) + (\nu'_{22}\kappa'_{12} - \nu'_{21}\kappa'_{22})\Psi \\ (\nu'_{32}\kappa'_{11} - \nu'_{31}\kappa'_{21}) + (\nu'_{32}\kappa'_{12} - \nu'_{31}\kappa'_{22})\Psi \end{pmatrix} D_1. \tag{C11}$$

The complex Poynting vector in the kDB-system expressed in terms of D_1 then becomes:

$$\mathbf{S}_{\text{kDB}} = \frac{1}{2}\mathbf{s}_{\text{kDB}}\, p^* D_1 D_1^*, \tag{C12}$$

where

$$\mathbf{s}_{\text{kDB}} = \begin{pmatrix} s_{11} + s_{12}\Psi + s_{13}\Psi^* + s_{14}\Psi\Psi^* \\ s_{21} + s_{22}\Psi + s_{23}\Psi^* + s_{24}\Psi\Psi^* \\ s_{31} + s_{32}\Psi + s_{33}\Psi^* + s_{34}\Psi\Psi^* \end{pmatrix}, \tag{C13a}$$

and

$$\begin{aligned} s_{11} &= (\nu'_{32}\kappa'_{21} - \nu'_{22}\kappa'_{31})(\kappa'_{11})^* - (\nu'_{31}\kappa'_{21} - \nu'_{21}\kappa'_{31})(\kappa'_{21})^*, \\ s_{12} &= (\nu'_{32}\kappa'_{22} - \nu'_{22}\kappa'_{32})(\kappa'_{11})^* - (\nu'_{31}\kappa'_{22} - \nu'_{21}\kappa'_{32})(\kappa'_{21})^*, \\ s_{13} &= (\nu'_{32}\kappa'_{21} - \nu'_{22}\kappa'_{31})(\kappa'_{12})^* - (\nu'_{31}\kappa'_{21} - \nu'_{21}\kappa'_{31})(\kappa'_{22})^*, \\ s_{14} &= (\nu'_{32}\kappa'_{22} - \nu'_{22}\kappa'_{32})(\kappa'_{12})^* - (\nu'_{31}\kappa'_{22} - \nu'_{21}\kappa'_{32})(\kappa'_{22})^*, \\ s_{21} &= (\nu'_{12}\kappa'_{31} - \nu'_{32}\kappa'_{11})(\kappa'_{11})^* - (\nu'_{11}\kappa'_{31} - \nu'_{31}\kappa'_{11})(\kappa'_{21})^*, \\ s_{22} &= (\nu'_{12}\kappa'_{32} - \nu'_{32}\kappa'_{12})(\kappa'_{11})^* - (\nu'_{11}\kappa'_{32} - \nu'_{31}\kappa'_{12})(\kappa'_{21})^*, \\ s_{23} &= (\nu'_{12}\kappa'_{31} - \nu'_{32}\kappa'_{11})(\kappa'_{12})^* - (\nu'_{11}\kappa'_{31} - \nu'_{31}\kappa'_{11})(\kappa'_{22})^*, \\ s_{24} &= (\nu'_{12}\kappa'_{32} - \nu'_{32}\kappa'_{12})(\kappa'_{12})^* - (\nu'_{11}\kappa'_{32} - \nu'_{31}\kappa'_{12})(\kappa'_{22})^*, \\ s_{31} &= (\nu'_{22}\kappa'_{11} - \nu'_{12}\kappa'_{21})(\kappa'_{11})^* - (\nu'_{21}\kappa'_{11} - \nu'_{11}\kappa'_{21})(\kappa'_{21})^*, \\ s_{32} &= (\nu'_{22}\kappa'_{12} - \nu'_{12}\kappa'_{22})(\kappa'_{11})^* - (\nu'_{21}\kappa'_{12} - \nu'_{11}\kappa'_{22})(\kappa'_{21})^*, \\ s_{33} &= (\nu'_{22}\kappa'_{11} - \nu'_{12}\kappa'_{21})(\kappa'_{12})^* - (\nu'_{21}\kappa'_{11} - \nu'_{11}\kappa'_{21})(\kappa'_{22})^*, \\ s_{34} &= (\nu'_{22}\kappa'_{12} - \nu'_{12}\kappa'_{22})(\kappa'_{12})^* - (\nu'_{21}\kappa'_{12} - \nu'_{11}\kappa'_{22})(\kappa'_{22})^*. \end{aligned} \tag{C13b}$$

The energy densities in the kDB-system can be written as

$$u_m = \frac{1}{4}\mathbf{H}\cdot\mathbf{B}^* = \frac{1}{4}\left(H_1 B_1^* + H_2 B_2^*\right) = \frac{p^*}{4p}\left(E_1^* D_1 + E_2^* D_2\right) = \frac{p^*}{p}u_e^*, \tag{C14a}$$

$$u_e = \frac{1}{4}\mathbf{E}\cdot\mathbf{D}^* = \frac{1}{4}\left(E_1 D_1^* + E_2 D_2^*\right) = \frac{1}{4}\left[(\kappa'_{11} + \kappa'_{12}\Psi) + (\kappa'_{21} + \kappa'_{22}\Psi)\Psi^*\right] D_1 D_1^*. \tag{C14b}$$

The energy density is independent of the coordinate system in which it is calculated, whereas the Poynting vector must be transformed back to the main coordinate frame $\mathbf{S} = \boldsymbol{e}_{\mathrm{kDB}}^T\, \mathbf{S}_{\mathrm{kDB}}$. This leads to the following expressions for the energy velocity:

$$\mathbf{v}_e = n_v^{-1}\mathrm{Re}\left(p^* \boldsymbol{e}_{\mathrm{kDB}}^T \mathbf{s}_{\mathrm{kDB}}\right), \tag{C15}$$

where

$$n_v = \mathrm{Re}\left(\frac{1}{p}\right)\mathrm{Re}\left[p(\kappa'_{11} + \kappa'_{12}\Psi) + p(\kappa'_{21} + \kappa'_{22}\Psi)\Psi^*\right]. \tag{C16}$$

If $\Psi \to \infty$, the Poynting vector and energy velocity can be calculated in terms of D_2, which implies multiplying the expressions with Ψ^{-1} $(\Psi^{-1})^*$.

When the eigenvalues are found, their ordering into upgoing and downgoing constituents can be determined from the direction of the z-component of the corresponding energy velocity. Moreover, the ordering of modes can be determined by matching the eigenvalue and the complex velocity in the dispersion relation in eq. (C9a). The choice of sign that corresponds to what mode can be established by considering what happens when the anisotropy simplifies into TIV. Then the fraction between D_1 or D_2 either approach zero or infinity depending on if the slowness corresponds to a TE- or a TM-mode.

APPENDIX D: MIXING THE qTE- AND qTM-MODES IN A LAYER

Consider reflection and transmission through a stack of three layers [from region (3) to (1) through layer (2)], and assume that the qTE- and qTM-modes have been switched when sorting the eigenvalues into the upgoing eigenvalue submatrix in region (2). Then, in region (2), the 'mixed' eigenvector submatrices and eigenvalue matrix are related to the corresponding 'correct' matrices as

$$\acute{\boldsymbol{N}}'_E = \begin{pmatrix} n_{12} & n_{11} \\ n_{22} & n_{21} \end{pmatrix} = \acute{\boldsymbol{N}}_E \boldsymbol{K}, \tag{D1a}$$

$$\acute{\boldsymbol{N}}'_H = \begin{pmatrix} n_{32} & n_{31} \\ n_{42} & n_{41} \end{pmatrix} = \acute{\boldsymbol{N}}_H \boldsymbol{K}, \tag{D1b}$$

$$\acute{\mathbf{p}}'_{\mathbf{z}} = \boldsymbol{K}\acute{\mathbf{p}}_{\mathbf{z}}\boldsymbol{K}, \tag{D1c}$$

where $\boldsymbol{K}$ is given by eq. (19). By using eq. (61), the $\boldsymbol{C}$ and $\boldsymbol{D}$-matrices between medium (3) and (2) become:

$$\acute{\boldsymbol{C}}' = \boldsymbol{K}\acute{\boldsymbol{C}}, \quad \acute{\boldsymbol{D}}' = \boldsymbol{K}\acute{\boldsymbol{D}}, \quad \hat{\boldsymbol{C}}' = \boldsymbol{K}\hat{\boldsymbol{C}}, \quad \text{and} \quad \hat{\boldsymbol{D}}' = \boldsymbol{K}\hat{\boldsymbol{D}}, \tag{D2}$$

since layer (2) has the mixed modes. Thus, the reflection coefficients are

$$\acute{\boldsymbol{t}}' = 2\left(\boldsymbol{K}\acute{\boldsymbol{C}} + \boldsymbol{K}\acute{\boldsymbol{D}}\right)^{-T} = \boldsymbol{K}\acute{\boldsymbol{t}}, \tag{D3a}$$

$$\acute{\boldsymbol{r}}' = -\left(\boldsymbol{K}\hat{\boldsymbol{C}} - \boldsymbol{K}\hat{\boldsymbol{D}}\right)^T \left(\boldsymbol{K}\acute{\boldsymbol{C}} + \boldsymbol{K}\acute{\boldsymbol{D}}\right)^{-T} = \acute{\boldsymbol{r}}, \tag{D3b}$$

$$\grave{\boldsymbol{r}}' = \left(\hat{\boldsymbol{C}} - \hat{\boldsymbol{D}}\right)\left(\boldsymbol{K}\grave{\boldsymbol{C}} + \boldsymbol{K}\grave{\boldsymbol{D}}\right)^{-1} = \boldsymbol{K}\grave{\boldsymbol{r}}, \tag{D3c}$$

$$\grave{\boldsymbol{t}}' = 2\left(\grave{\boldsymbol{C}} + \grave{\boldsymbol{D}}\right)^{-1} = \grave{\boldsymbol{t}}. \tag{D3d}$$

When inserted into the recursive formula in eq. (70), this leads to

$$\grave{\boldsymbol{R}}'_j = \boldsymbol{K}\mathrm{e}^{i\omega\acute{\mathbf{p}}_{\mathbf{z}}h_j}\boldsymbol{K}\left[\boldsymbol{K}\grave{\boldsymbol{r}}_j + \boldsymbol{K}\acute{\boldsymbol{t}}_j\grave{\boldsymbol{R}}_{j+1}(\boldsymbol{I} - \acute{\boldsymbol{r}}_j\grave{\boldsymbol{R}}_{j+1})^{-1}\grave{\boldsymbol{t}}_j\right]\mathrm{e}^{i\omega\grave{\mathbf{p}}_{\mathbf{z}}h_j} = \boldsymbol{K}\grave{\boldsymbol{R}}_j. \tag{D4}$$

In the propagation between medium (2) and (1), the same procedure yields the relations:

$$\acute{\boldsymbol{C}}' = \acute{\boldsymbol{C}}\boldsymbol{K}, \quad \acute{\boldsymbol{D}}' = \acute{\boldsymbol{D}}\boldsymbol{K}, \quad \check{\boldsymbol{C}}' = \check{\boldsymbol{C}}\boldsymbol{K}, \quad \text{and} \quad \check{\boldsymbol{D}}' = \check{\boldsymbol{D}}\boldsymbol{K}, \tag{D5}$$

which give the reflection coefficients

$$\acute{\boldsymbol{t}}' = 2\left(\acute{\boldsymbol{C}}\boldsymbol{K} + \acute{\boldsymbol{D}}\boldsymbol{K}\right)^{-T} = \acute{\boldsymbol{t}}\boldsymbol{K}, \tag{D6a}$$

$$\acute{\boldsymbol{r}}' = -\left(\hat{\boldsymbol{C}} - \hat{\boldsymbol{D}}\right)^T \left(\acute{\boldsymbol{C}}\boldsymbol{K} + \acute{\boldsymbol{D}}\boldsymbol{K}\right)^{-T} = \acute{\boldsymbol{r}}\boldsymbol{K}, \tag{D6b}$$

$$\grave{\boldsymbol{r}}' = \left(\acute{\boldsymbol{C}}\boldsymbol{K} + \acute{\boldsymbol{D}}\boldsymbol{K}\right)^{-T}\left(\check{\boldsymbol{C}}\boldsymbol{K} - \check{\boldsymbol{D}}\boldsymbol{K}\right)^T = \grave{\boldsymbol{r}}, \tag{D6c}$$

$$\grave{\boldsymbol{t}}' = 2\left(\grave{\boldsymbol{C}} + \grave{\boldsymbol{D}}\right)^{-1} = \grave{\boldsymbol{t}}. \tag{D6d}$$

When inserted into the recursive formula, this becomes

$$\grave{\boldsymbol{R}}'_{j-1} = \mathrm{e}^{i\omega\acute{\mathbf{p}}_{\mathbf{z}}h_{j-1}}\left[\grave{\boldsymbol{r}}_{j-1} + \acute{\boldsymbol{t}}_{j-1}\boldsymbol{K}\boldsymbol{K}\grave{\boldsymbol{R}}_j(\boldsymbol{I} - \acute{\boldsymbol{r}}_{j-1}\boldsymbol{K}\boldsymbol{K}\grave{\boldsymbol{R}}_j)^{-1}\grave{\boldsymbol{t}}_{j-1}\right]\mathrm{e}^{i\omega\grave{\mathbf{p}}_{\mathbf{z}}h_{j-1}} = \grave{\boldsymbol{R}}_{j-1}. \tag{D7}$$

The proof for mixing the downgoing modes is similar and leads to the same conclusion.

APPENDIX E: THE FRESNEL-EIGENVECTOR MATRIX IN TIV-MEDIA

The flux-normalized eigenvector leads to a symmetry in the transmission coefficients in eq. (122) that might not be appropriate for all purposes. In order to get the Fresnel transmission coefficients, a different scaling on the eigenvectors that make up the eigenvector matrix can be chosen:

$$\boldsymbol{N}_F = \frac{1}{\sqrt{2}p_\rho}\begin{pmatrix} p_y & p_x & p_y & p_x \\ -p_x & p_y & -p_x & p_y \\ p_y\frac{p_{z\mathrm{I}}}{\mu_h} & p_x\frac{\varepsilon_h}{p_{x\mathrm{II}}} & -p_y\frac{\varepsilon_{z\mathrm{I}}}{\mu_h} & -p_x\frac{\tilde{\varepsilon}_h}{p_{z\mathrm{II}}} \\ -p_x\frac{p_{z\mathrm{I}}}{\mu_h} & p_y\frac{\tilde{\varepsilon}_h}{p_{z\mathrm{II}}} & p_x\frac{p_{z\mathrm{I}}}{\mu_h} & -p_y\frac{\tilde{\varepsilon}_h}{p_{z\mathrm{II}}} \end{pmatrix},$$

$$\boldsymbol{N}_F^{-1} = \frac{1}{\sqrt{2}p_\rho}\begin{pmatrix} p_y & -p_x & p_y\frac{\mu_h}{p_{z\mathrm{I}}} & -p_x\frac{\mu_h}{p_{z\mathrm{I}}} \\ p_x & p_y & p_x\frac{p_{z\mathrm{II}}}{\tilde{\varepsilon}_h} & p_y\frac{p_{z\mathrm{II}}}{\tilde{\varepsilon}_h} \\ p_y & -p_x & -p_y\frac{\mu_h}{p_{z\mathrm{I}}} & p_x\frac{\mu_h}{p_{z\mathrm{I}}} \\ p_x & p_y & -p_x\frac{p_{x\mathrm{II}}}{\tilde{\varepsilon}_h} & -p_y\frac{p_{x\mathrm{II}}}{\tilde{\varepsilon}_h} \end{pmatrix}. \tag{E1}$$

With the choice in eq. (E1), the downgoing reflection matrix $\grave{\boldsymbol{r}}$ are as given in eq. (121) with $\acute{\boldsymbol{r}} = -\grave{\boldsymbol{r}}$. The upgoing and downgoing transmission matrices are:

$$\grave{\boldsymbol{t}} = \begin{pmatrix} \frac{2\mu_h^+\, p_{z\mathrm{I}}^-}{\mu_h^+\, p_{z\mathrm{I}}^- + \mu_h^-\, p_{z\mathrm{I}}^+} & 0 \\ 0 & \frac{2\tilde{\varepsilon}_h^-\, p_{z\mathrm{II}}^+}{\tilde{\varepsilon}_h^-\, p_{z\mathrm{II}}^+ + \tilde{\varepsilon}_h^+\, p_{z\mathrm{II}}^-} \end{pmatrix}, \quad \acute{\boldsymbol{t}} = \begin{pmatrix} \frac{2\mu_h^-\, p_{z\mathrm{I}}^+}{\mu_h^+\, p_{z\mathrm{I}}^- + \mu_h^-\, p_{z\mathrm{I}}^+} & 0 \\ 0 & \frac{2\tilde{\varepsilon}_h^+\, p_{z\mathrm{II}}^-}{\tilde{\varepsilon}_h^-\, p_{z\mathrm{II}}^+ + \tilde{\varepsilon}_h^+\, p_{z\mathrm{II}}^-} \end{pmatrix}. \tag{E2}$$

Note that the Fresnel transmission matrices are not symmetric, i.e. $\grave{\boldsymbol{t}} \neq \acute{\boldsymbol{t}}$, by contrast to the relation in eq. (122).

APPENDIX F: EM FIELDS FOR TIV-MEDIA IN CYLINDRICAL COORDINATES

When all the layers in the stratified model are either TIV or isotropic, the double Fourier integral over the horizontal wavenumbers k_x and k_y in eq. (6b) can be rewritten into a single integral in terms of Bessel functions and the polar horizontal wavenumber k_ρ. Thus, it is convenient to introduce cylindrical coordinates:

$$k_\rho = \sqrt{k_x^2 + k_y^2}, \qquad k_x = k_\rho \cos\alpha, \qquad k_y = k_\rho \sin\alpha, \tag{F1a}$$

$$\rho = \sqrt{x^2 + y^2}, \qquad x = \rho\cos\beta, \qquad y = \rho\sin\beta, \tag{F1b}$$

where α is the polar angle in the wavenumber domain, β is the angle in the spatial domain, and ρ is the polar radius. The inverse Fourier transform from the wavenumber domain back to the spatial domain (eq. (6b) without the time and frequency part), can then be rewritten as

$$\int_{-\infty}^{\infty}\int_{-\infty}^{\infty} dk_x dk_y\, \phi(k_x, k_y)\,\mathrm{e}^{ik_x x + ik_y y} = \int_0^{2\pi}\int_0^{\infty} d\xi dk_\rho\, k_\rho\, \phi\left(k_\rho, \xi\right)\, \mathrm{e}^{ik_\rho\rho\sin\xi}, \tag{F2}$$

where $\xi = \alpha - \beta + \pi/2$. The exponential term that contains the sine function, can be expressed by a series of Bessel functions (Gradshteyn & Ryzhik 1980):

$$\exp\left(ik_\rho\rho\sin\xi\right) = \sum_{n=-\infty}^{\infty} J_n(k_\rho\rho)\mathrm{e}^{in\xi}. \tag{F3}$$

By using the property $J_{-n}(k_\rho\, \rho) = (-1)^n J_n(k_\rho\, \rho)$, one arrives at the representation:

$$J_0(k_\rho\rho) = \frac{1}{2\pi}\int_0^{2\pi} d\xi\ \mathrm{e}^{ik_\rho\rho\sin\xi}, \tag{F4a}$$

$$J_1(k_\rho\rho) = \frac{1}{2\pi i}\int_0^{2\pi} d\xi\ \sin\xi\ \mathrm{e}^{ik_\rho\rho\sin\xi}, \tag{F4b}$$

$$J_2(k_\rho\rho) = \frac{1}{2\pi}\int_0^{2\pi} d\xi\ \cos 2\xi\ \mathrm{e}^{ik_\rho\rho\sin\xi}, \tag{F4c}$$

where the following relationship between J_0, J_1 and J_2 holds:

$$J_0(k_\rho\rho) + J_2(k_\rho\rho) = \frac{2}{k_\rho\rho}J_1(k_\rho\rho). \tag{F5}$$

Since the RT-response is symmetric about the vertical axis in a TIV or isotropic medium, the angle α is *explicitly* present in the field expressions in eqs (133), (137), (140), and (142) in these cases. Thus, the angle-dependence in the wavenumber domain can be accounted for by the higher orders of the Bessel functions. Now, rewrite the cosine and sine terms that contain α into expressions that contain ξ and β. Since terms involving $\cos\xi$ and $\sin 2\xi$ do not contribute to the Bessel expansion, this means that

$$\cos\alpha \rightarrow \sin\xi\cos\beta, \qquad \sin\alpha \rightarrow \sin\xi\sin\beta, \tag{F6a}$$

$$\cos 2\alpha \rightarrow -\cos 2\xi\cos 2\beta, \qquad \sin 2\alpha \rightarrow -\cos 2\xi\sin 2\beta. \tag{F6b}$$

The field components in cylindrical coordinates are furthermore obtained from the Cartesian components by the rotation:

$$\begin{pmatrix}\Psi_\rho\\ \Psi_\beta\\ \Psi_z\end{pmatrix} = \begin{pmatrix}\cos\beta & \sin\beta & 0\\ -\sin\beta & \cos\beta & 0\\ 0 & 0 & 1\end{pmatrix}\begin{pmatrix}\Psi_x\\ \Psi_y\\ \Psi_z\end{pmatrix}. \tag{F7}$$

where $\mathbf{\Psi} = \{\mathbf{E}, \mathbf{H}\}$.

In the following subsections, the electromagnetic field expressions in a TIV-medium for the four different source types are given in terms of cylindrical coordinates. In a numerical implementation cylindrical coordinates are advantageous since they imply evaluation of one integral instead of a double integral. The integral over the horizontal angles is contained within the Bessel functions as seen from eq. (F4). The vertical slownesses $p_{z\mathrm{I}}$ and $p_{z\mathrm{II}}$ that will be used in the following equations are dependent on $k_\rho = \omega p_\rho$ as described in eq. (119).

F1 EM-field from a HED

From the expressions in eq. (133) the following field components from a HED is derived:

$$E_\rho = -\frac{Il_x}{4\pi}\cos\beta\left[\mathcal{I}^{TM}_{A0} + \frac{1}{\rho}\left(\mathcal{I}^{TE}_{A1} - \mathcal{I}^{TM}_{A1}\right)\right], \tag{F8a}$$

$$E_\beta = -\frac{Il_x}{4\pi}\sin\beta\left[-\mathcal{I}^{TE}_{A0} + \frac{1}{\rho}\left(\mathcal{I}^{TE}_{A1} - \mathcal{I}^{TM}_{A1}\right)\right], \tag{F8b}$$

$$H_\rho = +\frac{Il_x}{4\pi}\sin\beta\left[-\mathcal{I}^{TE}_{D0} + \frac{1}{\rho}\left(\mathcal{I}^{TE}_{D1} - \mathcal{I}^{TM}_{D1}\right)\right], \tag{F8c}$$

$$H_\beta = -\frac{Il_x}{4\pi}\cos\beta\left[\mathcal{I}^{TM}_{D0} + \frac{1}{\rho}\left(\mathcal{I}^{TE}_{D1} - \mathcal{I}^{TM}_{D1}\right)\right], \tag{F8d}$$

$$E_z = +\frac{Il_x}{4\pi}\frac{i\cos\beta}{\omega\tilde{\varepsilon}_v}\int_0^\infty dk_\rho k_\rho^2\, J_1(k_\rho\rho)\, g^{TM}_D(p_{z\mathrm{II}}), \tag{F8e}$$

$$H_z = +\frac{Il_x}{4\pi}\frac{i\sin\beta}{\omega\mu_v}\int_0^\infty dk_\rho k_\rho^2\, J_1(k_\rho\rho)\, g^{TE}_A(p_{z\mathrm{I}}), \tag{F8f}$$

where

$$\mathcal{I}^{TE}_{A0} = \int_0^\infty dk_\rho k_\rho\, J_0(k_\rho\rho)\, g^{TE}_A(p_{z\mathrm{I}}), \qquad \mathcal{I}^{TE}_{A1} = \int_0^\infty dk_\rho\, J_1(k_\rho\rho)\, g^{TE}_A(p_{z\mathrm{I}}), \tag{F8g}$$

$$\mathcal{I}^{TM}_{A0} = \int_0^\infty dk_\rho k_\rho\, J_0(k_\rho\rho)\, g^{TM}_A(p_{z\mathrm{II}}), \qquad \mathcal{I}^{TM}_{A1} = \int_0^\infty dk_\rho\, J_1(k_\rho\rho)\, g^{TM}_A(p_{z\mathrm{II}}), \tag{F8h}$$

$$\mathcal{I}^{TE}_{D0} = \int_0^\infty dk_\rho k_\rho\, J_0(k_\rho\rho)\, g^{TE}_D(p_{z\mathrm{I}}), \qquad \mathcal{I}^{TE}_{D1} = \int_0^\infty dk_\rho\, J_1(k_\rho\rho)\, g^{TE}_D(p_{z\mathrm{I}}), \tag{F8i}$$

$$\mathcal{I}^{TM}_{D0} = \int_0^\infty dk_\rho k_\rho\, J_0(k_\rho\rho)\, g^{TM}_D(p_{z\mathrm{II}}), \qquad \mathcal{I}^{TM}_{D1} = \int_0^\infty dk_\rho\, J_1(k_\rho\rho)\, g^{TM}_D(p_{z\mathrm{II}}), \tag{F8j}$$

and

$$g^{TE}_A(p_{z\mathrm{I}}) = \sqrt{\frac{\mu_h}{p_{z\mathrm{I}}}}\,\sqrt{\frac{\mu_h}{p_{z\mathrm{I}}}}^{s}\,\mathcal{R}^{TE}_A(p_{z\mathrm{I}}), \qquad g^{TM}_A(p_{z\mathrm{II}}) = \sqrt{\frac{p_{z\mathrm{II}}}{\tilde{\varepsilon}_h}}\,\sqrt{\frac{p_{z\mathrm{II}}}{\tilde{\varepsilon}_h}}^{s}\,\mathcal{R}^{TM}_A(p_{z\mathrm{II}}), \tag{F9a}$$

$$g^{TE}_D(p_{z\mathrm{I}}) = -\sqrt{\frac{p_{z\mathrm{I}}}{\mu_h}}\,\sqrt{\frac{\mu_h}{p_{z\mathrm{I}}}}^{s}\,\mathcal{R}^{TE}_D(p_{z\mathrm{I}}), \qquad g^{TM}_D(p_{z\mathrm{II}}) = -\sqrt{\frac{\tilde{\varepsilon}_h}{p_{z\mathrm{II}}}}\,\sqrt{\frac{p_{z\mathrm{II}}}{\tilde{\varepsilon}_h}}^{s}\,\mathcal{R}^{TM}_D(p_{z\mathrm{II}}), \tag{F9b}$$

where the RT-amplitudes are given by eq. (134).

F2 EM-field from a HMD

From the expressions in eq. (137) the field components from a HMD can be calculated:

$$E_\rho = -\frac{i\omega\mu_h^s I a_x}{4\pi}\sin\beta\left[\ \mathcal{I}_{B0}^{TM} + \frac{1}{\rho}\left(\mathcal{I}_{B1}^{TE} - \mathcal{I}_{B1}^{TM}\right)\right], \tag{F10a}$$

$$E_\beta = +\frac{i\omega\mu_h^s I a_x}{4\pi}\cos\beta\left[-\mathcal{I}_{B0}^{TE} + \frac{1}{\rho}\left(\mathcal{I}_{B1}^{TE} - \mathcal{I}_{B1}^{TM}\right)\right], \tag{F10b}$$

$$H_\rho = -\frac{i\omega\mu_h^s I a_x}{4\pi}\cos\beta\left[-\mathcal{I}_{C0}^{TE} + \frac{1}{\rho}\left(\mathcal{I}_{C1}^{TE} - \mathcal{I}_{C1}^{TM}\right)\right], \tag{F10c}$$

$$H_\beta = -\frac{i\omega\mu_h^s I a_x}{4\pi}\sin\beta\left[\ \mathcal{I}_{C0}^{TM} + \frac{1}{\rho}\left(\mathcal{I}_{C1}^{TE} - \mathcal{I}_{C1}^{TM}\right)\right], \tag{F10d}$$

$$E_z = -\frac{I a_x}{4\pi}\frac{\mu_h^s}{\tilde{\varepsilon}_v}\sin\beta\int_0^\infty dk_\rho k_\rho^2\, J_1(k_\rho\rho)\, g_C^{TM}(p_{z\mathrm{II}}), \tag{F10e}$$

$$H_z = +\frac{I a_x}{4\pi}\frac{\mu_h^s}{\mu_v}\cos\beta\int_0^\infty dk_\rho k_\rho^2\, J_1(k_\rho\rho)\, g_B^{TE}(p_{z\mathrm{I}}), \tag{F10f}$$

where

$$\mathcal{I}_{B0}^{TE} = \int_0^\infty dk_\rho k_\rho\, J_0(k_\rho\rho)\, g_B^{TE}(p_{z\mathrm{I}}), \qquad \mathcal{I}_{B1}^{TE} = \int_0^\infty dk_\rho\, J_1(k_\rho\rho)\, g_B^{TE}(p_{z\mathrm{I}}), \tag{F10g}$$

$$\mathcal{I}_{B0}^{TM} = \int_0^\infty dk_\rho k_\rho\, J_0(k_\rho\rho)\, g_B^{TM}(p_{z\mathrm{II}}), \qquad \mathcal{I}_{B1}^{TM} = \int_0^\infty dk_\rho\, J_1(k_\rho\rho)\, g_B^{TM}(p_{z\mathrm{II}}), \tag{F10h}$$

$$\mathcal{I}_{C0}^{TE} = \int_0^\infty dk_\rho k_\rho\, J_0(k_\rho\rho)\, g_C^{TE}(p_{z\mathrm{I}}), \qquad \mathcal{I}_{C1}^{TE} = \int_0^\infty dk_\rho\, J_1(k_\rho\rho)\, g_C^{TE}(p_{z\mathrm{I}}), \tag{F10i}$$

$$\mathcal{I}_{C0}^{TM} = \int_0^\infty dk_\rho k_\rho\, J_0(k_\rho\rho)\, g_C^{TM}(p_{z\mathrm{II}}), \qquad \mathcal{I}_{C1}^{TM} = \int_0^\infty dk_\rho\, J_1(k_\rho\rho)\, g_C^{TM}(p_{z\mathrm{II}}), \tag{F10j}$$

and

$$g_B^{TE}(p_{z\mathrm{I}}) = \sqrt{\frac{\mu_h}{p_{z\mathrm{I}}}}\sqrt{\frac{p_{z\mathrm{I}}}{\mu_h}}^{s}\mathcal{R}_B^{TE}(p_{z\mathrm{I}}), \qquad g_B^{TM}(p_{z\mathrm{II}}) = \sqrt{\frac{p_{z\mathrm{II}}}{\tilde{\varepsilon}_h}}\sqrt{\frac{\tilde{\varepsilon}_h}{p_{z\mathrm{II}}}}^{s}\mathcal{R}_B^{TM}(p_{z\mathrm{II}}), \tag{F11a}$$

$$g_C^{TE}(p_{z\mathrm{I}}) = -\sqrt{\frac{p_{z\mathrm{I}}}{\mu_h}}\sqrt{\frac{p_{z\mathrm{I}}}{\mu_h}}^{s}\mathcal{R}_C^{TE}(p_{z\mathrm{I}}), \qquad g_C^{TM}(p_{z\mathrm{II}}) = -\sqrt{\frac{\tilde{\varepsilon}_h}{p_{z\mathrm{II}}}}\sqrt{\frac{\tilde{\varepsilon}_h}{p_{z\mathrm{II}}}}^{s}\mathcal{R}_C^{TM}(p_{z\mathrm{II}}), \tag{F11b}$$

where the RT-amplitudes are given by eq. (138).

F3 EM-field from a VED

The field components from a VED are obtained from eq. (140):

$$E_\rho = +\frac{I l_z}{4\pi}\frac{i}{\omega\tilde{\varepsilon}_v^s}\int_0^\infty dk_\rho k_\rho^2\, J_1(k_\rho\rho)\, g_B^{TM}(p_{z\mathrm{II}}), \tag{F12a}$$

$$H_\beta = +\frac{I l_z}{4\pi}\frac{i}{\omega\tilde{\varepsilon}_v^s}\int_0^\infty dk_\rho k_\rho^2\, J_1(k_\rho\rho)\, g_C^{TM}(p_{z\mathrm{II}}), \tag{F12b}$$

$$E_z = -\frac{I l_z}{4\pi}\frac{1}{\omega^2\tilde{\varepsilon}_v\tilde{\varepsilon}_v^s}\int_0^\infty dk_\rho k_\rho^3\, J_0(k_\rho\rho)\, g_C^{TM}(p_{z\mathrm{II}}) + \frac{I l_z}{4\pi}\frac{1}{i\omega\tilde{\varepsilon}_v^s}\delta(z-z_s)\delta(x)\delta(y). \tag{F12c}$$

F4 EM-field from a VMD

The field components from a VMD are obtained from eq. (142):

$$E_\beta = -\frac{I a_z}{4\pi}\int_0^\infty dk_\rho k_\rho^2\, J_1(k_\rho\rho)\, g_A^{TE}(p_{z\mathrm{I}}), \tag{F13a}$$

$$H_\rho = +\frac{I a_z}{4\pi}\int_0^\infty dk_\rho k_\rho^2\, J_1(k_\rho\rho)\, g_D^{TE}(p_{z\mathrm{I}}), \tag{F13b}$$

$$H_z = +\frac{Ia_z}{4\pi}\frac{i}{\omega\mu_v}\int_0^\infty dk_\rho k_\rho^3\, J_0(k_\rho\rho)\, g_A^{TE}(p_{zI}) - \frac{Ia_z}{4\pi}\delta(z-z_s)\delta(x)\delta(y). \tag{F13c}$$

F5 RT-amplitudes with source and receiver in the same layer

Consider the responses in eq. (F9) and (F11) with the source at $z_s = 0$, and the receiver within the same layer at z. The RT-responses can then be combined into a single expression for $z < z_s$ and $z > z_s$, and the RT-expressions in eqs (134) and (138) can be split into a direct and reflected field contribution:

$$\mathcal{R}_A = e^{i\omega p_z|z|} + R_A, \qquad R_A = \frac{\grave{R}_s(1+\acute{R}_s)e^{-i\omega p_z z} + \acute{R}_s(1+\grave{R}_s)e^{i\omega p_z z}}{1-\acute{R}_s\grave{R}_s}, \tag{F14a}$$

$$\mathcal{R}_B = \mathrm{sgn}(z)e^{i\omega p_z|z|} + R_B, \quad R_B = \frac{\grave{R}_s(1-\acute{R}_s)e^{-i\omega p_z z} - \acute{R}_s(1-\grave{R}_s)e^{i\omega p_z z}}{1-\acute{R}_s\grave{R}_s}, \tag{F14b}$$

$$-\mathcal{R}_C = e^{i\omega p_z|z|} + R_C, \qquad R_C = \frac{-\grave{R}_s(1-\acute{R}_s)e^{-i\omega p_z z} - \acute{R}_s(1-\grave{R}_s)e^{i\omega p_z z}}{1-\acute{R}_s\grave{R}_s}, \tag{F14c}$$

$$-\mathcal{R}_D = \mathrm{sgn}(z)e^{i\omega p_z|z|} + R_D, \quad R_D = \frac{-\grave{R}_s(1+\acute{R}_s)e^{-i\omega p_z z} + \acute{R}_s(1+\grave{R}_s)e^{i\omega p_z z}}{1-\acute{R}_s\grave{R}_s}. \tag{F14d}$$

In the expressions, $p_z = p_{zI}$ for the TE-mode, and $p_z = p_{zII}$ for the TM-mode.

APPENDIX G: UP/DOWN-SEPARATION AND FREE SURFACE REMOVAL

Consider an isotropic source medium in which the electromagnetic fields from a dipole antenna e.g. HED is recorded. The propagator matrix method with its implicit splitting of fields into upgoing and downgoing components, can be useful in processing real data from e.g. a marine CSEM/SBL experiment in shallow water. A possible choice of the eigenvector matrix that diagonalize the system matrix into upgoing and downgoing components of the electric field, is (Amundsen *et al.* 2006)

$$\boldsymbol{N}_A = \begin{pmatrix} \boldsymbol{I} & \boldsymbol{I} \\ \boldsymbol{N}_2 & -\boldsymbol{N}_2 \end{pmatrix}, \quad \boldsymbol{N}_A^{-1} = \frac{1}{2}\begin{pmatrix} \boldsymbol{I} & \boldsymbol{N}_2^{-1} \\ \boldsymbol{I} & -\boldsymbol{N}_2^{-1} \end{pmatrix}, \tag{G1}$$

where in isotropic media

$$\boldsymbol{N}_2 = \frac{1}{\mu p_z}\begin{pmatrix} \mu\tilde{\varepsilon} - p_y^2 & p_x p_y \\ p_x p_y & \mu\tilde{\varepsilon} - p_x^2 \end{pmatrix}, \quad \boldsymbol{N}_2^{-1} = \frac{1}{\tilde{\varepsilon} p_z}\begin{pmatrix} \mu\tilde{\varepsilon} - p_x^2 & -p_x p_y \\ -p_x p_y & \mu\tilde{\varepsilon} - p_y^2 \end{pmatrix}. \tag{G2}$$

In this case, the eigenvector matrix is normalized with respect to the electric amplitude which leads to the relations

$$E_x = E_x^U + E_x^D \quad \text{and} \quad E_y = E_y^U + E_y^D. \tag{G3}$$

Now $\boldsymbol{b} = \boldsymbol{N}_A\, \boldsymbol{w}_A$, where $\boldsymbol{w}_A = (E_x^U\ E_y^U\ E_x^D\ E_y^D)^T$. The quantity E^U describes the part of the electric field that is upgoing, and E^D describes the downgoing electric field. From the equations for up/down-separation where $\boldsymbol{N}_A$ is arranged to give $E_x = E_x^U + E_x^D$, one thus gets

$$E_x^U = \frac{1}{2}\left(E_x - \frac{p_x p_y}{\tilde{\varepsilon} p_z}H_x - \frac{\mu\tilde{\varepsilon} - p_x^2}{\tilde{\varepsilon} p_z}H_y\right), \tag{G4a}$$

$$E_x^D = \frac{1}{2}\left(E_x + \frac{p_x p_y}{\tilde{\varepsilon} p_z}H_x + \frac{\mu\tilde{\varepsilon} - p_x^2}{\tilde{\varepsilon} p_z}H_y\right). \tag{G4b}$$

When inserting the field expressions from eq. (133) into eq. (G4) with the appropriate simplifications for isotropic media with source and receiver within the same layer (eq. F14), one gets:

$$E_x^U = \frac{Il_x}{2}\left[\frac{\mu p_y^2}{p_\rho p_z} f\left(-z, R_A^{TE}, -R_D^{TE}\right) + \frac{p_x^2 p_z}{\tilde{\varepsilon} p_\rho} f\left(-z, R_A^{TM}, -R_D^{TM}\right)\right], \tag{G5a}$$

$$E_x^D = \frac{Il_x}{2}\left[\frac{\mu p_y^2}{p_\rho p_z} f\left(z, R_A^{TE}, R_D^{TE}\right) + \frac{p_x^2 p_z}{\tilde{\varepsilon} p_\rho} f\left(z, R_A^{TM}, R_D^{TM}\right)\right], \tag{G5b}$$

where

$$f(z, R_A, R_D) = \frac{1+\mathrm{sgn}(z)}{2}\, e^{i\omega p_z|z|} + \frac{R_A + R_D}{2}. \tag{G6}$$

From eqs (F14a) and (F14d), the following relations can be derived:

$$\frac{R_A - R_D}{2} = \frac{1}{1-\grave{R}_s\acute{R}_s}\grave{R}_s(1+\acute{R}_s)e^{-i\omega p_z z}, \tag{G7a}$$

$$\frac{R_A + R_D}{2} = \frac{1}{1 - \grave{R}_s \acute{R}_s} \acute{R}_s (1 + \grave{R}_s) \mathrm{e}^{i\omega p_z z}. \tag{G7b}$$

The TE- and TM-mode are not separated in these expressions. In order to derive expressions with separated modes, the eigenvector matrix can be chosen as in eq. (E1). Then the mode-field vector describes the upgoing and downgoing TE- and TM-modes. In isotropic media

$$\begin{pmatrix} U^{TE} \\ U^{TM} \\ D^{TE} \\ D^{TM} \end{pmatrix} = \boldsymbol{N}_F^{-1} \boldsymbol{b} = \frac{1}{\sqrt{2} p_\rho} \begin{pmatrix} p_y & -p_x & p_y \frac{\mu}{p_z} & -p_x \frac{\mu}{p_z} \\ p_x & p_y & p_x \frac{p_z}{\tilde{\varepsilon}} & p_y \frac{p_z}{\tilde{\varepsilon}} \\ p_y & -p_x & -p_y \frac{\mu}{p_z} & p_x \frac{\mu}{p_z} \\ p_x & p_y & -p_x \frac{p_z}{\tilde{\varepsilon}} & -p_y \frac{p_z}{\tilde{\varepsilon}} \end{pmatrix} \begin{pmatrix} E_x \\ E_y \\ -H_y \\ H_x \end{pmatrix}. \tag{G8}$$

By inserting the field expressions from eq. (133) with the appropriate simplifications for isotropic media with source and receiver within the same layer, one then gets

$$U^{TE} = \frac{Il_x}{2\sqrt{2} p_\rho} \left(\frac{\mu p_y}{p_z} \left\{ [1 - \mathrm{sgn}(z)] \mathrm{e}^{i\omega p_z |z|} + R_A^{TE} - R_D^{TE} \right\} \right), \tag{G9a}$$

$$U^{TM} = \frac{Il_x}{2\sqrt{2} p_\rho} \left(\frac{p_z p_x}{\tilde{\varepsilon}} \left\{ [1 - \mathrm{sgn}(z)] \mathrm{e}^{i\omega p_z |z|} + R_A^{TM} - R_D^{TM} \right\} \right), \tag{G9b}$$

$$D^{TE} = \frac{Il_x}{2\sqrt{2} p_\rho} \left(\frac{\mu p_y}{p_z} \left\{ [1 + \mathrm{sgn}(z)] \mathrm{e}^{i\omega p_z |z|} + R_A^{TE} + R_D^{TE} \right\} \right), \tag{G9c}$$

$$D^{TM} = \frac{Il_x}{2\sqrt{2} p_\rho} \left(\frac{p_z p_x}{\tilde{\varepsilon}} \left\{ [1 + \mathrm{sgn}(z)] \mathrm{e}^{i\omega p_z |z|} + R_A^{TM} + R_D^{TM} \right\} \right). \tag{G9d}$$

Here the upgoing and downgoing fields are a mix of the electric and magnetic field.

In a marine CSEM/SBL experiment, the receiver is normally situated below the receiver, i.e. $z > 0$ in eq. (F14). The reflection response from the lower stack can thus be obtained by dividing the upgoing component by the downgoing component. The reflection responses for the TE- and TM-polarization components hence become:

$$\frac{U^{TE}}{D^{TE}} = \grave{R}_b^{TE} \quad \text{and} \quad \frac{U^{TM}}{D^{TM}} = \grave{R}_b^{TM}, \tag{G10}$$

where $\grave{R}_b$ is the reflection response from the lower stack at the receiver (*cf.* Fig. 4). The decomposition matrix from eq. (120) would give the same results since the difference between the eigenvectors lies within a normalization factor. By using the reflection response from the lower stack when calculating the electromagnetic field from an artificial source, one might say that one in this way has removed the free surface from the original data set. In order to do the free surface removal with the procedure described here, a 2-D data set with $z > z_s$ and which contains all the horizontal components of the electromagnetic field, is needed.